

[Click here to view linked References](#)

The frog inner ear: picture perfect?

Matthew J. Mason¹

Johannes M. Segenhout²

Ariadna Cobo-Cuan³

Patricia M. Quiñones⁴

Pim van Dijk^{2,5}

¹ University of Cambridge

Department of Physiology, Development & Neuroscience

Downing Street

Cambridge CB2 3EG

U.K.

Tel. +44 1223 333829

Fax +44 1223 333840

mjm68@cam.ac.uk

² University of Groningen

University Medical Center Groningen

Department of Otorhinolaryngology, Head & Neck Surgery

P.O. Box 30.001

9700 RB Groningen

The Netherlands

jmsegenhout@hotmail.com

p.van.dijk@umcg.nl

1
2
3
4
5
6
7
8
9
10
11
12
13
14
15
16
17
18
19
20
21
22
23
24
25
26
27
28
29
30
31
32
33
34
35
36
37
38
39
40
41
42
43
44
45
46
47
48
49
50
51
52
53
54
55
56
57
58
59
60
61
62
63
64
65

27 ³ Department of Animal and Human Biology
28 Havana University
29 Street 25 No. 455
30 Havana CP 10400
31 Cuba
32 cobo_cuan@fbio.uh.cu
33
34 ⁴ Department of Physics and Astronomy
35 1-129 Knudsen Hall, 475 Portola Plaza
36 University of California Los Angeles
37 Los Angeles, CA 90095
38 U.S.A.
39 yukiq@ucla.edu
40
41 ⁵ University of Groningen
42 Graduate School of Medical Sciences, Research School of Behavioral and Cognitive Neurosciences
43 P.O. Box 196
44 9700 AD Groningen
45 The Netherlands
46 p.van.dijk@umcg.nl

Abstract

47
48 Many recent accounts of the frog peripheral auditory system have reproduced Wever's (1973)
49 schematic cross-section of the ear of a leopard frog. We sought to investigate to what extent this
50 diagram is an accurate and representative depiction of the anuran inner ear, using three-
51 dimensional reconstructions made from serial sections of *Rana pipiens*, *Eleutherodactylus limbatus*
52 and *Xenopus laevis*.

53 In *Rana*, three discrete contact membranes were found to separate the posterior otic (=
54 endolymphatic) labyrinth from the periotic (= perilymphatic) system: those of the amphibian and
55 basilar recesses and the contact membrane of the saccule. The amphibian 'tegmentum vasculosum'
56 was distinguishable as a thickened epithelial lining within a posterior recess of the superior saccular
57 chamber. These features were also identified in *Eleutherodactylus*, but in this tiny frog the relative
58 proportions of the semicircular canals and saccule resemble those of ranid tadpoles. There appeared
59 to be a complete fluid pathway between the right and left periotic labyrinths in this species, crossing
60 the cranial cavity. *Xenopus* lacks a tegmentum vasculosum and a contact membrane of the saccule;
61 the *Xenopus* ear is further distinguished by a lateral passage separating stapes from periotic cistern
62 and a more direct connection between periotic cistern and basilar recess. The basilar and lagenar
63 recesses are conjoined in this species.

64 Wever's diagram of the inner ear of *Rana* retains its value for diagrammatic purposes but it is not
65 anatomically accurate, nor representative of all frogs. Although Wever identified the contact
66 membrane of the saccule, most recent studies of frog inner ear anatomy have overlooked both this
67 and the amphibian tegmentum vasculosum. These structures deserve further attention.

Keywords

70 Inner ear; frog; amphibian papilla; basilar papilla; tegmentum vasculosum; contact membrane

71

72 Introduction

73 The inner ear structures of ranid frogs have been the subject of detailed anatomical accounts dating
74 back over 150 years, many of which were written in German (see e.g. Deiters, 1862; Hasse, 1868;
75 Retzius, 1881; Gaupp, 1904). Among the best known of the English-language descriptions are those
76 of Ernest Glen Wever. The first figure from Wever's 1973 paper in *Journal of Morphology*
77 (reproduced here as Fig. 1A) shows "A schematic representation of the ear and labyrinth of *Rana*
78 *pipiens*, in frontal section". An almost identical diagram appeared in two of Wever's later
79 publications including his 1985 book *The Amphibian Ear*, which remains the most comprehensive
80 account of the subject. It has been reproduced, sometimes in a modified form, in review papers (e.g.
81 Fay and Popper, 1985; Lewis and Narins, 1999; Simmons et al., 2007; Gridi-Papp and Narins, 2010), a
82 leading text-book on amphibian biology (Duellman and Trueb, 1986) and several other articles. As
83 such, it must be the world's most widely-consulted scientific illustration of an amphibian peripheral
84 auditory system. However, as explained below, there is some uncertainty as to the species depicted,
85 the orientation and the accuracy of this important diagram.

86 The species examined

87 The taxonomy of the North American ranid frogs is currently in a state of flux (Dubois, 2007; Hillis,
88 2007; Pauly et al., 2009). Some authors place leopard frogs in the genus *Lithobates*, but following
89 Hillis' (2007) recommendation, we retain the genus *Rana* for North American ranids.

90 Wever (1973) stated that his illustration shows the ear of *Rana pipiens*, but in his 1985 book he
91 distinguished between this species (the northern leopard frog) and the very similar "*Rana utricularia*
92 *sphenocephala*", now *R. sphenocephala utricularia* (the southern leopard frog). Wever (1985) did not
93 make it clear which of these species is represented in the figure of interest to us here, which appears
94 in slightly modified form as his Fig. 3-17. However, another illustration also reproduced from his
95 1973 paper (Fig. 3-79 in Wever, 1985) is labelled as *R. sphenocephala*. Wever's 1973 paper may

1
2
3
4
5
6
7
8
9
10
11
12
13
14
15
16
17
18
19
20
21
22
23
24
25
26
27
28
29
30
31
32
33
34
35
36
37
38
39
40
41
42
43
44
45
46
47
48
49
50
51
52
53
54
55
56
57
58
59
60
61
62
63
64
65

96 therefore describe the ear of the southern leopard frog, but it is likely that the ears of these two
97 species are practically identical. The articles that have reproduced Wever's illustration have often
98 implied that a generalized anuran morphology is represented.

99 **The orientation of Wever's illustration**

100 Within his 1973 paper, Wever stated that he sectioned his specimens in "a horizontal plane (dorsal
101 to ventral)...frontally (anterior to posterior) or laterally (right to medial, then continued from medial
102 to left)". This description is somewhat confusing, and perhaps for this reason Wever later redefined
103 the three planes. In Wever's (1985) figure 3-34, a frontal plane is clearly shown dividing the head
104 into dorsal and ventral components. Such a plane would pass through most of the teeth on both left
105 and right maxillae and may be considered horizontal. A sagittal plane vertically divides the head into
106 left and right components. A transverse plane is a vertical plane perpendicular to the frontal and
107 sagittal planes, which divides the head into anterior and posterior components. These definitions
108 agree with the standard veterinary anatomical nomenclature (Blood and Studdert, 1999) and are
109 those used in the present study. In our interpretation, "horizontal" (Wever, 1973) is actually frontal,
110 "lateral" (Wever, 1973) is actually sagittal and "frontal" (Wever, 1973) is actually transverse.

111 The present study focuses on the first figure from Wever (1973), the caption of which reads "the ear
112 and labyrinth...in frontal section" (Fig. 1A). Was this in fact a transverse section, according to
113 standard nomenclature?

114 **The accuracy of Wever's illustration**

115 When preparing a previous article (van Dijk et al., 2011), two of the current authors had reason to
116 question the accuracy of Wever's 1973 diagram. Wever shows the extrastapes (= extracolumella) as
117 a very short extension of the bony stapes shaft (*stapes pars media*), connecting it to the centre of
118 the tympanic membrane (Fig. 1). It would be natural to assume that this apparatus must operate as
119 a stiff piston, an inflection of the tympanic membrane driving the stapes directly into the inner ear.
120 In reality, the extrastapes is much longer than this and has an angled articulation with the *pars*

121 *media*: the stapes/extrastapes system works as a flexible, first-order lever (Jørgensen and
122 Kanneworff, 1998; Mason and Narins, 2002; Werner, 2003).

123 Turning to the inner ear, Wever shows three pathways for “fluid flow” to pass between the stapes
124 on the right of his diagram to the periotic (= perilymphatic) sac on the left, one via the amphibian
125 papilla, a second via the basilar papilla and a third between the two papillae, each being indicated by
126 arrows in Fig. 1A. The endolymph within the otic (= endolymphatic) labyrinth in frogs is separated
127 from the perilymph within the periotic labyrinth by so-called ‘contact membranes’ (Fig. 1B), so fluid
128 cannot actually flow between the two systems and the three arrows should instead be taken to
129 indicate three pathways of acoustic energy flow. In their more recent account of energy flow
130 pathways through the ear of the bullfrog (*Rana catesbeiana*), Purgue & Narins (2000a, b) considered
131 the routes passing through the amphibian and basilar recesses but made no mention of Wever’s
132 middle pathway. Purgue & Narins regarded the periotic canal as an alternative route for low-
133 frequency energy flow which bypasses the otic system entirely, but this is not labelled in Wever’s
134 diagram and there is scant reference to it in his written descriptions. Four potential pathways for
135 sound energy flow between stapes and periotic sac have therefore been described in frogs, but are
136 all four consistently present?

137 In this study, histological sections were made from the inner ears of three species of frogs, including
138 leopard frogs (these were believed to be *Rana pipiens* rather than *R. sphenoccephala*, but this could
139 not be confirmed beyond doubt by the suppliers). Photomicrographs and three-dimensional
140 reconstructions were used to assess the accuracy of Wever’s accounts and other recent descriptions
141 of ranid inner ear morphology.

142 While leopard frogs are in the family Ranidae, within the Ranoidea clade of the Neobatrachia,
143 *Eleutherodactylus limbatus* (Eleutherodactylidae) is placed within the other major neobatrachian
144 clade, the Hyloidea (Hoegg et al., 2004). *Xenopus laevis*, family Pipidae, is an aquatic
145 ‘archaeobatrachian’, the ‘Archaeobatrachia’ being a paraphyletic assemblage of frogs which

146 diverged before the Neobatrachia (Hoegg et al., 2004). In order to assess whether Wever's diagram
147 is representative of a more diverse range of frogs, the leopard frog ear was compared here with the
148 ears of *E. limbatus*, one of the world's smallest frogs, and with those of *X. laevis*.

Materials and methods

149
150
151 Twelve frogs from three different species were used in this study. Three leopard frogs believed to be
152 *Rana pipiens* (40-50 g body mass) were obtained from Charles D. Sullivan Co. Inc. (Nashville, TN,
153 U.S.A.) via Exoterra Schaudi GmbH, Holzheim, Germany. They were housed at the University of
154 Groningen laboratory animal facilities. The frogs were euthanized using the double pith procedure
155 and then decapitated. The lower jaw was removed and the remaining part of the head was divided
156 sagittally. Skin was removed and small holes were made in various places in the skull, away from the
157 structures of interest, to improve fluid impregnation. The ears were fixed by immersion in a 10%
158 neutral buffered formalin solution (pH 7.4) for at least 24 hours at 4°C. The fresh corpse of a male
159 *Rana pipiens*, originating from Nasco (Fort Atkinson, WI, U.S.A.), was used for micro-computed
160 tomography (micro-CT) scanning, as described below.

161 Two *Eleutherodactylus limbatus* specimens (each around 0.2 g body mass) were captured at Las
162 Terrazas, Artemisa province, Cuba. They were euthanized by double pithing and decapitation, the
163 palatal skin was removed and their heads were preserved in 10% formalin and sent to Groningen for
164 further processing. The head of one specimen was halved prior to sectioning, while the other was
165 sectioned whole.

166 Six *Xenopus laevis* specimens (males 55-60 g, females 120-220 g, all gonadectomized body masses)
167 were obtained as fresh corpses from a breeding colony in the Wellcome Trust/Cancer Research U.K.
168 Gurdon Institute, Cambridge, U.K. They had been euthanized via tricaine overdose followed by
169 cooling, as part of another study. The otic capsules of one male and one female specimen were cut

170 out and placed in 4% buffered formaldehyde solution within two hours of euthanasia. They were
171 then sent to the University of Groningen where they were processed as the *Rana* specimens. A
172 micro-CT scan was made of the head of another male specimen at the University of Cambridge, and
173 the head was then dissected under light microscopy. The remaining three specimens, two females
174 and a male, were also dissected.

175 Animal care and euthanasia procedures conformed to local and national regulations and were
176 approved by the appropriate institutional Animal Care and Use Committees.

177 **Histological procedures**

178 After fixation the *Rana* and *Xenopus* specimens were rinsed in distilled water, refreshed several
179 times. All subsequent steps were performed on a rolling bank to keep the specimens moving in the
180 experimental solutions. Decalcification took place in a 10% EDTA solution (Sigma, ED5SS, pH 7.34) at
181 a temperature of 50°C in a microwave oven (T/T MEGA microwave histo-processor, Milestone), in
182 four sessions of twelve hours. After decalcification the specimens were rinsed again in distilled water
183 and dehydrated in a graded, seven-step ethanol series (30%, 50%, 70%, 90%, 96%, 100%, 100%)
184 where each step took one hour and solutions were refreshed three times. If necessary, specimens
185 were stored overnight in 70% ethanol. Next, specimens were placed in a 100% ethanol/
186 hydroxypropyl methacrylate (HPMA) solution (50:50) for 4-8 hours and then put in pure HPMA
187 solution for 24-48 hours. The specimens were then embedded in pure HPMA solution with addition
188 of a plasticizer (around 25:1). The HPMA solution contained 45 ml HPMA, 5 ml ethylene glycol
189 monobutyl ether, 0.5 g benzoyl peroxide, 1.25 ml glycerol and 0.25 ml ethylene glycol
190 dimethacrylate. The plasticizer consisted of 1 ml n,n-dimethylaniline and 10 ml polyethylene glycol
191 400.

192 The *Eleutherodactylus* sections were prepared using a faster procedure owing to time constraints.
193 The decalcification was performed in only two steps of 7 and 12 hours and the ethanol dehydration
194 series was also slightly altered (30% for 30 minutes, three times; 70% for 30 minutes, three times;

195 90% for 10 minutes, three times; 96% for 10 minutes, three times and 100% for 15 minutes, twice).

196 The specimens were placed in the ethanol/HPMA solution for two sessions of 1 hour, then
197 overnight.

198 After polymerization, transverse sections of 4 μm thickness were cut using a motorized microtome
199 (HM350S, Microm, Heidelberg, Germany). In some cases, the otoconial mass of the saccule, if
200 identified during the sectioning procedure, was removed from the embedded specimen using a fine
201 needle so as to avoid damaging the microtome. A subset of sections was stained with toluidine blue
202 1% (10 min) and contrast-stained with basic fuchsin (15-20 s).

203 **3-D reconstruction from serial sections**

204 Digital photographs of *Rana* and *Xenopus* sections were made with an Olympus Camedia C-5050
205 digital camera and stored as tiff files. Digital photographs of the smaller *Eleutherodactylus*
206 specimens were made using a Leica DM RXA microscope fitted with a Colorview 1 MP camera (Soft
207 Imaging System), working with AnalySiS software (Olympus). Individual files, in some cases reduced
208 in size by cropping and/or conversion to greyscale, were then loaded into ImageJ 1.45s (W. Rasband,
209 2011, National Institutes of Health) and autoregistered using the StackReg plug-in (P. Thévenaz,
210 2011, Biomedical Imaging Group, Swiss Federal Institute of Technology, Lausanne; see Thévenaz et
211 al., 1998). StackReg uses a recursive procedure based on rigid-body translation and rotation to align
212 each consecutive section. WinSurf 4.0 (S. Lozanoff & D. Moody, 2001) was then used to construct
213 three-dimensional images, following visual identification of relevant structures. Where wall
214 thickness was significant, the internal rather than external walls of the otic and periotic labyrinths
215 were traced and modelled. The choice of interval between sections used to make the final
216 reconstruction depended upon the size of the structure being reconstructed and the level of detail
217 required. In the production of Fig. 12, MicroView 2.1.2 (GE Healthcare, 2006) was used to reorient
218 the registered image stacks.

219 One potential problem with 3D reconstruction from serial sections is systematic misalignment of the
220 sections, resulting in a distorted (skewed or twisted) representation, and it can also be difficult to
221 determine orientation. *Eleutherodactylus* was small enough that a whole head could be sectioned
222 and reconstructions from right and left ears compared. In the case of *Rana* and *Xenopus*, the
223 reconstructions from serial sections were compared with micro-CT reconstructions of the whole
224 skull and the ear regions within it (see below). Although soft tissue could not be visualized in our CT
225 scans, hard-tissue structures including otic capsule walls and stapes shaft provided sufficient
226 landmarks for comparison with the serial section reconstructions.

227 Photomicrographs and reconstructions were laterally inverted where necessary, to facilitate
228 comparison.

229 **Micro-CT reconstructions**

230 Micro-CT images were obtained of the head of one male *Xenopus* specimen at the University of
231 Cambridge. The posterior part of the head was skinned and tissues between the mandibles were
232 removed. The head was then wrapped in cellophane to reduce the rate of drying, and the head was
233 scanned using a Metris X-Tek HMX 160 micro-CT scanner operating at 50 kV and 50 μ A with no
234 prefilter. The stepping rotational angle was 0.5 degrees. The software used in the processing of the
235 scan data included iXS Integrated X-ray System Control version 4.1.29 (X-Tek Systems Ltd., 2002),
236 NGI CT Control version 1.5.4 (X-Tek Systems Ltd., 2005) and CT-Pro 2.0 (Metris, 2008). At UCLA, a
237 micro-CT scan was made of the head of one male *Rana pipiens* specimen, immersed in a buffered
238 salt solution within a sample holder. A desktop micro-CT machine was used (MicroCT 40; Scanco
239 Medical, Bassersdorf, Switzerland), operating at 55 kV and 145 μ A with a 0.5 mm Al prefilter. The
240 stepping rotational angle was 0.36 degrees. The image was processed using Scanco proprietary
241 software. For both animals, the voxels in the scan images were of 30 μ m side length.

242 VGStudio Max 2.0.1 (Volume Graphics GmbH, 2008), MicroView 2.1.2 and WinSurf 4.0 were used to
243 construct 3D images from the CT data obtained. The CT reconstructions were used to verify that the

244 reconstructions made from serial sections of *Rana* and *Xenopus* were not distorted, and to
245 determine their orientation relative to the skull.

246

247 Results

248 WinSurf reconstructions of the inner ears of the three anuran species are presented for comparison
249 in Fig. 2. There was no evidence of systematic distortion of the reconstructions made from serial
250 sections, as determined by comparison between different ears and/or comparison with micro-CT
251 reconstructions. Histological artefacts inevitably affected the reconstructions, however, as described
252 below.

253 *Rana pipiens*

254 Reconstructions of the inner ear of *Rana* are shown in Figs. 2 and 3, and photomicrographs of
255 sections of particular interest are presented as Figs. 4 and 5.

256 Considering first the otic labyrinth, the saccule is partially divided by a central constriction into
257 inferior and superior compartments (Fig. 3). The **inferior saccule** is an ovoid chamber, flattened
258 rostromedially. The saccular macula (sensory epithelium) is at the centre of the flattened surface.
259 The **superior saccule** has an expanded dorsal chamber and four relatively small, posterior
260 diverticula:

- 261 1) The prominent **amphibian recess** (Figs. 3, 4A, B, 5B) extends medially from the dorsomedial
262 part of the superior saccule before turning caudally. The sensory epithelium on its dorsal wall is
263 known as the **amphibian papilla**, although this term is sometimes used to refer to the whole
264 chamber and its contents.
- 265 2) The **lagenar recess** (Figs. 3, 4A) extends medially from the caudoventral part of the superior
266 saccule, below the amphibian recess. Its sensory epithelium covers its medial wall.

1
2
3
4
5
6
7
8
9
10
11
12
13
14
15
16
17
18
19
20
21
22
23
24
25
26
27
28
29
30
31
32
33
34
35
36
37
38
39
40
41
42
43
44
45
46
47
48
49
50
51
52
53
54
55
56
57
58
59
60
61
62
63
64
65

267 3) A third small diverticulum, the only one to lack a sensory end-organ, extends caudally from the
268 dorsolateral part of the superior saccule (Fig. 3). The thick epithelium forming the internal lining
269 of this diverticulum is known as the **tegmentum vasculosum** (Figs. 4A, 5D). This lining extends
270 rostrally into the posterior part of the superior saccular chamber.

271 4) The **basilar recess** (Figs. 3, 4A, 5A) is located between the cavity of the tegmentum vasculosum
272 and the lagenar recess. Its sensory epithelium (**basilar papilla**) lies on its medial wall.

273 Rostral to the amphibian recess, the superior saccule communicates via a constricted region, the
274 utriculo-saccular foramen, with the elongated **utricular chamber**. The sensory epithelium of the
275 utricle is on the ventral wall of the free, rostral portion of this chamber, which then divides to form
276 the ampullae of the anterior and lateral **semicircular canals** (Fig. 2). From the caudal end of the
277 utricular chamber arise the other end of the lateral semicircular canal and the **crus commune**, a
278 short, vertical segment representing the convergence of the anterior and posterior semicircular
279 canals (Fig. 3). The ampulla of the posterior semicircular canal is located just underneath the caudal-
280 most part of the lateral semicircular canal; the two are not in contact.

281 We turn now to the periotic system, which may be divided (after Lombard, 1977) into periotic tissue
282 and the periotic labyrinth proper. **Periotic tissue** is the connective tissue found separating both otic
283 and periotic labyrinths from the walls of the otic capsule. In places, it takes the form of condensed
284 and cartilage-like 'limbic tissue' (Wever, 1973). Limbic tissue forms a thin layer around the
285 membranes of the semi-circular canals and utriculus, but it is much thicker around the amphibian
286 and basilar recesses (Figs. 5A, B). The lagenar recess and part of the tegmentum vasculosum are also
287 supported by limbic tissue. Elsewhere, the periotic tissue consists of little more than a diffuse
288 collection of fibres within a fluid space. The semicircular canals, within their thin shells of limbic
289 tissue, are separated from the otic capsule walls by such a fluid space, as is much of the superior
290 saccule (Figs. 4A, B).

1
2
3
4
5
6
7
8
9
10
11
12
13
14
15
16
17
18
19
20
21
22
23
24
25
26
27
28
29
30
31
32
33
34
35
36
37
38
39
40
41
42
43
44
45
46
47
48
49
50
51
52
53
54
55
56
57
58
59
60
61
62
63
64
65

291 The other component of the periotic system, the **periotic labyrinth**, is a membranous sac of complex
292 shape containing apparently acellular fluid. Its three main subdivisions are the periotic cistern, the
293 periotic canal and the periotic sac. The capacious **periotic cistern** (Figs. 3, 4A, B) almost completely
294 surrounds the inferior sacculle, extending around it on the medial side as far dorsally as the utricular
295 chamber. A diverticulum of the lateral part of the periotic cistern extends through a narrow, oval-
296 shaped foramen in the wall of the otic capsule and turns sharply rostrally to expand into a **lateral**
297 **chamber** (Figs. 2-4). The cartilaginous **operculum** lies immediately over the foramen (Figs. 4A, B),
298 while the **stapes footplate** is rostral to this. The footplate comprises the expanded medial part of the
299 bony *pars media* and, around its periphery, the U-shaped, cartilaginous *pars interna*. The operculum
300 and stapes footplate interlock: a flange of the *pars interna* extends a short distance medial to the
301 operculum, while the rostromedial corner of the operculum fills the gap between the *pars interna*
302 and a ventral process of the *pars media* which articulates with the otic capsule.

303 The **periotic canal** is a long, narrow tube which ascends dorsally from the lateral part of the periotic
304 cistern and wraps closely around the anterior aspect of the superior sacculle (Figs. 2, 3). There is a
305 thin, shared membrane between periotic and otic labyrinths throughout this course. The periotic
306 canal then parts from the sacculle near the *crus commune*, turns sharply caudolaterally and bends
307 down around the lateral semicircular canal to meet the superior sacculle again between the
308 amphibian recess and the diverticulum of the tegmentum vasculosum. The oval region of apposition
309 found here between otic and periotic labyrinths is the **contact membrane of the sacculle** (Figs. 3,
310 5C), identified in all three specimens of *Rana pipiens* just lateral to the contact membrane of the
311 amphibian recess. The contact membrane of the sacculle has 33-76% (n=3 ears) of the area of the
312 contact membrane of the amphibian recess and it is more than twice as thick, but it still represents a
313 relatively thin window between otic and periotic labyrinths, in a region where much of the otic
314 system is surrounded by thick limbic tissue.

1
2
3
4
5
6
7
8
9
10
11
12
13
14
15
16
17
18
19
20
21
22
23
24
25
26
27
28
29
30
31
32
33
34
35
36
37
38
39
40
41
42
43
44
45
46
47
48
49
50
51
52
53
54
55
56
57
58
59
60
61
62
63
64
65

315 The periotic canal then turns ventromedially to form an elongated, curved contact membrane with
316 the lateral wall of the amphibian recess (Fig. 5B). Leaving the otic capsule, the canal runs for a short
317 distance parallel to the *recessus partis basilaris*, a blind-ending periotic diverticulum heading
318 rostrally towards the basilar recess (Figs. 3, 5A). There is a small contact membrane between the
319 apposed tips of the *recessus partis basilaris* and the basilar recess (Fig. 5A), which is 6-14% (n=3 ears)
320 of the area of the contact membrane of the amphibian recess. The sections of the three *Rana*
321 specimens stopped at this point, so the relationship between the *recessus partis basilaris* and the
322 rest of the periotic system could not be examined. From the literature (see e.g. Lewis and Narins,
323 1999), the *recessus partis basilaris* and the periotic canal are expected to communicate with each
324 other via the **periotic sac**, a caudal expansion of the periotic canal which projects out of the otic
325 capsule.

326

327 *Eleutherodactylus limbatus*

328 Reconstructions of the inner ear of *Eleutherodactylus* are shown in Figs. 2 and 6, and
329 photomicrographs of sections of particular interest are presented as Figs. 7-9.

330 There is no distinct lateral chamber in *Eleutherodactylus* but the footplate and operculum lie at an
331 angle to each other such that their inner surfaces form a bowl-like concavity. The stapes footplate is
332 relatively small; as in *Rana*, it sends a prominent cartilaginous flange under the large operculum. The
333 inferior saccule/periotic cistern region had evidently collapsed to a greater or lesser extent in all four
334 ears examined because it had pulled away from surrounding structures, but its original shape could
335 be determined as the region enclosed between otic capsule, stapes and operculum. The other parts
336 of the inner ear escaped distortion in at least one specimen.

337 Given the size of the chamber in which it is contained, the inferior saccule must be relatively much
338 smaller than that of *Rana* or *Xenopus*, while the semicircular canals are much wider relative to their

1
2
3
4
5
6
7
8
9
10
11
12
13
14
15
16
17
18
19
20
21
22
23
24
25
26
27
28
29
30
31
32
33
34
35
36
37
38
39
40
41
42
43
44
45
46
47
48
49
50
51
52
53
54
55
56
57
58
59
60
61
62
63
64
65

339 length (Fig. 2). A narrow diverticulum lined with a tegmentum vasculosum extends from the saccular
340 cavity just dorsolateral to the basilar recess (Figs. 6, 7A, B, 8A, C).

341 The periotic canal (Fig. 6) is relatively longer and more convoluted than in *Rana*. Because the
342 superior saccule is little inflated in *Eleutherodactylus*, the canal, where it emerges from the periotic
343 cistern, is initially not in such close contact with the saccular cavity. However, after turning caudally
344 a diverticulum of the central part of the periotic canal extends downwards and comes into intimate
345 apposition with the superior saccular cavity (Figs. 6, 7B). As in *Rana*, the periotic canal then
346 separates from the otic labyrinth and runs across the lateral semicircular canal en route to the
347 amphibian recess. The contact membrane of the saccule (Figs. 6, 8B) is located just rostral to the
348 contact membrane of the amphibian recess (Figs. 6, 7A, 8A). The contact membrane of the saccule
349 has 26-41% (n=3 ears) of the area of the contact membrane of the amphibian recess. The contact
350 membrane of the basilar recess is around 5-15% (n=4 ears) of the area of the amphibian recess
351 contact membrane.

352 The *recessus partis basilaris* of the periotic labyrinth (Fig. 6) originates from the periotic sac, which
353 extends out of the otic capsule and into the brain-case. In the whole-head sections which were made
354 from one *Eleutherodactylus* specimen, the periotic sac appears to extend underneath the brain to
355 meet and freely communicate with its contralateral counterpart (Fig. 9). A second fluid space just
356 below this periotic space extends between right and left round windows. The two fluid spaces are
357 separated by a membrane which may be meningeal in origin. It was unclear whether this membrane
358 had simply separated from the basicranial bones due to shrinkage, or whether it really does separate
359 two fluid compartments *in vivo*. The membrane was everted into both the periotic sac and the
360 *recessus partis basilaris* in all four ears examined, perhaps due to shrinkage of the periotic system.

361

362 *Xenopus laevis*

1
2 363 Reconstructions of the inner ear of *Xenopus* are shown in Figs. 2 and 10, and photomicrographs of
3
4 364 sections of particular interest are presented as Figs. 8D and 11.

5
6
7
8 365 In the sectioned female *Xenopus* specimen, the anterior semicircular canal was damaged, there was
9
10 366 a bubble in the saccular region and the sections did not include the lateral passage or stapes. In the
11
12 367 male specimen, the utricular and lagenar cavities had collapsed, as judged from a comparison of
13
14 368 shapes between the two specimens and the fact that these structures had pulled away from the otic
15
16 369 capsule walls. The periotic cistern had pulled away from the otic capsule wall in both specimens.
17
18
19 370 Despite these shrinkage artefacts, the essential features of the inner ear remained intact in at least
20
21 371 one of the two specimens, permitting the following description.

22
23
24
25 372 The saccular chamber is relatively large and shifted dorsally compared to that of *Rana* (Fig. 2); it is
26
27 373 not divided into superior and inferior compartments. The anterior and especially the lateral
28
29 374 semicircular canals are elongated rostro-caudally; the posterior canal is shorter. The amphibian
30
31 375 recess projects as a diverticulum from the caudomedial end of the sacculle, and ventral to this
32
33 376 extends a second diverticulum which divides into the basilar recess laterally and the prominent
34
35 377 lagenar recess medially (Fig. 10). No special subcavity of the saccular chamber containing a
36
37 378 tegmentum vasculosum could be found.

38
39
40
41
42
43 379 The periotic cistern completely enwraps the sacculle (Fig. 10) and is interposed between this and the
44
45 380 basilar recess, giving rise to a 'tympanal area' rostralateral to the basilar recess (Figs. 8D, 11; see
46
47 381 Discussion). The relatively short, sickle-shaped periotic canal runs very close to the dorsal part of the
48
49 382 periotic cistern, but the two remain separate (Fig. 2). Although the periotic canal is also close to the
50
51 383 dorsal wall of the saccular cavity, the two are not in such close apposition as in *Rana* and
52
53 384 *Eleutherodactylus* and there is no distinct contact membrane of the sacculle. The periotic canal forms
54
55 385 a small contact membrane with the amphibian recess before turning caudally and expanding into
56
57
58
59
60
61
62
63
64
65

1
2 386 the periotic sac, which forms a second contact membrane directly with the basilar recess (Figs. 10,
3 387 11). The periotic sac then extends out of the otic cavity.

4
5 388 No trace of an operculum was identified in *Xenopus*. The stapes footplate caps the end of a tubular
6
7 389 passage projecting laterally from the otic capsule (Figs. 2, 11). The contents of this passage had
8
9
10 390 picked up a pale blue stain in the histological sections, suggesting that a precipitate had formed
11
12 391 there. The periotic cistern was not similarly stained and was clearly separated from the stapes
13
14 392 footplate by whatever was in this lateral passage. In gross dissection of frogs of both sexes, the
15
16 393 lateral passage was found to be filled with a clear, colourless fluid. A very thin membrane was seen
17
18 394 at the medial end of the passage, separating its contents from the periotic cistern. The lateral end
19
20 395 was sealed by the tough membrane of the oval window.
21
22
23
24

25 396 Although the reconstructions made from the male and female *Xenopus* specimens were generally
26
27 397 very similar, the female's inner ear apparatus, particularly the saccular chamber, was more
28
29 398 elongated rostro-caudally. The contact membrane of the amphibian recess was just over twice the
30
31 399 area of the contact membrane of the basilar recess in the female, whereas in the male the contact
32
33 400 membrane of the basilar recess was 1.5 times the area of that of the amphibian recess.
34
35
36
37

38 401

41 402 **Discussion**

43 403 **Wever's diagram**

44
45 404 Wever's (1973) schematic section through the ear of a leopard frog (Fig. 1A) has been widely
46
47 405 reproduced in the literature. Although presented as a "frontal section", Wever did not claim that his
48
49 406 diagram was based on a single, histological section and he may have amalgamated several slides in
50
51 407 its construction. In order to address this possibility, MicroView software was used to reorient a stack
52
53 408 of registered *Rana* section photomicrographs and section it in a new plane, thus revealing a 'virtual
54
55 409 section' through the inner ear. The orientation was chosen such that the 'virtual section' (Fig. 12A)
56
57
58
59
60
61
62
63
64
65

1
2
3
4
5
6
7
8
9
10
11
12
13
14
15
16
17
18
19
20
21
22
23
24
25
26
27
28
29
30
31
32
33
34
35
36
37
38
39
40
41
42
43
44
45
46
47
48
49
50
51
52
53
54
55
56
57
58
59
60
61
62
63
64
65

410 was as close to Wever's illustration as possible, the main criteria being that the section should show
411 both amphibian and basilar recesses as well as the lateral chamber of the inner ear. Falling
412 somewhere between frontal and transverse planes, its orientation is best described as oblique (Fig.
413 12C).

414 Assuming that our original section photomicrographs were well-aligned, which by comparison with
415 CT scan data appeared to be the case, our 'virtual section' shows Wever's schematic figure to be
416 anatomically inaccurate in several respects. The orientation of the stapes footplate in our 'virtual
417 section' differs substantially, revealing the process of the stapes *pars media* which articulates with
418 the otic capsule (marked with an asterisk in Fig. 12B). It is easy to visualise the stapes footplate
419 rocking about this process, as has been shown to be the case in ranid frogs (Jørgensen and
420 Kanneworff, 1998; Mason and Narins, 2002; Werner, 2003), rather than acting as a piston as
421 Wever's diagram might imply. Our 'virtual section' also passes through all three semicircular canals,
422 but only touches the periphery of the operculum. It does not include the contact membrane of the
423 sacculle.

424 Wever's figure therefore appears not to represent a single, real section through the ear, but it is
425 useful in diagrammatically illustrating the likely pathways for acoustic energy flow from the stapes to
426 the amphibian and basilar papillae, and thence to the round window. Acoustic energy is also thought
427 to be able to pass from periotic cistern to round window via the periotic canal, bypassing the otic
428 labyrinth and auditory papillae entirely (Purgue and Narins, 2000a, b). That portion of the periotic
429 canal which ascends from the periotic cistern is visible in both our 'virtual section' (Fig. 12B) and
430 Wever's diagram (Fig. 1B), but Wever (1973, 1985) made surprisingly little mention of the canal in
431 his otherwise detailed descriptions of frog inner ears.

432 Of the other schematic illustrations of the frog inner ear which exist in the literature, that of
433 Frishkopf & Goldstein (1963) may be the best-known. More obviously diagrammatic than Wever's

1
2 434 illustration, this older representation shows the periotic and semicircular canals, and it represents
3 435 the extrastapes more accurately.
4

5 436 *The ears of Eleutherodactylus and Xenopus*

6
7 437 The inner ear of *Eleutherodactylus limbatus* was found generally to resemble that of *Rana*, but there
8
9
10 438 were some pronounced differences in terms of the relative sizes and shapes of the various
11
12 439 structures. These differences were not highlighted by Wever (1985), who examined three other
13
14 440 *Eleutherodactylus* species. The very small saccule and the relatively short, wide semicircular canals
15
16
17 441 (Fig. 2) closely resemble reconstructions of the inner ear in 'stage 8' *Rana temporaria* tadpoles (30
18
19 442 mm long, just before emergence of hindlimbs) made by Birkmann (1940). *E. limbatus* has direct
20
21 443 development which omits a tadpole stage, but our frogs had been vocalizing in life and were
22
23 444 therefore believed to be reproductively mature. The inner ear of this species may therefore be
24
25
26 445 paedomorphic.
27

28
29
30 446 The inner ear of *Xenopus laevis* has been described, among others, by Paterson (1949, 1960), Wever
31
32 447 (1985) and Bever et al. (2003). Our reconstructions of *Xenopus* ears largely agree with their
33
34 448 descriptions. The saccular cavity contains a dense otoconial mass (very obvious in the CT scans)
35
36
37 449 which, relative to the rest of the inner ear, is much larger and more dorsally positioned than its
38
39 450 equivalent in *Rana* and *Eleutherodactylus*. The size and position of the saccular cavity in *Xenopus*
40
41 451 gives its inner ear a striking morphological similarity to that of the fish *Gobius niger*, as illustrated by
42
43 452 Retzius (1881). The possible functional convergence between these two aquatic species remains to
44
45
46 453 be explored.
47

48
49
50 454 The association of the basilar papilla with the lagenar recess in urodeles, caecilians and amniotes has
51
52 455 been said to be the "single most influential piece of evidence supporting a [basilar papilla] homology
53
54 456 among all terrestrial vertebrates", but the separate opening of the basilar recess into the saccule in
55
56
57 457 frogs was seen as a complication to this theory (Smotherman and Narins, 2004). We have found that
58
59
60
61
62
63
64
65

1
2 458 the basilar and lagenar recesses are in fact conjoined in *Xenopus* (Fig. 10), suggesting that this
3
4 459 represents the primitive condition for all lissamphibians and perhaps tetrapods in general.

5
6 460 At the caudal end of the basilar recess, periotic contact occurs via the periotic sac directly in
7
8 461 *Xenopus*, rather than via a *recessus partis basilaris*. Rostrally, the recess is separated from the
9
10 462 periotic cistern by a thin “tympal area”, discussed later. These features have been previously
11
12 463 described by Paterson (1949, 1960).

13
14
15
16 464 In *Xenopus*, the periotic cistern is separated from the stapes footplate by the fluid contained within a
17
18 465 tubular extension of the otic capsule (Fig. 11). A shorter separation between stapes and cistern is
19
20 466 shown in Wever’s (1985) diagrams of the ear of this frog, but Wever found a much longer, fluid-filled
21
22 467 “lateral passage” in the related species *Pipa pipa*. In both our histological slides of *Xenopus* and
23
24 468 Wever’s slides of *Pipa* it looked like a precipitate had formed within this lateral passage, but not in
25
26 469 the periotic labyrinth. Paterson (1960) found only a short lateral passage in her immature specimen
27
28 470 of *Pipa* which she refers to as a “fossa fenestrae ovalis”, filled with “delicate connective tissue”; she
29
30 471 did not describe anything similar in *Xenopus*. Perhaps the separation between footplate and periotic
31
32 472 labyrinth increases in pipids as the skull grows, such that it is less obvious in younger specimens. The
33
34 473 lateral chamber of *Rana* differs from the lateral passage of *Xenopus* because the rapid lateral
35
36 474 chamber has a narrower connection with the main otic capsule, it bends sharply rostrally to reach
37
38 475 the stapes footplate and it is filled with a diverticulum of the periotic cistern. The rapid lateral
39
40 476 chamber is also in contact with the operculum, an element lacking in *Xenopus*.

41
42
43
44
45
46
47 477 The otic labyrinth in the female *Xenopus* was around 1.5 times the linear dimensions of that of the
48
49 478 male. The saccular cavity was more elongated in the female and there was a difference in the
50
51 479 relative sizes of the contact membranes of the amphibian and basilar recesses, noted earlier. Further
52
53 480 investigation of a larger number of specimens is needed in order to establish whether these inner
54
55 481 ear differences represent sexual dimorphism, which has been observed in the middle ear of this
56
57 482 species (Mason et al., 2009).
58
59
60
61

483

484 **The blind branch of the periotic canal**

485 The discrete “blind branch” of the periotic canal which Purgue & Narins (2000b) found in the bullfrog
486 *Rana catesbeiana* could not be identified in the *Rana* or *Eleutherodactylus* specimens examined
487 here. However, the membranous wall of the periotic canal as it curves around the superior sacculle
488 was particularly thin in *Rana pipiens*, and in some slides it appeared to be ruptured. An apparent
489 short diverticulum found in the female *Xenopus* specimen only (Fig. 10) might also have been the
490 result of periotic canal rupture. Purgue & Narins injected silicone into the periotic labyrinth of their
491 frogs to make casts: it is possible that they experienced a similar problem.

492

493 **The contact membranes**

494 Harrison (1902) referred to three ‘tympanal areas’ in the frog inner ear where otic and periotic
495 labyrinths are in particularly close apposition. One of these is the extensive, membranous division
496 between periotic cistern and sacculle, while the other two ‘tympanal areas’ are now more generally
497 known as the ‘contact membranes’ of the amphibian and basilar recesses. To these three may be
498 added the contact membrane of the sacculle and an additional ‘tympanal area’ in *Xenopus*, discussed
499 later.

500 Sound energy from stapedial vibrations is widely presumed to enter the otic labyrinth through the
501 first ‘tympanal area’ between periotic cistern and sacculle (the membrane surrounding the inferior
502 saccular chamber, labelled IS in Fig. 4, forms part of this). The division between the periotic and otic
503 systems remains very thin where the periotic canal wraps around the anterior wall of the superior
504 sacculle; a special, ventral diverticulum of the canal makes additional contact with the superior
505 sacculle in *Eleutherodactylus* (Figs. 6, 7B).

1
2
3
4
5
6
7
8
9
10
11
12
13
14
15
16
17
18
19
20
21
22
23
24
25
26
27
28
29
30
31
32
33
34
35
36
37
38
39
40
41
42
43
44
45
46
47
48
49
50
51
52
53
54
55
56
57
58
59
60
61
62
63
64
65

506 In both *Rana* and *Eleutherodactylus*, the periotic canal separates from the saccule but returns to
507 meet the otic labyrinth at three contact membranes within the otherwise thickened limbic tissue at
508 the posterior end of the otic capsule. The contact membranes of the amphibian and basilar recesses
509 represent pathways through which sound energy can travel from the otic labyrinth back into the
510 periotic system, via the auditory epithelia of the amphibian and basilar papillae (Purgue and Narins,
511 2000a, b). Although not considered by Purgue & Narins, Wever (1973) showed in his diagram a third
512 contact membrane located between the two papillae, marked only with a tiny arrow (Fig. 1A). Wever
513 wrote that “this thin area acts as a bypass and allows some fraction of the fluid motion to go directly
514 into the perilymphatic duct [= periotic canal] without being detected”. This membrane between
515 superior saccule and periotic canal was described in *Rana catesbeiana* by Lewis (1976), who referred
516 to it as the “contact membrane of the saccule”. Lewis & Narins (1999) state that it is found in “the
517 more derived anurans”, referring this statement to Lewis (1984); Lewis & Narins may have meant
518 Lewis’ 1976 publication.

519 The contact membrane of the saccule was identified in this study in both *Rana* (Figs. 3, 5C) and
520 *Eleutherodactylus* (Figs. 6, 8B), located close to the contact membrane of the amphibian recess.
521 Although it appears to be thicker than the other two contact membranes, it might indeed represent
522 a second route by which sound energy could bypass the amphibian and basilar papillae, additional to
523 the periotic canal route described by Purgue & Narins (2000a, b). The frequency-dependent
524 impedance of such a bypass, and hence its functional significance, remains to be determined. The
525 so-called ‘round window’ within the metotic fissure, which may not be homologous with the round
526 window of other tetrapods (Henson, 1974), represents a point of pressure release for all these
527 routes (Wever, 1985).

528 As well as the usual contact membrane at the posterior end of the basilar recess, *Xenopus* has an
529 additional ‘tympanal area’ between the rostralateral wall of this recess and a posterior extension of
530 the periotic cistern (Paterson, 1949, 1960). Of the frogs studied here only *Xenopus* has this

1 531 'tympanal area' (Figs. 8D, 11) because its basilar and lagenar recesses both arise from the same
2 532 caudoventral diverticulum of the saccular cavity (Fig. 10; see earlier), and part of the periotic cistern
3
4 533 has come to occupy the space between this diverticulum and the saccule proper. Elsewhere, the
5
6 534 membranous walls of the basilar recess are enclosed within thick limbic tissue (Fig. 8D). In principle,
7
8
9 535 acoustic energy might flow from periotic cistern through this 'tympanal area' directly into the basilar
10
11 536 recess, exiting at the posterior end of the recess via the contact membrane formed here with the
12
13 537 periotic sac. This short and direct pathway through the basilar recess was represented
14
15 538 diagrammatically by Wever (1985).
16
17
18

19 539 **The tegmentum vasculosum**

20
21
22 540 'Tegmentum vasculosum', literally meaning 'vascular covering', is a term most often used to
23
24 541 describe the well-vascularized, thickened wall of the cochlear duct in birds and crocodylians.
25
26 542 Separating the scala media from the scala vestibuli, this archosaur tegmentum vasculosum is
27
28 543 believed to combine the roles of the stria vascularis and Reissner's membrane in mammals (Baird,
29
30 544 1974; Lewis et al., 1985; Hossler et al., 2002). The same term has long been used in the German
31
32 545 anatomical literature to describe the thickened layer of epithelial cells found in the superior saccule
33
34 546 of certain frogs (e.g. Deiters, 1862; Hasse, 1868; Kuhn, 1880; Retzius, 1881; Gaupp, 1904; Birkmann,
35
36 547 1940; Hagmann and Giebel, 1978). Retzius (1881) described a tegmentum vasculosum in *Bufo*, *Hyla*
37
38 548 and *Pelobates* but found it to be very poorly-developed in *Alytes*; it is not found in *Ascaphus* or
39
40 549 *Liopelma* (Wagner, 1934), nor in pipids including *Xenopus* (Paterson, 1960; this study). Although
41
42 550 lacking in some 'archaeobatrachians', the tegmentum vasculosum has apparently been identified in
43
44 551 all neobatrachian ears in which it has been sought. It is not found in urodeles (Birkmann, 1940).
45
46
47
48
49
50

51 552 Retzius (1881) produced several illustrations of the otic labyrinth of *Rana esculenta*, which were
52
53 553 redrawn and modified by Gaupp (1904). Retzius and Gaupp both labelled the whole of the superior
54
55 554 saccular wall as the tegmentum vasculosum, as did Birkmann (1940) in his reconstructions of the otic
56
57 555 labyrinth of *Rana temporaria*. Several illustrations from Gaupp and Birkmann were redrawn by
58
59
60
61
62
63
64
65

1
2
3
4
5
6
7
8
9
10
11
12
13
14
15
16
17
18
19
20
21
22
23
24
25
26
27
28
29
30
31
32
33
34
35
36
37
38
39
40
41
42
43
44
45
46
47
48
49
50
51
52
53
54
55
56
57
58
59
60
61
62
63
64
65

556 Wever (1985) in *The Amphibian Ear*, but in each case the region originally labelled as tegmentum
557 vasculosum was relabelled as part of the sacculle. In the present study, the tegmentum vasculosum
558 was readily identifiable in *Rana* and *Eleutherodactylus* as a thickened epithelium lining an otherwise
559 unoccupied diverticulum of the saccular chamber. However, the extent of its vascularization could
560 not be ascertained and, as Gaupp (1904) noted, its rostral borders are indistinct in *Rana*. A
561 tegmentum vasculosum was not found in *Xenopus*.

562 Wever (1985) made only one, brief mention of the anuran tegmentum vasculosum in his book
563 (p.78), in which he commented on the mistake of “early anatomists” in assigning to it a sensory
564 function. Nevertheless, the unusual epithelium suggests a functional distinction from the rest of the
565 superior saccular chamber. Haggmann & Giebel (1978), working on *Rana temporaria*, confirmed that
566 this region is richly vascularized and found high levels of metabolic enzymatic activity. This supports
567 the contention that the tegmentum vasculosum in frogs is responsible for the secretion of
568 endolymph, like the tegmentum of archosaurs and the stria vascularis of mammals. Subsequent
569 studies of endolymph secretion in frogs, however, have focused on the dark cells located in the
570 utricle and semicircular canal ampullae (Burnham and Stirling, 1984; Bernard et al., 1986); the
571 anuran tegmentum vasculosum has fallen into obscurity.

572

573 **The apparent interaural fluid connection in *Eleutherodactylus***

574 Of the frogs examined, sections through the whole head were only available for one specimen of
575 *Eleutherodactylus*. Although our interpretation may have been affected by shrinkage, these sections
576 appeared to show the left and right periotic sacs converging to form a fluid space immediately
577 beneath the brain (Fig. 9). Wever (1978) showed that vibrations applied to the operculum of one ear
578 in a salamander can excite the contralateral ear: his proposed mechanism involved a similar
579 intracranial pathway below the brain, but he believed that the two periotic sacs in his species
580 communicated only indirectly, via the cerebrospinal fluid. Harrison (1902) challenged the notion of

1 581 earlier authors that amphibians possess a connection between the periotic system and a “subdural
2 582 space”.

3
4
5 583 Such a fluid system extending between the two ears via the cranial cavity might be functionally
6
7 584 significant in (1) communicating vibrations from the cerebrospinal fluid to the inner ears, (2)
8
9 585 acoustically coupling the two ears, which might affect sound localization, or (3) providing increased
10
11 586 possibilities for pressure release from the inner ear, affecting sensitivity. Further work is clearly
12
13 587 needed to confirm the presence of an interaural fluid connection in *Eleutherodactylus* and other
14
15 588 frogs, so as to assess whether this condition is widespread among anurans.
16
17
18
19
20

21 589

22 23 24 590 **Conclusion**

25
26 591 The anuran inner ear is a complex, three-dimensional structure consisting of the intertwined canals
27
28 592 of the periotic and otic labyrinths. Although his representation appears not to be anatomically
29
30 593 accurate, Wever’s (1973) diagram of the leopard frog inner ear does an admirable job of clearly
31
32 594 illustrating some of the possible routes of acoustic energy flow from stapes to round window. Its
33
34 595 main shortcoming in this respect is that it does not label the periotic canal, which represents
35
36 596 another potential route. Although some anatomical differences were identified, the inner ear of
37
38 597 *Eleutherodactylus* is broadly similar to that of *Rana*, so Wever’s diagram is clearly representative of a
39
40 598 wider range of neobatrachian frogs. The illustration is less useful in describing the ear of *Xenopus*; to
41
42 599 what extent this reflects the ‘archaeobatrachian’ status of *Xenopus* or its aquatic habits remains to
43
44 600 be determined.
45
46
47
48
49

50
51 601 The tegmentum vasculosum and the contact membrane of the saccule, found here in *Rana* and
52
53 602 *Eleutherodactylus* but not *Xenopus*, have been neglected in the recent literature and deserve further
54
55 603 attention from auditory physiologists. The intriguing possibility of a fluid pathway extending
56
57 604 between right and left ears also demands investigation.
58
59
60
61
62
63
64
65

605

Acknowledgements

606

607

608 The authors wish to thank Emanuel Mora for his help and support with this project. Dave Simpson
609 kindly provided the *Xenopus* specimens. The CT scan of *Xenopus* was made by Alan Heaver of the
610 University of Cambridge Department of Engineering, with thanks going also to Norman Fleck for the
611 use of his equipment. The authors are very grateful to Dolores Bozovic, Alan D. Grinnell, Tammy
612 Hoang, Victoria Sandoval and Felix E. Schweizer for facilitating the *Rana* CT scan, which was made by
613 Ting-Ling Chang at the UCLA School of Dentistry, Division of Advanced Prosthodontics. Stephan
614 Kamrad helped with translations. The research of JMS and PvD was supported by the Heinsius
615 Houbolt Foundation and is part of the research program *Healthy Ageing and Communication* of the
616 Department of Otorhinolaryngology at the University Medical Center Groningen. Finally, the authors
617 wish to thank the reviewers and editors of the manuscript for their very helpful comments.

618

619

Conflicts of interest

620

621

622 The authors declare that they have no conflicts of interest.

623

References

624

625

- 626 Baird IL (1974) Anatomical features of the inner ear in submammalian vertebrates. In: Handbook of
627 Sensory Physiology, volume V/1: Auditory System (Keidel WD, Neff WD, eds), pp 159-212.
628 Berlin: Springer-Verlag.
629 Bernard C, Ferrary E, Sterkers O (1986) Production of endolymph in the semicircular canal of the frog
630 *Rana esculenta*. *Journal of Physiology* 371:17-28.

- 631 Bever MM, Jean YY, Fekete DM (2003) Three-dimensional morphology of inner ear development in
 1 632 *Xenopus laevis*. *Developmental Dynamics* 227:422–430.
- 2 633 Birkmann K (1940) Morphologisch-anatomische Untersuchungen zur Entwicklung des häutigen
 3 634 Labyrinthes der Amphibien. *Zeitschrift für Anatomie und Entwicklungsgeschichte* 110:443-
 4 635 488.
- 5 636 Blood DC, Studdert VP (1999) *Saunders Comprehensive Veterinary Dictionary, 2nd Edition.*
 6 637 Edinburgh: W.B. Saunders.
- 7 638 Burnham JA, Stirling CE (1984) Quantitative localization of Na-K pump site in frog inner ear dark cells.
 8 639 *Hearing Research* 13:261-268.
- 9 640 Deiters O (1862) Ueber das innere Gehörorgan der Amphibien. *Archiv für Anatomie, Physiologie und*
 10 641 *Wissenschaftliche Medizin* 1862:262-275, 277-310.
- 11 642 Dubois A (2007) Naming taxa from cladograms: a cautionary tale. *Molecular Phylogenetics and*
 12 643 *Evolution* 42:317-330.
- 13 644 Duellman WE, Trueb L (1986) *Biology of Amphibians*. Baltimore: The Johns Hopkins University Press.
- 14 645 Fay RR, Popper AN (1985) The octavolateralis system. In: *Functional Vertebrate Morphology*
 15 646 (Hildebrand M, Bramble DM, Liem KF, Wake DB, eds), pp 291-316. London: Belknap Press.
- 16 647 Frishkopf LS, Goldstein MH (1963) Responses to acoustic stimuli from single units in the eighth nerve
 17 648 of the bullfrog. *Journal of the Acoustical Society of America* 35:1219-1228.
- 18 649 Gaupp E (1904) A. Ecker's und R. Wiedersheim's Anatomie des Frosches, part 3, 2nd Edition.
 19 650 Braunschweig: Druck und Verlag von Friedrich Vieweg und Sohn.
- 20 651 Gridi-Papp M, Narins PM (2010) Seismic detection and communication in amphibians. In: *The Use of*
 21 652 *Vibrations in Communication: Properties, Mechanisms and Function across Taxa* (O'Connell-
 22 653 Rodwell CE, ed), pp 69-83. Kerala: Research Signpost.
- 23 654 Hagmann B, Giebel W (1978) Enzymhistochemische Untersuchungen am Innenohr des Frosches
 24 655 (*Rana temporaria*). *Archives of Oto-Rhino-Laryngology* 220:89-103.
- 25 656 Harrison HS (1902) On the perilymphatic spaces of the amphibian ear. *Internationale Monatsschrift*
 26 657 *für Anatomie und Physiologie* 19:221-261.
- 27 658 Hasse C (1868) *Das Gehörorgan der Frösche*, Reprinted from *Zeitschrift für wissenschaftliche*
 28 659 *Zoologie*, Bd. 18 Edition. Leipzig: Verlag von Wilhelm Engelmann.
- 29 660 Henson OW (1974) Comparative anatomy of the middle ear. In: *Handbook of Sensory Physiology*,
 30 661 volume V/1: Auditory System (Keidel WD, Neff WD, eds), pp 39-110. Berlin: Springer-Verlag.
- 31 662 Hillis DM (2007) Constraints in naming parts of the Tree of Life. *Molecular Phylogenetics and*
 32 663 *Evolution* 42:331-338.
- 33 664 Hoegg S, Vences M, Brinkmann H, Meyer A (2004) Phylogeny and comparative substitution rates of
 34 665 frogs inferred from sequences of three nuclear genes. *Molecular Biology and Evolution*
 35 666 21:1188-1200.
- 36 667 Hossler FE, Olson KR, Musil G, McKamey MI (2002) Ultrastructure and blood supply of the
 37 668 tegmentum vasculosum in the cochlea of the duckling. *Hearing Research* 164:155-165.
- 38 669 Jørgensen MB, Kannevorff M (1998) Middle ear transmission in the grass frog, *Rana temporaria*.
 39 670 *Journal of Comparative Physiology A* 182:59-64.
- 40 671 Kuhn (1880) Ueber das häutige Labyrinth der Amphibien. *Archiv für Mikroskopische Anatomie*
 41 672 17:479-550.
- 42 673 Lewis ER (1976) Surface morphology of the bullfrog amphibian papilla. *Brain, Behavior and Evolution*
 43 674 13:196-215.
- 44 675 Lewis ER (1984) On the frog amphibian papilla. *Scanning Electron Microscopy* 1984 (IV):1899-1913.
- 45 676 Lewis ER, Narins PM (1999) The acoustic periphery of amphibians: anatomy and physiology. In:
 46 677 *Comparative Hearing: Fish and Amphibians* (Fay RR, Popper AN, eds), pp 101-154. New York:
 47 678 Springer.
- 48 679 Lewis ER, Leverenz EL, Bialek WS (1985) *The Vertebrate Inner Ear*. Boca Raton: CRC Press, Inc.
- 49 680 Lombard RE (1977) Comparative morphology of the inner ear in salamanders (*Caudata: Amphibia*).
 50 681 Basel: S. Karger.

682 Mason MJ, Narins PM (2002) Vibrometric studies of the middle ear of the bullfrog *Rana catesbeiana*
683 I. The extrastapes. *Journal of Experimental Biology* 205:3153-3165.

684 Mason MJ, Wang M, Narins PM (2009) Structure and function of the middle ear apparatus of the
685 aquatic frog, *Xenopus laevis*. *Proceedings of the Institute of Acoustics* 31:13-21.

686 Paterson NF (1949) The development of the inner ear of *Xenopus laevis*. *Proceedings of the*
687 *Zoological Society of London* 119:269–291.

688 Paterson NF (1960) The inner ear of some members of the Pipidae (Amphibia). *Proceedings of the*
689 *Zoological Society of London* 134:509-546.

690 Pauly GB, Hillis DM, Cannatella DC (2009) Taxonomic freedom and the role of official lists of species
691 names. *Herpetologica* 65:115–128.

692 Purgue AP, Narins PM (2000a) A model for energy flow in the inner ear of the bullfrog (*Rana*
693 *catesbeiana*). *Journal of Comparative Physiology A* 186: 489-495.

694 Purgue AP, Narins PM (2000b) Mechanics of the inner ear of the bullfrog (*Rana catesbeiana*): the
695 contact membranes and the periotic canal. *Journal of Comparative Physiology A* 186: 481-
696 488.

697 Retzius G (1881) Das Gehörorgan der Wirbelthiere. Morphologisch-Histologische Studien. I. Das
698 Gehörorgan der Fische und Amphibien. Stockholm: Samson & Wallin.

699 Simmons DD, Meenderink SWF, Vassilakis PN (2007) Anatomy, physiology, and function of auditory
700 end-organs in the frog inner ear. In: *Hearing and Sound Communication in Amphibians*
701 (Narins PM, Feng AS, Fay RR, Popper AN, eds), pp 184-220. New York: Springer.

702 Smotherman M, Narins P (2004) Evolution of the amphibian ear. In: *Evolution of the Vertebrate*
703 *Auditory System* (Manley GA, Popper AN, Fay RR, eds), pp 164-199. New York: Springer.

704 Thévenaz P, Ruttimann UE, Unser M (1998) A pyramid approach to subpixel registration based on
705 intensity. *IEEE Transactions on Image Processing* 7:27-41.

706 van Dijk P, Mason MJ, Schoffelen RLM, Narins PM, Meenderink SWF (2011) Mechanics of the frog
707 ear. *Hearing Research* 273:46-58.

708 Wagner DS (1934) The structure of the inner ear in relation to the reduction of the middle ear in the
709 Liopelmidae (Noble). *Anatomischer Anzeiger* 79:20-36.

710 Werner YL (2003) Mechanical leverage in the middle ear of the American bullfrog, *Rana catesbeiana*.
711 *Hearing Research* 175:54-65.

712 Wever EG (1973) The ear and hearing in the frog, *Rana pipiens*. *Journal of Morphology* 141:461-477.

713 Wever EG (1978) Sound transmission in the salamander ear. *Proceedings of the National Academy of*
714 *Sciences of the USA* 75:529-530.

715 Wever EG (1985) *The Amphibian Ear*. Princeton: Princeton University Press.

716

Figure Captions

717

718

Fig. 1

720 A: Ernest Glen Wever's schematic diagram of the peripheral auditory apparatus of a ranid frog. The

721 original caption is included. From: Wever, E.G. (1973) The ear and hearing in the frog, *Rana pipiens*.

722 *Journal of Morphology* 141(4): 461-477. Copyright © 1973 Wiley-Liss, Inc. B: A representation of the

723 same diagram with the colour-coding used elsewhere in this paper, to facilitate comparison between

724 figures. Where Wever's nomenclature differs from that used in the present paper, structures have

725 been relabelled. Additionally, based on the interpretations of the present study, new labels have

726 been introduced for structures that were not explicitly identified in Wever's original diagram,

727 including the contact membranes which separate otic and periotic labyrinths.

728 Colour code: white = otic labyrinth (endolymph); green = periotic labyrinth (perilymph); red =

729 sensory epithelium; dark grey = limbic tissue; cream = bone; yellow = cartilage.

730

Fig. 2

732 WinSurf reconstructions of the left inner ear structures of (left) *Xenopus laevis*, male specimen,

733 (middle) *Rana pipiens*, (right) *Eleutherodactylus limbatus*. Lateral views are shown in the top row,

734 dorsal views in the bottom row. *Eleutherodactylus* reconstructions are 2.5× enlarged relative to the

735 others. In the *Eleutherodactylus* sections used for these reconstructions, the periotic cistern in the

736 region marked with an asterisk, which lies lateral to the very small saccular cavity, had collapsed. Its

737 approximate shape has been restored here by comparison with the contralateral ear and the extent

738 of the space available for it within the otic capsule. Colour code: white = otic labyrinth (endolymph);

739 green = periotic labyrinth (perilymph); red = sensory epithelium; semitranslucent grey = internal

740 walls of the otic capsule.

1
2
3
4
5
6
7
8
9
10
11
12
13
14
15
16
17
18
19
20
21
22
23
24
25
26
27
28
29
30
31
32
33
34
35
36
37
38
39
40
41
42
43
44
45
46
47
48
49
50
51
52
53
54
55
56
57
58
59
60
61
62
63
64
65

741 Key to this and subsequent figures: AR = amphibian recess (endolymph); AS = anterior semicircular
742 canal; B = brain; BR = basilar recess (endolymph); CA = contact membrane of amphibian recess; CB =
743 contact membrane of basilar recess; CC = *crus commune* (confluence of anterior and posterior
744 semicircular canals); CS = contact membrane of saccule; IS = inferior saccular chamber; LC = lateral
745 chamber; LP = lateral passage; LR = lagenar recess (endolymph); LS = lateral semicircular canal; LT =
746 limbic tissue; O = operculum; PC = periotic canal; POC = periotic cistern; POS = periotic sac; PS =
747 posterior semicircular canal; PT = periotic tissue; PU = posterior utricular cavity; RPB = *recessus partis*
748 *basilaris* (perilymph); RW = round window; S = saccule; SPI = stapes *pars interna*; SPM = stapes *pars*
749 *media*; SS = superior saccular chamber; TV = tegmentum vasculosum, or the saccular diverticulum
750 within which this epithelial lining is found; VIII = branch of eighth cranial nerve.

751

752 Fig. 3

753 WinSurf reconstructions of left inner ear structures of *Rana pipiens*, seen from an approximately
754 posterior view. The reconstruction on the left shows the otic labyrinth (white), sensory epithelia
755 (red) and contact membranes separating endo- and perilymph (purple). Part of the posterior
756 semicircular canal has been removed to reveal the diverticula of the superior saccule. The
757 reconstruction on the right shows the same, with the periotic labyrinth added in (semitranslucent
758 green). Scale bar 2.5 mm. See Fig. 2 caption for full list of abbreviations.

759

760 Fig. 4

761 Composite photomicrographs of two approximately transverse sections through the posterior part
762 of the inner ear of *Rana pipiens*. Section B is in a plane 240 μm anterior to Section A. Relative to the
763 centre of each photomicrograph, dorsal is upwards and slightly away from the viewer, lateral is to

1
2 764 the left. Scale bar applies to both A and B and represents 1 mm. See Fig. 2 caption for full list of
3 abbreviations.

4
5 766

6
7
8
9 **Fig. 5**

10
11 768 Photomicrographs of sections through the inner ear of *Rana pipiens*. A: Basilar recess (BR;
12 endolymph), *recessus partis basilaris* (RPB; perilymph) and contact membrane of basilar recess (CB)
13 separating the two. B: Amphibian recess (AR) and its contact membrane (CA), expanded from Fig.
14 769 4A. C: Periotic canal (PC) and contact membrane of the sacculle (CS), expanded from Fig. 4B. D:
15
16 770 Tegmentum vasculosum (TV), expanded from Fig. 4A. All scale bars 200 μ m. See Fig. 2 caption for full
17
18 771 list of abbreviations.
19
20
21 772
22
23 773

24
25
26 774

27
28
29
30 **Fig. 6**

31
32 776 WinSurf reconstructions of left inner ear structures of *Eleutherodactylus limbatus*, seen from an
33
34 777 approximately lateral view. Part of the lateral semicircular canal has been removed to reveal the
35
36 778 contact membrane of the amphibian recess (CA) and the contact membrane of the sacculle (CS). The
37
38 779 reconstruction on the left shows the otic labyrinth and associated structures only; the reconstruction
39
40 780 on the right includes the dorsal and posterior parts (only) of the periotic labyrinth. The asterisk
41
42 781 indicates the ventral diverticulum of the central part of the periotic canal, which is closely apposed
43
44 782 to the superior saccular chamber (SS). Scale bar 0.5 mm. Colour code: white = otic labyrinth
45
46 783 (endolymph); semitranslucent green = periotic labyrinth (perilymph); red = sensory epithelium;
47
48 784 purple = contact membrane separating endo- and perilymph. See Fig. 2 caption for full list of
49
50 785 abbreviations.

51
52
53
54 786

787 **Fig. 7**

788 Composite photomicrographs of two sections through the inner ear of *Eleutherodactylus limbatus*.

789 Section A is in an approximately transverse plane, through the posterior part of the inner ear.

790 Relative to the centre of the photomicrograph, dorsal is upwards and slightly away from the viewer,

791 lateral is to the left. Section B is in an oblique plane (between transverse and sagittal), taken from

792 the ear on the contralateral side to Section A and laterally inverted to aid comparison. Relative to

793 the centre of the photomicrograph, dorsal is upwards, lateral is to the left and away from the

794 viewer. Note in particular the membrane marked with an asterisk, located between the ventral

795 diverticulum of the central part of the periotic canal (PC) and the superior saccular chamber (SS). The

796 membranous labyrinth has pulled away from the otic capsule wall on the right hand side. Scale bar

797 applies to both A and B and represents 200 μm . See Fig. 2 caption for full list of abbreviations.

798

799 **Fig. 8**

800 Photomicrographs of sections through the inner ears of *Eleutherodactylus limbatus* and *Xenopus*

801 *laevis*. A: Tegmentum vasculosum (TV), amphibian recess (AR) and its contact membrane (CA) in *E.*

802 *limbatus*, scale bar 100 μm . B: Periotic canal (PC) and the contact membrane of the sacculle (CS) in *E.*

803 *limbatus*, scale bar 100 μm . C: Tegmentum vasculosum of *E. limbatus*, scale bar 50 μm . D: Basilar

804 recess (BR) of *X. laevis* (female specimen), scale bar 200 μm . The asterisk indicates the additional

805 'tympanal area' identified by Paterson (1949, 1960), located just rostralateral to the basilar recess

806 (see text). See Fig. 2 caption for full list of abbreviations.

807

808 **Fig. 9**

809 Photomicrograph of a transverse section through the head of *Eleutherodactylus limbatus*, at the

810 level of the posterior half of the otic capsule. The three fluid compartments collectively denoted '1'

1
2
3
4
5
6
7
8
9
10
11
12
13
14
15
16
17
18
19
20
21
22
23
24
25
26
27
28
29
30
31
32
33
34
35
36
37
38
39
40
41
42
43
44
45
46
47
48
49
50
51
52
53
54
55
56
57
58
59
60
61
62
63
64
65

811 appear to be separate in this section, but inspection of other sections in the same series suggests
812 that they are actually part of one continuous fluid system extending between the periotic labyrinths
813 of each ear and passing underneath the brain (B). The left-hand arrow marked '1' points to the left
814 periotic sac, which can be seen emerging from the left otic capsule. Within the capsule, it is
815 immediately adjacent to the amphibian recess (AR), from which it is separated by a thin contact
816 membrane. Between fluid space 1 and the base of the skull is a second fluid space (2), which is also
817 continuous across the head and extends between the two round windows (RW). Distortion resulting
818 from shrinkage may have changed the relative sizes of fluid spaces 1 and 2. Scale bar 0.5 mm. See
819 Fig. 2 caption for full list of abbreviations.

820
821 **Fig. 10**

822 WinSurf reconstructions of left inner ear structures of *Xenopus laevis* (female specimen), seen from
823 an approximately caudoventral view. Part of the posterior semicircular canal has been removed to
824 reveal the diverticula of the saccule. The reconstruction on the left shows the otic labyrinth and
825 associated structures only; the reconstruction on the right includes all but the most rostralateral
826 part of the periotic labyrinth too. The anterior semicircular canal had been obliterated in the slides
827 used to make this reconstruction and the saccular cavity was distorted owing to the presence of a
828 bubble. The presumed original shape of the saccule (S) has been restored here. The asterisk
829 indicates a short, blind branch of the periotic canal (see text). Scale bar 1.5 mm. Colour code: white =
830 otic labyrinth (endolymph); semitranslucent green = periotic labyrinth (perilymph); red = sensory
831 epithelium; purple = contact membrane separating endo- and perilymph. See Fig. 2 caption for full
832 list of abbreviations.

834 **Fig. 11**

835 Photomicrograph of an oblique section through the inner ear of *Xenopus laevis* (male specimen).

836 Note that the periotic cistern (POC), the contents of which have picked up only a small amount of

837 stain, is separated from the stapes footplate (SPI and SPM) by the lateral passage (LP), which is filled

838 with diffuse material staining pale blue. The contact membrane of the basilar recess is the thin

839 membrane between the basilar recess (BR) and the periotic sac (POS); the membrane marked with

840 an asterisk between the basilar recess and the periotic cistern (POC) is Paterson's (1949, 1960)

841 additional 'tympanal area' (see text). Relative to the centre of the picture, dorsal is upwards and

842 away from the viewer, lateral is to the left and towards the viewer. Scale bar 1 mm. See Fig. 2

843 caption for full list of abbreviations.

844

845 **Fig. 12**

846 Reconstructions created from a stack of serial section images of the ear of *Rana pipiens*, digitally

847 resectioned in a plane as close as possible to Wever's 1973 illustration (Fig. 1). See text for details.

848 The extrastapes, tympanic membrane, periotic sac and round window were not within the original

849 sections and are consequently not shown in these reconstructions. A: 'Virtual section'; the faint,

850 diagonal striations indicate the planes of the original section photomicrographs from which this was

851 reconstructed. B: Expanded, diagrammatic illustration of the same. Out of the plane of this particular

852 section, the periotic canal is in communication with the periotic fluid which abuts the contact

853 membranes of the amphibian and basilar recesses; these regions are all components of the periotic

854 labyrinth and are hence shaded in green. The asterisk indicates a process of the stapes *pars media*

855 which articulates with the otic capsule. C: WinSurf reconstructions of the right inner ear of *R. pipiens*

856 from (left) lateral, (middle) posterior and (right) dorsal views, showing the position of the 'virtual

857 section' as a grey plane. The stapes and operculum are included in these reconstructions but the

858 internal walls of the otic capsule are not. Both scale bars 2 mm. Colour code: white = otic labyrinth

859 (endolymph); green = periotic labyrinth (perilymph); dark grey = limbic tissue; lighter grey = looser

- 1
- 2
- 3
- 4
- 5
- 6
- 7
- 8
- 9
- 10
- 11
- 12
- 13
- 14
- 15
- 16
- 17
- 18
- 19
- 20
- 21
- 22
- 23
- 24
- 25
- 26
- 27
- 28
- 29
- 30
- 31
- 32
- 33
- 34
- 35
- 36
- 37
- 38
- 39
- 40
- 41
- 42
- 43
- 44
- 45
- 46
- 47
- 48
- 49
- 50
- 51
- 52
- 53
- 54
- 55
- 56
- 57
- 58
- 59
- 60
- 61
- 62
- 63
- 64
- 65

860 periotic tissue; cream = bone; yellow = cartilage.

861

1
2
3
4
5
6
7
8
9
10
11
12
13
14
15
16
17
18
19
20
21
22
23
24
25
26
27
28
29
30
31
32
33
34
35
36
37
38
39
40
41
42
43
44
45
46
47
48
49
50
51
52
53
54
55
56
57
58
59
60
61
62
63
64
65

1
2
3
4
5
6
7
8
9
10
11
12
13
14
15
16
17
18
19
20
21
22
23
24
25
26
27
28
29
30
31
32
33
34
35
36
37
38
39
40
41
42
43
44
45
46
47
48
49
50
51
52
53
54
55
56
57
58
59
60
61
62
63
64
65

The frog inner ear: picture perfect?

Matthew J. Mason¹

Johannes M. Segenhout²

Ariadna Cobo-Cuan³

Patricia M. Quiñones⁴

Pim van Dijk^{2,5}

¹ University of Cambridge

Department of Physiology, Development & Neuroscience

Downing Street

Cambridge CB2 3EG

U.K.

Tel. +44 1223 333829

Fax +44 1223 333840

mjm68@cam.ac.uk

² University of Groningen

University Medical Center Groningen

Department of Otorhinolaryngology, Head & Neck Surgery

P.O. Box 30.001

9700 RB Groningen

The Netherlands

jmsegenhout@hotmail.com

p.van.dijk@umcg.nl

1
2
3
4
5
6
7
8
9
10
11
12
13
14
15
16
17
18
19
20
21
22
23
24
25
26
27
28
29
30
31
32
33
34
35
36
37
38
39
40
41
42
43
44
45
46
47
48
49
50
51
52
53
54
55
56
57
58
59
60
61
62
63
64
65

27 ³ Department of Animal and Human Biology
28 Havana University
29 Street 25 No. 455
30 Havana CP 10400
31 Cuba
32 cobo_cuan@fbio.uh.cu
33
34 ⁴ Department of Physics and Astronomy
35 1-129 Knudsen Hall, 475 Portola Plaza
36 University of California Los Angeles
37 Los Angeles, CA 90095
38 U.S.A.
39 yukiq@ucla.edu
40
41 ⁵ University of Groningen
42 Graduate School of Medical Sciences, Research School of Behavioral and Cognitive Neurosciences
43 P.O. Box 196
44 9700 AD Groningen
45 The Netherlands
46 p.van.dijk@umcg.nl

Abstract

47
48 Many recent accounts of the frog peripheral auditory system have reproduced Wever's (1973)
49 schematic cross-section of the ear of a leopard frog. We sought to investigate to what extent this
50 diagram is an accurate and representative depiction of the anuran inner ear, using three-
51 dimensional reconstructions made from serial sections of *Rana pipiens*, *Eleutherodactylus limbatus*
52 and *Xenopus laevis*.

53 In *Rana*, three discrete contact membranes were found to separate the posterior otic (=
54 endolymphatic) labyrinth from the periotic (= perilymphatic) system: those of the amphibian and
55 basilar recesses and the contact membrane of the saccule. The amphibian 'tegmentum vasculosum'
56 was distinguishable as a thickened epithelial lining within a posterior recess of the superior saccular
57 chamber. These features were also identified in *Eleutherodactylus*, but in this tiny frog the relative
58 proportions of the semicircular canals and saccule resemble those of ranid tadpoles. There appeared
59 to be a complete fluid pathway between the right and left periotic labyrinths in this species, crossing
60 the cranial cavity. *Xenopus* lacks a tegmentum vasculosum and a contact membrane of the saccule;
61 the *Xenopus* ear is further distinguished by a lateral passage separating stapes from periotic cistern
62 and a more direct connection between periotic cistern and basilar recess. The basilar and lagenar
63 recesses are conjoined in this species.

64 Wever's diagram of the inner ear of *Rana* retains its value for diagrammatic purposes but it is not
65 anatomically accurate, nor representative of all frogs. Although Wever identified the contact
66 membrane of the saccule, most recent studies of frog inner ear anatomy have overlooked both this
67 and the amphibian tegmentum vasculosum. These structures deserve further attention.

Keywords

70 Inner ear; frog; amphibian papilla; basilar papilla; tegmentum vasculosum; contact membrane

71

Introduction

72
73 The inner ear structures of ranid frogs have been the subject of detailed anatomical accounts dating
74 back over 150 years, many of which were written in German (see e.g. Deiters, 1862; Hasse, 1868;
75 Retzius, 1881; Gaupp, 1904). Among the best known of the English-language descriptions are those
76 of Ernest Glen Wever. The first figure from Wever's 1973 paper in *Journal of Morphology*
77 (reproduced here as Fig. 1A) shows "A schematic representation of the ear and labyrinth of *Rana*
78 *pipiens*, in frontal section". An almost identical diagram appeared in two of Wever's later
79 publications including his 1985 book *The Amphibian Ear*, which remains the most comprehensive
80 account of the subject. It has been reproduced, sometimes in a modified form, in **high-profile** review
81 papers (e.g. **Fay and Popper, 1985; Lewis and Narins, 1999; Simmons et al., 2007; Gridi-Papp and**
82 **Narins, 2010**), a leading text-book on amphibian biology (**Duellman and Trueb, 1986**) and several
83 other articles. **As such, it** must be the world's most widely-consulted scientific illustration of an
84 amphibian peripheral auditory system. However, as explained below, there is some uncertainty as to
85 the species depicted, the orientation and the accuracy of this important diagram.

The species examined

86
87 The taxonomy of the North American ranid frogs is currently in a state of flux (Dubois, 2007; Hillis,
88 2007; Pauly et al., 2009). Some authors place leopard frogs in the genus *Lithobates*, but following
89 Hillis' (2007) recommendation, we retain the genus *Rana* for North American ranids.

90 Wever (1973) stated that his illustration shows the ear of *Rana pipiens*, but in his 1985 book he
91 distinguished between this species (the northern leopard frog) and the very similar "*Rana utricularia*
92 *sphenocephala*", now *R. sphenocephala utricularia* (the southern leopard frog). Wever (1985) did not
93 make it clear which of these species is represented in the figure of interest to us here, **which appears**
94 **in slightly modified form as his Fig. 3-17**. However, another illustration also reproduced from his
95 1973 paper (Fig. 3-79 in Wever, 1985) is **clearly** labelled as *R. sphenocephala*. Wever's 1973 paper

1
2
3
4
5
6
7
8
9
10
11
12
13
14
15
16
17
18
19
20
21
22
23
24
25
26
27
28
29
30
31
32
33
34
35
36
37
38
39
40
41
42
43
44
45
46
47
48
49
50
51
52
53
54
55
56
57
58
59
60
61
62
63
64
65

96 may therefore describe the ear of the southern leopard frog, but it is likely that the ears of these two
97 species are practically identical. The articles that have reproduced Wever's illustration have often
98 implied that a generalized anuran morphology is represented (Table 1).

99 **The orientation of Wever's illustration**

100 Within his 1973 paper, Wever stated that he sectioned his specimens in "a horizontal plane (dorsal
101 to ventral)...frontally (anterior to posterior) or laterally (right to medial, then continued from medial
102 to left)". This description is somewhat confusing, and perhaps for this reason Wever later redefined
103 the three planes. In Wever's (1985) figure 3-34, a frontal plane is clearly shown dividing the head
104 into dorsal and ventral components. Such a plane would pass through most of the teeth on both left
105 and right maxillae and may be considered horizontal. A sagittal plane vertically divides the head into
106 left and right components. A transverse plane is a vertical plane perpendicular to the frontal and
107 sagittal planes, which divides the head into anterior and posterior components. These definitions
108 agree with the standard veterinary anatomical nomenclature (Blood and Studdert, 1999) and are
109 those used in the present study. In our interpretation, "horizontal" (Wever, 1973) is actually frontal,
110 "lateral" (Wever, 1973) is actually sagittal and "frontal" (Wever, 1973) is actually transverse.

111 The present study focuses on the first figure from Wever (1973), the caption of which reads "the ear
112 and labyrinth...in frontal section" (Fig. 1A). Was this in fact a transverse section, according to
113 standard nomenclature?

114 **The accuracy of Wever's illustration**

115 When preparing a previous article (van Dijk et al., 2011), two of the current authors had reason to
116 question the accuracy of Wever's 1973 diagram. Wever shows the extrastapes (= extracolumella) as
117 a very short extension of the bony stapes shaft (*stapes pars media*), connecting it to the centre of
118 the tympanic membrane (Fig. 1). It would be natural to assume that this apparatus must operate as
119 a stiff piston, an inflection of the tympanic membrane driving the stapes directly into the inner ear.
120 In reality, the extrastapes is much longer than this and has an angled articulation with the *pars*

121 *media*: the stapes/extrastapes system works as a flexible, first-order lever (Jørgensen and
122 Kanneworff, 1998; Mason and Narins, 2002; Werner, 2003).

123 Turning to the inner ear, Wever shows three pathways for “fluid flow” to pass between the stapes
124 on the right of his diagram to the periotic (= perilymphatic) sac on the left, one via the amphibian
125 papilla, a second via the basilar papilla and a third between the two papillae, each being indicated by
126 arrows in Fig. 1A. The endolymph within the otic (= endolymphatic) labyrinth in frogs is separated
127 from the perilymph within the periotic labyrinth by so-called ‘contact membranes’ (Fig. 1B), so fluid
128 cannot actually flow between the two systems and the three arrows should instead be taken to
129 indicate three pathways of acoustic energy flow. In their more recent account of energy flow
130 pathways through the ear of the bullfrog (*Rana catesbeiana*), Purgue & Narins (2000a, b) considered
131 the routes passing through the amphibian and basilar recesses but made no mention of Wever’s
132 middle pathway. Purgue & Narins regarded the periotic canal as an alternative route for low-
133 frequency energy flow which bypasses the otic system entirely, but this is not labelled in Wever’s
134 diagram and there is scant reference to it in his written descriptions. Four potential pathways for
135 sound energy flow between stapes and periotic sac in frogs have therefore been described in frogs,
136 but are all four consistently present?

137 In this study, histological sections were made from the inner ears of three species of frogs, including
138 leopard frogs (these were believed to be *Rana pipiens* rather than *R. sphenocephala*, but this could
139 not be confirmed beyond doubt by the suppliers). Photomicrographs and three-dimensional
140 reconstructions were used to assess the accuracy of Wever’s accounts and other recent descriptions
141 of ranid inner ear morphology.

142 While leopard frogs are in the family Ranidae, within the Ranoidea clade of the Neobatrachia,
143 *Eleutherodactylus limbatus* (Eleutherodactylidae) is placed within the other major neobatrachian
144 clade, the Hyloidea (Hoegg et al., 2004). *Xenopus laevis*, family Pipidae, is an aquatic
145 ‘archaeobatrachian’, the ‘Archaeobatrachia’ being a paraphyletic assemblage of frogs which

146 diverged before the Neobatrachia (Hoegg et al., 2004). In order to assess whether **Wever's diagram**
147 **the ranid ear** is representative of a more diverse range of frogs, the leopard frog ear was compared
148 here with the ears of *E. limbatus*, one of the world's smallest frogs, and with those of *X. laevis*.

150 **Materials and methods**

151 Twelve frogs from three different species were used in this study. Three leopard frogs believed to be
152 *Rana pipiens* (40-50 g body mass) were obtained from Charles D. Sullivan Co. Inc. (Nashville, TN,
153 U.S.A.) via Exoterra Schaudi GmbH, Holzheim, Germany. They were housed at the University of
154 Groningen laboratory animal facilities. The frogs were euthanized using the double pith procedure
155 and then decapitated. The lower jaw was removed and the remaining part of the head was divided
156 sagittally. ~~This resulted in two preparations, each containing one complete ear.~~ Skin was removed
157 and small holes were made in various places in the skull, away from the structures of interest, to
158 improve fluid impregnation. The ears were fixed by immersion in a 10% neutral buffered formalin
159 solution (pH 7.4) for at least 24 hours at 4°C. **The fresh corpse of a male *Rana pipiens*, originating**
160 **from Nasco (Fort Atkinson, WI, U.S.A.), was used for micro-computed tomography (micro-CT)**
161 **scanning, as described below.**

162 Two *Eleutherodactylus limbatus* specimens (each around 0.2 g body mass) were captured at Las
163 Terrazas, Artemisa province, Cuba. They were euthanized by double pithing and decapitation, the
164 palatal skin was removed and their heads were preserved in 10% formalin and sent to Groningen for
165 further processing. The head of one specimen was halved prior to sectioning, while the other was
166 sectioned whole.

167 Six *Xenopus laevis* specimens (males 55-60 g, females 120-220 g, all gonadectomized body masses)
168 were obtained as fresh corpses from a breeding colony in the Wellcome Trust/Cancer Research U.K.
169 Gurdon Institute, Cambridge, U.K. They had been euthanized via tricaine overdose followed by

170 cooling, as part of another study. The otic capsules of one male and one female specimen were cut
171 out and placed in 4% buffered formaldehyde solution within two hours of euthanasia. They were
172 then sent to the University of Groningen where they were processed as the *Rana* specimens. A
173 micro-CT scan was made of the head of another male specimen at the University of Cambridge, and
174 the head was then dissected under light microscopy. The remaining three specimens, two females
175 and a male, were also dissected.

176 Animal care and euthanasia procedures conformed to local and national regulations and were
177 approved by the appropriate institutional Animal Care and Use Committees.

178 **Histological procedures**

179 After fixation the *Rana* and *Xenopus* specimens were rinsed in distilled water, refreshed several
180 times. All subsequent steps were performed on a rolling bank to keep the specimens moving in the
181 experimental solutions. Decalcification took place in a 10% EDTA solution (Sigma, ED5SS, pH 7.34) at
182 a temperature of 50°C in a microwave oven (T/T MEGA microwave histo-processor, Milestone), in
183 four sessions of twelve hours. After decalcification the specimens were rinsed again in distilled water
184 and dehydrated in a graded, seven-step ethanol series (30%, 50%, 70%, 90%, 96%, 100%, 100%)
185 where each step took one hour and solutions were refreshed three times. If necessary, specimens
186 were stored overnight in 70% ethanol. Next, specimens were placed in a 100% ethanol/
187 hydroxypropyl methacrylate (HPMA) solution (50:50) for 4-8 hours and then put in pure HPMA
188 solution for 24-48 hours. The specimens were then embedded in pure HPMA solution with addition
189 of a plasticizer (around 25:1). The HPMA solution contained 45 ml HPMA, 5 ml ethylene glycol
190 monobutyl ether, 0.5 g benzoyl peroxide, 1.25 ml glycerol and 0.25 ml ethylene glycol
191 dimethacrylate. The plasticizer consisted of 1 ml n,n-dimethylaniline and 10 ml polyethylene glycol
192 400.

193 The *Eleutherodactylus* sections were prepared using a faster procedure owing to time constraints.
194 The decalcification was performed in only two steps of 7 and 12 hours and the ethanol dehydration

195 series was also slightly altered (30% for 30 minutes, three times; 70% for 30 minutes, three times;
196 90% for 10 minutes, three times; 96% for 10 minutes, three times and 100% for 15 minutes, twice).
197 The specimens were placed in the ethanol/HPMA solution for two sessions of 1 hour, then
198 overnight.

199 After polymerization, transverse sections of 4 μm thickness were cut using a motorized microtome
200 (HM350S, Microm, Heidelberg, Germany). In some cases, the otoconial mass of the saccule, if
201 identified during the sectioning procedure, was removed from the embedded specimen using a fine
202 needle so as to avoid damaging the microtome. A subset of sections was stained with toluidine blue
203 1% (10 min) and contrast-stained with basic fuchsin (15-20 s).

204 **3-D reconstruction from serial sections**

205 Digital photographs of *Rana* and *Xenopus* sections were made with an Olympus Camedia C-5050
206 digital camera and stored as tiff files. Digital photographs of the smaller *Eleutherodactylus*
207 specimens were made using a Leica DM RXA microscope fitted with a Colorview 1 MP camera (Soft
208 Imaging System), working with AnalySiS software (Olympus). Individual files, in some cases reduced
209 in size by cropping and/or conversion to greyscale, were then loaded into ImageJ 1.45s (W. Rasband,
210 2011, National Institutes of Health) and autoregistered using the StackReg plug-in (P. Thévenaz,
211 2011, Biomedical Imaging Group, Swiss Federal Institute of Technology, Lausanne; see Thévenaz et
212 al., 1998). StackReg uses a recursive procedure based on rigid-body translation and rotation to align
213 each consecutive section. WinSurf 4.0 (S. Lozanoff & D. Moody, 2001) was then used to construct
214 three-dimensional images, following visual identification of relevant structures. Where wall
215 thickness was significant, the internal rather than external walls of the otic and periotic labyrinths
216 were traced and modelled. The choice of interval between sections used to make the final
217 reconstruction depended upon the size of the structure being reconstructed and the level of detail
218 required. In the production of Fig. 12, MicroView 2.1.2 (GE Healthcare, 2006) was used to reorient
219 the registered image stacks.

220 One potential problem with 3D reconstruction from serial sections is systematic misalignment of the
221 sections, resulting in a distorted (skewed or twisted) representation, and it can also be difficult to
222 determine orientation. *Eleutherodactylus* was small enough that a whole head could be sectioned
223 and reconstructions from right and left ears compared. In the case of *Rana* and *Xenopus*, the
224 reconstructions from serial sections were compared with micro-CT reconstructions of the whole
225 skull and the ear regions within it (see below). Although soft tissue could not be visualized in our CT
226 scans, hard-tissue structures including otic capsule walls and stapes shaft provided sufficient
227 landmarks for comparison with the serial section reconstructions.

228 Photomicrographs and reconstructions were laterally inverted where necessary, to facilitate
229 comparison.

230 **Micro-CT reconstructions**

231 Micro-CT images were obtained of the head of one male *Xenopus* specimen at the University of
232 Cambridge. The posterior part of the head was skinned and tissues between the mandibles were
233 removed. The head was then wrapped in cellophane to reduce the rate of drying, and the head was
234 scanned using a Metris X-Tek HMX 160 micro-CT scanner operating at 50 kV and 50 μ A with no
235 prefilter. The stepping rotational angle was 0.5 degrees. The software used in the processing of the
236 scan data included iXS Integrated X-ray System Control version 4.1.29 (X-Tek Systems Ltd., 2002),
237 NGI CT Control version 1.5.4 (X-Tek Systems Ltd., 2005) and CT-Pro 2.0 (Metris, 2008). At UCLA, a
238 micro-CT scan was made of the head of one male *Rana pipiens* specimen, immersed in a buffered
239 salt solution within a sample holder. A desktop micro-CT machine was used (MicroCT 40; Scanco
240 Medical, Bassersdorf, Switzerland), operating at 55 kV and 145 μ A with a 0.5 mm Al prefilter. The
241 stepping rotational angle was 0.36 degrees. The image was processed using Scanco proprietary
242 software. For both animals, the voxels in the scan images were of 30 μ m side length.

243 VGStudio Max 2.0.1 (Volume Graphics GmbH, 2008), MicroView 2.1.2 and WinSurf 4.0 were used to
244 construct 3D images from the CT data obtained. The CT reconstructions were used to verify that the

245 reconstructions made from serial sections of *Rana* and *Xenopus* were not distorted, and to
246 determine their orientation relative to the skull.

247

248 Results

249 WinSurf reconstructions of the inner ears of the three anuran species are presented for comparison
250 in Fig. 2. There was no evidence of systematic distortion of the reconstructions made from serial
251 sections, as determined by comparison between different ears and/or comparison with micro-CT
252 reconstructions. Histological artefacts inevitably affected the reconstructions, however, as described
253 below.

254 *Rana pipiens*

255 Reconstructions of the inner ear of *Rana* are shown in Figs. 2 and 3, and photomicrographs of
256 sections of particular interest are presented as Figs. 4 and 5.

257 Considering first the otic labyrinth, the saccule is partially divided by a central constriction into
258 inferior and superior compartments (Fig. 3). The **inferior saccule** is an ovoid chamber, flattened
259 rostromedially. The saccular macula (sensory epithelium) is at the centre of the flattened surface.
260 The **superior saccule** has an expanded dorsal chamber and four relatively small, posterior
261 diverticula:

- 262 1) The prominent **amphibian recess** (Figs. 3, 4A, B, 5B) extends medially from the dorsomedial
263 part of the superior saccule before turning caudally. The sensory epithelium on its dorsal wall is
264 known as the **amphibian papilla**, although this term is sometimes used to refer to the whole
265 chamber and its contents.
- 266 2) The **lagenar recess** (Figs. 3, 4A) extends medially from the caudoventral part of the superior
267 saccule, below the amphibian recess. Its sensory epithelium covers its medial wall.

1
2
3
4
5
6
7
8
9
10
11
12
13
14
15
16
17
18
19
20
21
22
23
24
25
26
27
28
29
30
31
32
33
34
35
36
37
38
39
40
41
42
43
44
45
46
47
48
49
50
51
52
53
54
55
56
57
58
59
60
61
62
63
64
65

268 3) A third small diverticulum, the only one to lack a sensory end-organ, extends caudally from the
269 dorsolateral part of the superior saccule (Fig. 3). The thick epithelium forming the internal lining
270 of this diverticulum is known as the **tegmentum vasculosum** (Figs. 4A, 5D). This lining extends
271 rostrally into the posterior part of the superior saccular chamber.

272 4) The **basilar recess** (Figs. 3, 4A, 5A) is located between the cavity of the tegmentum vasculosum
273 and the lagenar recess. Its sensory epithelium (**basilar papilla**) lies on its medial wall.

274 Rostral to the amphibian recess, the superior saccule communicates via a constricted region, the
275 utriculo-saccular foramen, with the elongated **utricular chamber**. The sensory epithelium of the
276 utricle is on the ventral wall of the free, rostral portion of this chamber, which then divides to form
277 the ampullae of the anterior and lateral **semicircular canals** (Fig. 2). From the caudal end of the
278 utricular chamber arise the other end of the lateral semicircular canal and the **crus commune**, a
279 short, vertical segment representing the convergence of the anterior and posterior semicircular
280 canals (Fig. 3). The ampulla of the posterior semicircular canal is located just underneath the caudal-
281 most part of the lateral semicircular canal; the two are not in contact.

282 We turn now to the periotic system, which may be divided (after Lombard, 1977) into periotic tissue
283 and the periotic labyrinth proper. **Periotic tissue** is the connective tissue found separating both otic
284 and periotic labyrinths from the walls of the otic capsule. In places, it takes the form of condensed
285 and cartilage-like 'limbic tissue' (Wever, 1973). Limbic tissue forms a thin layer around the
286 membranes of the semi-circular canals and utriculus, but it is much thicker around the amphibian
287 and basilar recesses (Figs. 5A, B). The lagenar recess and part of the tegmentum vasculosum are also
288 supported by limbic tissue. Elsewhere, the periotic tissue consists of little more than a diffuse
289 collection of fibres within a fluid space. The semicircular canals, within their thin shells of limbic
290 tissue, are separated from the otic capsule walls by such a fluid space, as is much of the superior
291 saccule (Figs. 4A, B).

292 The other component of the periotic system, the **periotic labyrinth**, is a membranous sac of complex
1
2 293 shape containing apparently acellular fluid. Its three main subdivisions are the periotic cistern, the
3
4 294 periotic canal and the periotic sac. The capacious **periotic cistern** (Figs. 3, 4A, B) almost completely
5
6
7 295 surrounds the inferior sacculle, extending around it on the medial side as far dorsally as the utricular
8
9 296 chamber. A diverticulum of the lateral part of the periotic cistern extends through a narrow, oval-
10
11 297 shaped foramen in the wall of the otic capsule and turns sharply rostrally to expand into a **lateral**
12
13
14 298 **chamber** (Figs. 2-4). The cartilaginous **operculum** lies immediately over the foramen (Figs. 4A, B),
15
16 299 while the **stapes footplate** is rostral to this. The footplate comprises the expanded medial part of the
17
18
19 300 bony *pars media* and, around its periphery, the U-shaped, cartilaginous *pars interna*. The operculum
20
21 301 and stapes footplate interlock: a flange of the *pars interna* extends a short distance medial to the
22
23 302 operculum, while the rostromedial corner of the operculum fills the gap between the *pars interna*
24
25 303 and a ventral process of the *pars media* which articulates with the otic capsule.

29 304 The **periotic canal** is a long, narrow tube which ascends dorsally from the lateral part of the periotic
30
31 305 cistern and wraps closely around the anterior aspect of the superior sacculle (Figs. 2, 3). There is a
32
33 306 thin, shared membrane between periotic and otic labyrinths throughout this course. The periotic
34
35 307 canal then parts from the sacculle near the *crus commune*, turns sharply caudolaterally and bends
36
37 308 down around the lateral semicircular canal to meet the superior sacculle again between the
38
39 309 amphibian recess and the diverticulum of the tegmentum vasculosum. The oval region of apposition
40
41 310 found here between otic and periotic labyrinths is the **contact membrane of the sacculle** (Figs. 3,
42
43 311 5C), identified in all three specimens of *Rana pipiens* just lateral to the contact membrane of the
44
45 312 amphibian recess. The contact membrane of the sacculle has 33-76% (n=3 ears) of the area of the
46
47 313 contact membrane of the amphibian recess and it is more than twice as thick, but it still represents a
48
49 314 relatively thin window between otic and periotic labyrinths, in a region where much of the otic
50
51 315 system is surrounded by thick limbic tissue.

1
2
3
4
5
6
7
8
9
10
11
12
13
14
15
16
17
18
19
20
21
22
23
24
25
26
27
28
29
30
31
32
33
34
35
36
37
38
39
40
41
42
43
44
45
46
47
48
49
50
51
52
53
54
55
56
57
58
59
60
61
62
63
64
65

316 The periotic canal then turns ventromedially to form an elongated, curved contact membrane with
317 the lateral wall of the amphibian recess (Fig. 5B). Leaving the otic capsule, the canal runs for a short
318 distance parallel to the *recessus partis basilaris*, a blind-ending periotic diverticulum heading
319 rostrally towards the basilar recess (Figs. 3, 5A). There is a small contact membrane between the
320 apposed tips of the *recessus partis basilaris* and the basilar recess (Fig. 5A), which is 6-14% (n=3 ears)
321 of the area of the contact membrane of the amphibian recess. The sections of the three *Rana*
322 specimens stopped at this point, so the relationship between the *recessus partis basilaris* and the
323 rest of the periotic system could not be examined. From the literature (see e.g. Lewis and Narins,
324 1999), the *recessus partis basilaris* and the periotic canal are expected to communicate with each
325 other via the **periotic sac**, a caudal expansion of the periotic canal which projects out of the otic
326 capsule.

327

328 *Eleutherodactylus limbatus*

329 Reconstructions of the inner ear of *Eleutherodactylus* are shown in Figs. 2 and 6, and
330 photomicrographs of sections of particular interest are presented as Figs. 7-9.

331 There is no distinct lateral chamber in *Eleutherodactylus* but the footplate and operculum lie at an
332 angle to each other such that their inner surfaces form a bowl-like concavity. The stapes footplate is
333 relatively small; as in *Rana*, it sends a prominent cartilaginous flange under the large operculum. The
334 inferior saccule/periotic cistern region had evidently collapsed to a greater or lesser extent in all four
335 ears examined because it had pulled away from surrounding structures, but its original shape could
336 be determined as the region enclosed between otic capsule, stapes and operculum. The other parts
337 of the inner ear escaped distortion in at least one specimen.

338 Given the size of the chamber in which it is contained, the inferior saccule must be relatively much
339 smaller than that of *Rana* or *Xenopus*, while the semicircular canals are much wider relative to their

1
2 340 length (Fig. 2). A narrow diverticulum lined with a tegmentum vasculosum extends from the saccular
3 341 cavity just dorsolateral to the basilar recess (Figs. 6, 7A, B, 8A, C).

4
5 342 The periotic canal (Fig. 6) is relatively longer and more convoluted than in *Rana*. Because the
6
7 343 superior saccule is little inflated in *Eleutherodactylus*, the periotic canal, where it emerges from the
8
9 344 periotic cistern, is initially not in such close contact with the saccular cavity. However, after turning
10
11 345 caudally a diverticulum of the central part of the periotic canal extends downwards and comes into
12
13 346 intimate apposition with the superior saccular cavity (Figs. 6, 7B). As in *Rana*, the periotic canal then
14
15 347 separates from the otic labyrinth and runs across the lateral semicircular canal en route to the
16
17 348 amphibian recess. The contact membrane of the saccule (Figs. 6, 8B) is located just rostral to the
18
19 349 contact membrane of the amphibian recess (Figs. 6, 7A, 8A). The contact membrane of the saccule
20
21 350 has 26-41% (n=3 ears) of the area of the contact membrane of the amphibian recess. The contact
22
23 351 membrane of the basilar recess is around 5-15% (n=4 ears) of the area of the amphibian recess
24
25 352 contact membrane.

26
27
28
29
30
31
32 353 The *recessus partis basilaris* of the periotic labyrinth (Fig. 6) originates from the periotic sac, which
33
34 354 extends out of the otic capsule and into the brain-case. In the whole-head sections which were made
35
36 355 from one *Eleutherodactylus* specimen, the periotic sac appears to extend underneath the brain to
37
38 356 meet and freely communicate with its contralateral counterpart (Fig. 9). A second fluid space just
39
40 357 below this periotic space extends between right and left round windows. The two fluid spaces are
41
42 358 separated by a membrane which may be meningeal in origin. It was unclear whether this membrane
43
44 359 had simply separated from the basicranial bones due to shrinkage, or whether it really does separate
45
46 360 two fluid compartments *in vivo*. The membrane was everted into both the periotic sac and the
47
48 361 *recessus partis basilaris* in all four ears examined, perhaps due to shrinkage of the periotic system.

49
50
51
52
53
54 362

363 *Xenopus laevis*

1
2 364 Reconstructions of the inner ear of *Xenopus* are shown in Figs. 2 and 10, and photomicrographs of
3
4 365 sections of particular interest are presented as Figs. 8D and 11.

6
7
8 366 In the sectioned female *Xenopus* specimen, the anterior semicircular canal was damaged, there was
9
10 367 a bubble in the saccular region and the sections did not include the lateral passage or stapes. In the
11
12 368 male specimen, the utricular and lagenar cavities had collapsed, as judged from a comparison of
13
14 369 shapes between the two specimens and the fact that these structures had pulled away from the otic
15
16 370 capsule walls. The periotic cistern had pulled away from the otic capsule wall in both specimens.
17
18
19 371 Despite these shrinkage artefacts, the essential features of the inner ear remained intact in at least
20
21
22 372 one of the two specimens, permitting the following description.

23
24
25 373 The saccular chamber is relatively large and shifted dorsally compared to that of *Rana* (Fig. 2); it is
26
27 374 not divided into superior and inferior compartments. The anterior and especially the lateral
28
29 375 semicircular canals are elongated rostro-caudally; the posterior canal is shorter. The amphibian
30
31
32 376 recess projects as a diverticulum from the caudomedial end of the sacculle, and ventral to this
33
34 377 extends a second diverticulum which divides into the basilar recess laterally and the prominent
35
36 378 lagenar recess medially (Fig. 10). No special subcavity of the saccular chamber containing a
37
38
39 379 tegmentum vasculosum could be found.

40
41
42
43 380 The periotic cistern completely enwraps the sacculle (Fig. 10) and is interposed between this and the
44
45 381 basilar recess, giving rise to a 'tympanal area' rostralateral to the basilar recess (Figs. 8D, 11; see
46
47 382 Discussion). The relatively short, sickle-shaped periotic canal runs very close to the dorsal part of the
48
49
50 383 periotic cistern, but the two remain separate (Fig. 2). Although the periotic canal is also close to the
51
52 384 dorsal wall of the saccular cavity, the two are not in such close apposition as in *Rana* and
53
54 385 *Eleutherodactylus* and there is no distinct contact membrane of the sacculle. The periotic canal forms
55
56
57 386 a small contact membrane with the amphibian recess before turning caudally and expanding into
58
59
60
61
62
63
64
65

1
2 387 the periotic sac, which forms a second contact membrane directly with the basilar recess (Figs. 10,
3 388 11). The periotic sac then extends out of the otic cavity.

4
5 389 No trace of an operculum was identified in *Xenopus*. The stapes footplate caps the end of a tubular
6
7 390 passage projecting laterally from the otic capsule (Figs. 2, 11). The contents of this passage had
8
9 391 picked up a pale blue stain in the histological sections, suggesting that a precipitate had formed
10
11 392 there. The periotic cistern was not similarly stained and was clearly separated from the stapes
12
13 393 footplate by whatever was in this lateral passage. In gross dissection of frogs of both sexes, the
14
15 394 lateral passage was found to be filled with a clear, colourless fluid. A very thin membrane was seen
16
17 395 at the medial end of the passage, separating its contents from the periotic cistern. The lateral end
18
19 396 was sealed by the tough membrane of the oval window.

20
21
22 397 Although the reconstructions made from the male and female *Xenopus* specimens were generally
23
24 398 very similar, the female's inner ear apparatus, particularly the saccular chamber, was more
25
26 399 elongated rostro-caudally. The contact membrane of the amphibian recess was just over twice the
27
28 400 area of the contact membrane of the basilar recess in the female, whereas in the male the contact
29
30 401 membrane of the basilar recess was 1.5 times the area of that of the amphibian recess.

31
32
33
34
35
36
37
38 402

39 40 41 403 **Discussion**

42 43 44 404 **Wever's diagram**

45
46 405 Wever's (1973) schematic section through the ear of a leopard frog (Fig. 1A) has been widely
47
48 406 reproduced in the literature. Although presented as a "frontal section", Wever did not claim that his
49
50 407 diagram was based on a single, histological section and he may have amalgamated several slides in
51
52 408 its construction. In order to address this possibility, MicroView software was used to reorient a stack
53
54 409 of registered *Rana* section photomicrographs and section it in a new plane, thus revealing a 'virtual
55
56 410 section' through the inner ear. The orientation was chosen such that the 'virtual section' (Fig. 12A)

1
2
3
4
5
6
7
8
9
10
11
12
13
14
15
16
17
18
19
20
21
22
23
24
25
26
27
28
29
30
31
32
33
34
35
36
37
38
39
40
41
42
43
44
45
46
47
48
49
50
51
52
53
54
55
56
57
58
59
60
61
62
63
64
65

411 was as close to Wever's illustration as possible, the main criteria being that the section should show
412 both amphibian and basilar recesses as well as the lateral chamber of the inner ear. Falling
413 somewhere between frontal and transverse planes, its orientation is best described as oblique (Fig.
414 12C).

415 Assuming that our original section photomicrographs were well-aligned, which by comparison with
416 CT scan data appeared to be the case, our 'virtual section' shows Wever's schematic figure to be
417 anatomically inaccurate in several respects. The orientation of the stapes footplate in our 'virtual
418 section' differs substantially, revealing the process of the stapes *pars media* which articulates with
419 the otic capsule (marked with an asterisk in Fig. 12B). It is easy to visualise the stapes footplate
420 rocking about this process, as has been shown to be the case in ranid frogs (Jørgensen and
421 Kanneworff, 1998; Mason and Narins, 2002; Werner, 2003), rather than acting as a piston as
422 Wever's diagram might imply. Our 'virtual section' also passes through all three semicircular canals,
423 but only touches the periphery of the operculum. It does not include the contact membrane of the
424 sacculle.

425 Wever's figure therefore appears not to represent a single, real section through the ear, but it is
426 useful in diagrammatically illustrating the likely pathways for acoustic energy flow from the stapes to
427 the amphibian and basilar papillae, and thence to the round window. Acoustic energy is also thought
428 to be able to pass from periotic cistern to round window via the periotic canal, bypassing the otic
429 labyrinth and auditory papillae entirely (Purgue and Narins, 2000a, b). That portion of the periotic
430 canal which ascends from the periotic cistern is visible in both our 'virtual section' (Fig. 12B) and
431 Wever's diagram (Fig. 1B), but Wever (1973, 1985) made surprisingly little mention of the canal in
432 his otherwise detailed descriptions of frog inner ears.

433 Of the other schematic illustrations of the frog inner ear which exist in the literature, that of
434 Frishkopf & Goldstein (1963) may be the best-known. More obviously diagrammatic than Wever's

1
2 435 illustration, this older representation shows the periotic and semicircular canals, and it represents
3 436 the extrastapes more accurately.
4

5 437 *The ears of Eleutherodactylus and Xenopus*

6
7 438 The inner ear of *Eleutherodactylus limbatus* was found generally to resemble that of *Rana*, but there
8
9
10 439 were some pronounced differences in terms of the relative sizes and shapes of the various
11
12 440 structures. These differences were not highlighted by Wever (1985), who examined three other
13
14 441 *Eleutherodactylus* species. The very small saccule and the relatively short, wide semicircular canals
15
16
17 442 (Fig. 2) closely resemble reconstructions of the inner ear in 'stage 8' *Rana temporaria* tadpoles (30
18
19 443 mm long, just before emergence of hindlimbs) made by Birkmann (1940). *E. limbatus* has direct
20
21 444 development which omits a tadpole stage, but our frogs had been vocalizing in life and were
22
23 445 therefore believed to be reproductively mature. The inner ear of this species may therefore be
24
25
26 446 paedomorphic.
27

28
29
30 447 The inner ear of *Xenopus laevis* has been described, among others, by Paterson (1949, 1960), Wever
31
32 448 (1985) and Bever et al. (2003). Our reconstructions of *Xenopus* ears largely agree with their
33
34 449 descriptions. The saccular cavity contains a dense otoconial mass (very obvious in the CT scans)
35
36
37 450 which, relative to the rest of the inner ear, is much larger and more dorsally positioned than its
38
39 451 equivalent in *Rana* and *Eleutherodactylus*. The size and position of the saccular cavity in *Xenopus*
40
41 452 gives its inner ear a striking morphological similarity to that of the fish *Gobius niger*, as illustrated by
42
43 453 Retzius (1881). The possible functional convergence between these two aquatic species remains to
44
45
46 454 be explored.
47

48
49
50 455 The association of the basilar papilla with the lagenar recess in urodeles, caecilians and amniotes has
51
52 456 been said to be the "single most influential piece of evidence supporting a [basilar papilla] homology
53
54 457 among all terrestrial vertebrates", but the separate opening of the basilar recess into the saccule in
55
56
57 458 frogs was seen as a complication to this theory (Smotherman and Narins, 2004). We have found that
58
59
60
61
62
63
64
65

1
2 459 the basilar and lagenar recesses are in fact conjoined in *Xenopus* (Fig. 10), suggesting that this
3
4 460 represents the primitive condition for all lissamphibians and perhaps tetrapods in general.

5
6 461 At the caudal end of the basilar recess, periotic contact occurs via the periotic sac directly in
7
8 462 *Xenopus*, rather than via a *recessus partis basilaris*. Rostrally, the recess is separated from the
9
10 463 periotic cistern by a thin “tympal area”, discussed later. These features have been previously
11
12 464 described by Paterson (1949, 1960).

13
14
15
16 465 In *Xenopus*, the periotic cistern is separated from the stapes footplate by the fluid contained within a
17
18 466 tubular extension of the otic capsule (Fig. 11). A shorter separation between stapes and cistern is
19
20 467 shown in Wever’s (1985) diagrams of the ear of this frog, but Wever found a much longer, fluid-filled
21
22 468 “lateral passage” in the related species *Pipa pipa*. In both our histological slides of *Xenopus* and
23
24 469 Wever’s slides of *Pipa* it looked like a precipitate had formed within this lateral passage, but not in
25
26 470 the periotic labyrinth. Paterson (1960) found only a short lateral passage in her immature specimen
27
28 471 of *Pipa* which she refers to as a “fossa fenestrae ovalis”, filled with “delicate connective tissue”; she
29
30 472 did not describe anything similar in *Xenopus*. Perhaps the separation between footplate and periotic
31
32 473 labyrinth increases in pipids as the skull grows, such that it is less obvious in younger specimens. The
33
34 474 lateral chamber of *Rana* differs from the lateral passage of *Xenopus* because the rapid lateral
35
36 475 chamber has a narrower connection with the main otic capsule, it bends sharply rostrally to reach
37
38 476 the stapes footplate and it is filled with a diverticulum of the periotic cistern. The rapid lateral
39
40 477 chamber is also in contact with the operculum, an element lacking in *Xenopus*.

41
42
43
44
45
46
47 478 The otic labyrinth in the female *Xenopus* was around 1.5 times the linear dimensions of that of the
48
49 479 male. The saccular cavity was more elongated in the female and there was a difference in the
50
51 480 relative sizes of the contact membranes of the amphibian and basilar recesses, noted earlier. Further
52
53 481 investigation of a larger number of specimens is needed in order to establish whether these inner
54
55 482 ear differences represent sexual dimorphism, which has been observed in the middle ear of this
56
57 483 species (Mason et al., 2009).
58
59
60
61
62
63
64
65

1
2
3
4
5
6
7
8
9
10
11
12
13
14
15
16
17
18
19
20
21
22
23
24
25
26
27
28
29
30
31
32
33
34
35
36
37
38
39
40
41
42
43
44
45
46
47
48
49
50
51
52
53
54
55
56
57
58
59
60
61
62
63
64
65

484 ~~Some other aspects of the inner ear of the three frog species studied that are worthy of particular~~
485 ~~attention are discussed in more detail in the sections to follow.~~

486

487 **The blind branch of the periotic canal**

488 The discrete “blind branch” of the periotic canal which Purgue & Narins (2000b) found in the bullfrog
489 *Rana catesbeiana* could not be identified in the *Rana* or *Eleutherodactylus* specimens examined
490 here. However, the membranous wall of the periotic canal as it curves around the superior sacculle
491 was particularly thin in *Rana pipiens*, and in some slides it appeared to be ruptured. An apparent
492 short diverticulum found in the female *Xenopus* specimen only (Fig. 10) might also have been the
493 result of periotic canal rupture. Purgue & Narins injected silicone into the periotic labyrinth of their
494 frogs to make casts: it is possible that they experienced a similar problem.

495

496 **The contact membranes**

497 Harrison (1902) referred to three ‘tympanal areas’ in the frog inner ear where otic and periotic
498 labyrinths are in particularly close apposition. One of these is the extensive, membranous division
499 between periotic cistern and sacculle, while the other two ‘tympanal areas’ are now more generally
500 known as the ‘contact membranes’ of the amphibian and basilar recesses. To these three may be
501 added the contact membrane of the sacculle and an additional ‘tympanal area’ in *Xenopus*, discussed
502 later.

503 Sound energy from stapedial vibrations is widely presumed to enter the otic labyrinth through the
504 first ‘tympanal area’ between periotic cistern and sacculle (the membrane surrounding the inferior
505 saccular chamber, labelled IS in Fig. 4, forms part of this). The division between the periotic and otic
506 systems remains very thin where the periotic canal wraps around the anterior wall of the superior

1
2 507 saccule; a special, ventral diverticulum of the canal makes additional contact with the superior
3 508 saccule in *Eleutherodactylus* (Figs. 6, 7B).

4
5 509 In both *Rana* and *Eleutherodactylus*, the periotic canal separates from the saccule but returns to
6
7 510 meet the otic labyrinth at three contact membranes within the otherwise thickened limbic tissue at
8
9 511 the posterior end of the otic capsule. The contact membranes of the amphibian and basilar recesses
10
11 512 represent pathways through which sound energy can travel from the otic labyrinth back into the
12
13 513 periotic system, via the auditory epithelia of the amphibian and basilar papillae (Purgue and Narins,
14
15 514 2000a, b). Although not considered by Purgue & Narins, Wever (1973) showed in his diagram a third
16
17 515 contact membrane located between the two papillae, marked only with a tiny arrow (Fig. 1A). Wever
18
19 516 wrote that “this thin area acts as a bypass and allows some fraction of the fluid motion to go directly
20
21 517 into the perilymphatic duct [= periotic canal] without being detected”. This membrane between
22
23 518 superior saccule and periotic canal was described in *Rana catesbeiana* by Lewis (1976), who referred
24
25 519 to it as the “contact membrane of the saccule”. Lewis & Narins (1999) state that it is found in “the
26
27 520 more derived anurans”, referring this statement to Lewis (1984); Lewis & Narins may have meant
28
29 521 Lewis’ 1976 publication.

30
31
32
33
34
35
36
37 522 The contact membrane of the saccule was identified in this study in both *Rana* (Figs. 3, 5C) and
38
39 523 *Eleutherodactylus* (Figs. 6, 8B), located close to the contact membrane of the amphibian recess.
40
41 524 Although it appears to be thicker than the other two contact membranes, it might indeed represent
42
43 525 a second route by which sound energy could bypass the amphibian and basilar papillae, additional to
44
45 526 the periotic canal route described by Purgue & Narins (2000a, b). The frequency-dependent
46
47 527 impedance of such a bypass, and hence its functional significance, remains to be determined. The
48
49 528 so-called ‘round window’ within the metotic fissure, which may not be homologous with the round
50
51 529 window of other tetrapods (Henson, 1974), represents a point of pressure release for all these
52
53 530 routes (Wever, 1985).

1
2
3
4
5
6
7
8
9
10
11
12
13
14
15
16
17
18
19
20
21
22
23
24
25
26
27
28
29
30
31
32
33
34
35
36
37
38
39
40
41
42
43
44
45
46
47
48
49
50
51
52
53
54
55
56
57
58
59
60
61
62
63
64
65

531 As well as the usual contact membrane at the posterior end of the basilar recess, *Xenopus* has an
532 additional ‘tympanal area’ between the rostrolateral wall of this recess and a posterior extension of
533 the periotic cistern (Paterson, 1949, 1960). Of the frogs studied here only *Xenopus* has this
534 ‘tympanal area’ (Figs. 8D, 11) because its basilar and lagenar recesses both arise from the same
535 caudoventral diverticulum of the saccular cavity (Fig. 10; see earlier), and part of the periotic cistern
536 has come to occupy the space between this diverticulum and the sacculle proper. Elsewhere, the
537 membranous walls of the basilar recess are enclosed within thick limbic tissue (Fig. 8D). In principle,
538 acoustic energy might flow from periotic cistern through this ‘tympanal area’ directly into the basilar
539 recess, exiting at the posterior end of the recess via the contact membrane formed here with the
540 periotic sac. This short and direct pathway through the basilar recess was represented
541 diagrammatically by Wever (1985).

542 **The tegmentum vasculosum**

543 ‘Tegmentum vasculosum’, literally meaning ‘vascular covering’, is a term most often used to
544 describe the well-vascularized, thickened wall of the cochlear duct in birds and crocodylians.
545 Separating the scala media from the scala vestibuli, this archosaur tegmentum vasculosum is
546 believed to combine the roles of the stria vascularis and Reissner’s membrane in mammals (Baird,
547 1974; Lewis et al., 1985; Hossler et al., 2002). The same term has long been used in the German
548 anatomical literature to describe the thickened layer of epithelial cells found in the superior sacculle
549 of certain frogs (e.g. Deiters, 1862; Hasse, 1868; Kuhn, 1880; Retzius, 1881; Gaupp, 1904; Birkmann,
550 1940; Hagmann and Giebel, 1978). Retzius (1881) described a tegmentum vasculosum in *Bufo*, *Hyla*
551 and *Pelobates* but found it to be very poorly-developed in *Alytes*; it is not found in *Ascaphus* or
552 *Liopelma* (Wagner, 1934), nor in pipids including *Xenopus* (Paterson, 1960; this study). Although
553 lacking in some ‘archaeobatrachians’, the tegmentum vasculosum has apparently been identified in
554 all neobatrachian ears in which it has been sought. It is not found in urodeles (Birkmann, 1940).

1
2
3
4
5
6
7
8
9
10
11
12
13
14
15
16
17
18
19
20
21
22
23
24
25
26
27
28
29
30
31
32
33
34
35
36
37
38
39
40
41
42
43
44
45
46
47
48
49
50
51
52
53
54
55 Retzius (1881) produced several illustrations of the otic labyrinth of *Rana esculenta*, which were
56 redrawn and modified by Gaupp (1904). Retzius and Gaupp both labelled the whole of the superior
57 saccular wall as the tegmentum vasculosum, as did Birkmann (1940) in his reconstructions of the otic
58 labyrinth of *Rana temporaria*. Several illustrations from Gaupp and Birkmann were redrawn by
59 Wever (1985) in *The Amphibian Ear*, but in each case the region originally labelled as tegmentum
60 vasculosum was relabelled as part of the sacculi. In the present study, the tegmentum vasculosum
61 was readily identifiable in *Rana* and *Eleutherodactylus* as a thickened epithelium lining an otherwise
62 unoccupied diverticulum of the saccular chamber. However, the extent of its vascularization could
63 not be ascertained and, as Gaupp (1904) noted, its rostral borders are indistinct in *Rana*. A
64 tegmentum vasculosum was not found in *Xenopus*.

55
56
57
58
59
60
61
62
63
64
65
66
67
68
69
70
71
72
73
74
75
76
77
78
79
80
81
82
83
84
85
86
87
88
89
90
91
92
93
94
95
96
97
98
99
100
101
102
103
104
105
106
107
108
109
110
111
112
113
114
115
116
117
118
119
120
121
122
123
124
125
126
127
128
129
130
131
132
133
134
135
136
137
138
139
140
141
142
143
144
145
146
147
148
149
150
151
152
153
154
155
156
157
158
159
160
161
162
163
164
165
166
167
168
169
170
171
172
173
174
175
176
177
178
179
180
181
182
183
184
185
186
187
188
189
190
191
192
193
194
195
196
197
198
199
200
201
202
203
204
205
206
207
208
209
210
211
212
213
214
215
216
217
218
219
220
221
222
223
224
225
226
227
228
229
230
231
232
233
234
235
236
237
238
239
240
241
242
243
244
245
246
247
248
249
250
251
252
253
254
255
256
257
258
259
260
261
262
263
264
265
266
267
268
269
270
271
272
273
274
275
276
277
278
279
280
281
282
283
284
285
286
287
288
289
290
291
292
293
294
295
296
297
298
299
300
301
302
303
304
305
306
307
308
309
310
311
312
313
314
315
316
317
318
319
320
321
322
323
324
325
326
327
328
329
330
331
332
333
334
335
336
337
338
339
340
341
342
343
344
345
346
347
348
349
350
351
352
353
354
355
356
357
358
359
360
361
362
363
364
365
366
367
368
369
370
371
372
373
374
375
376
377
378
379
380
381
382
383
384
385
386
387
388
389
390
391
392
393
394
395
396
397
398
399
400
401
402
403
404
405
406
407
408
409
410
411
412
413
414
415
416
417
418
419
420
421
422
423
424
425
426
427
428
429
430
431
432
433
434
435
436
437
438
439
440
441
442
443
444
445
446
447
448
449
450
451
452
453
454
455
456
457
458
459
460
461
462
463
464
465
466
467
468
469
470
471
472
473
474
475
476
477
478
479
480
481
482
483
484
485
486
487
488
489
490
491
492
493
494
495
496
497
498
499
500
501
502
503
504
505
506
507
508
509
510
511
512
513
514
515
516
517
518
519
520
521
522
523
524
525
526
527
528
529
530
531
532
533
534
535
536
537
538
539
540
541
542
543
544
545
546
547
548
549
550
551
552
553
554
555
556
557
558
559
560
561
562
563
564
565
566
567
568
569
570
571
572
573
574
575
576
577
578
579
580
581
582
583
584
585
586
587
588
589
590
591
592
593
594
595
596
597
598
599
600
601
602
603
604
605
606
607
608
609
610
611
612
613
614
615
616
617
618
619
620
621
622
623
624
625
626
627
628
629
630
631
632
633
634
635
636
637
638
639
640
641
642
643
644
645
646
647
648
649
650
651
652
653
654
655
656
657
658
659
660
661
662
663
664
665
666
667
668
669
670
671
672
673
674
675
676
677
678
679
680
681
682
683
684
685
686
687
688
689
690
691
692
693
694
695
696
697
698
699
700
701
702
703
704
705
706
707
708
709
710
711
712
713
714
715
716
717
718
719
720
721
722
723
724
725
726
727
728
729
730
731
732
733
734
735
736
737
738
739
740
741
742
743
744
745
746
747
748
749
750
751
752
753
754
755
756
757
758
759
760
761
762
763
764
765
766
767
768
769
770
771
772
773
774
775
776
777
778
779
780
781
782
783
784
785
786
787
788
789
790
791
792
793
794
795
796
797
798
799
800
801
802
803
804
805
806
807
808
809
810
811
812
813
814
815
816
817
818
819
820
821
822
823
824
825
826
827
828
829
830
831
832
833
834
835
836
837
838
839
840
841
842
843
844
845
846
847
848
849
850
851
852
853
854
855
856
857
858
859
860
861
862
863
864
865
866
867
868
869
870
871
872
873
874
875
876
877
878
879
880
881
882
883
884
885
886
887
888
889
890
891
892
893
894
895
896
897
898
899
900
901
902
903
904
905
906
907
908
909
910
911
912
913
914
915
916
917
918
919
920
921
922
923
924
925
926
927
928
929
930
931
932
933
934
935
936
937
938
939
940
941
942
943
944
945
946
947
948
949
950
951
952
953
954
955
956
957
958
959
960
961
962
963
964
965
966
967
968
969
970
971
972
973
974
975
976
977
978
979
980
981
982
983
984
985
986
987
988
989
990
991
992
993
994
995
996
997
998
999
1000

Wever (1985) made only one, brief mention of the anuran tegmentum vasculosum in his book
(p.78), in which he commented on the mistake of “early anatomists” in assigning to it a sensory
function. Nevertheless, the unusual epithelium suggests a functional distinction from the rest of the
superior saccular chamber. Hagmann & Giebel (1978), working on *Rana temporaria*, confirmed that
this region is richly vascularized and found high levels of metabolic enzymatic activity. This supports
the contention that the tegmentum vasculosum in frogs is responsible for the secretion of
endolymph, like the tegmentum of archosaurs and the stria vascularis of mammals. Subsequent
studies of endolymph secretion in frogs, however, have focused on the dark cells located in the
utricle and semicircular canal ampullae (Burnham and Stirling, 1984; Bernard et al., 1986); the
anuran tegmentum vasculosum has fallen into obscurity.

575 576 **The apparent interaural fluid connection in *Eleutherodactylus***

577
578
579
580
581
582
583
584
585
586
587
588
589
590
591
592
593
594
595
596
597
598
599
600
601
602
603
604
605
606
607
608
609
610
611
612
613
614
615
616
617
618
619
620
621
622
623
624
625
626
627
628
629
630
631
632
633
634
635
636
637
638
639
640
641
642
643
644
645
646
647
648
649
650
651
652
653
654
655
656
657
658
659
660
661
662
663
664
665
666
667
668
669
670
671
672
673
674
675
676
677
678
679
680
681
682
683
684
685
686
687
688
689
690
691
692
693
694
695
696
697
698
699
700
701
702
703
704
705
706
707
708
709
710
711
712
713
714
715
716
717
718
719
720
721
722
723
724
725
726
727
728
729
730
731
732
733
734
735
736
737
738
739
740
741
742
743
744
745
746
747
748
749
750
751
752
753
754
755
756
757
758
759
760
761
762
763
764
765
766
767
768
769
770
771
772
773
774
775
776
777
778
779
780
781
782
783
784
785
786
787
788
789
790
791
792
793
794
795
796
797
798
799
800
801
802
803
804
805
806
807
808
809
810
811
812
813
814
815
816
817
818
819
820
821
822
823
824
825
826
827
828
829
830
831
832
833
834
835
836
837
838
839
840
841
842
843
844
845
846
847
848
849
850
851
852
853
854
855
856
857
858
859
860
861
862
863
864
865
866
867
868
869
870
871
872
873
874
875
876
877
878
879
880
881
882
883
884
885
886
887
888
889
890
891
892
893
894
895
896
897
898
899
900
901
902
903
904
905
906
907
908
909
910
911
912
913
914
915
916
917
918
919
920
921
922
923
924
925
926
927
928
929
930
931
932
933
934
935
936
937
938
939
940
941
942
943
944
945
946
947
948
949
950
951
952
953
954
955
956
957
958
959
960
961
962
963
964
965
966
967
968
969
970
971
972
973
974
975
976
977
978
979
980
981
982
983
984
985
986
987
988
989
990
991
992
993
994
995
996
997
998
999
1000

Of the frogs examined, sections through the whole head were only available for one specimen of
Eleutherodactylus. Although our interpretation may have been affected by shrinkage, these sections
appeared to show the left and right periotic sacs converging to form a fluid space immediately

1 580 beneath the brain (Fig. 9). Wever (1978) showed that vibrations applied to the operculum of one ear
2 581 in a salamander can excite the contralateral ear: his proposed mechanism involved a similar
3
4 582 intracranial pathway below the brain, but he believed that the two periotic sacs in his species
5
6
7 583 communicated only indirectly, via the cerebrospinal fluid. Harrison (1902) challenged the notion of
8
9 584 earlier authors that amphibians possess a connection between the periotic system and a “subdural
10
11 585 space”.

12
13
14
15 586 Such a fluid system extending between the two ears via the cranial cavity might be functionally
16
17 587 significant in (1) communicating vibrations from the cerebrospinal fluid to the inner ears, (2)
18
19 588 acoustically coupling the two ears, which might affect sound localization, or (3) providing increased
20
21
22 589 possibilities for pressure release from the inner ear, affecting sensitivity. Further work is clearly
23
24 590 needed to confirm the presence of an interaural fluid connection in *Eleutherodactylus* and other
25
26 591 frogs, so as to assess whether this condition is widespread among anurans.

27
28
29
30 592

31 32 33 593 **Conclusion**

34
35
36 594 The anuran inner ear is a complex, three-dimensional structure consisting of the intertwined canals
37
38 595 of the periotic and otic labyrinths. Although his representation appears not to be anatomically
39
40 596 accurate, Wever’s (1973) diagram of the leopard frog inner ear does an admirable job of clearly
41
42 597 illustrating some of the possible routes of acoustic energy flow from stapes to round window. Its
43
44 598 main shortcoming in this respect is that it does not label the periotic canal, which represents
45
46 599 another potential route. Although some anatomical differences were identified, the inner ear of
47
48 600 *Eleutherodactylus* is broadly similar to that of *Rana*, so Wever’s diagram is clearly representative of a
49
50 601 wider range of neobatrachian frogs. The illustration is less useful in describing the ear of *Xenopus*; to
51
52 602 what extent this reflects the ‘archaeobatrachian’ status of *Xenopus* or its aquatic habits remains to
53
54 603 be determined.
55
56
57
58
59
60
61
62
63
64
65

1
2
3
4
5
6
7
8
9
10
11
12
13
14
15
16
17
18
19
20
21
22
23
24
25
26
27
28
29
30
31
32
33
34
35
36
37
38
39
40
41
42
43
44
45
46
47
48
49
50
51
52
53
54
55
56
57
58
59
60
61
62
63
64
65

604 The tegmentum vasculosum and the contact membrane of the saccule, found here in *Rana* and
605 *Eleutherodactylus* but not *Xenopus*, have been neglected in the recent literature and deserve further
606 attention from auditory physiologists. The intriguing possibility of a fluid pathway extending
607 between right and left ears also demands investigation.

Acknowledgements

608
609
610
611 The authors wish to thank Emanuel Mora for his help and support with this project. Dave Simpson
612 kindly provided the *Xenopus* specimens. The CT scan of *Xenopus* was made by Alan Heaver of the
613 University of Cambridge Department of Engineering, with thanks going also to Norman Fleck for the
614 use of his equipment. The authors are very grateful to Dolores Bozovic, Alan D. Grinnell, Tammy
615 Hoang, Victoria Sandoval and Felix E. Schweizer for facilitating the *Rana* CT scan, which was made by
616 Ting-Ling Chang at the UCLA School of Dentistry, Division of Advanced Prosthodontics. Stephan
617 Kamrad helped with translations. The research of JMS and PvD was supported by the Heinsius
618 Houbolt Foundation and is part of the research program *Healthy Ageing and Communication* of the
619 Department of Otorhinolaryngology at the University Medical Center Groningen. Finally, the authors
620 wish to thank the reviewers and editors of the manuscript for their very helpful comments.

Conflicts of interest

621
622
623
624
625 The authors declare that they have no conflicts of interest.
626

References

627

1

2

3 628

4

5

6 629

Baird IL (1974) Anatomical features of the inner ear in submammalian vertebrates. In: Handbook of Sensory Physiology, volume V/1: Auditory System (Keidel WD, Neff WD, eds), pp 159-212. Berlin: Springer-Verlag.

8 631

9 632

Bernard C, Ferrary E, Sterkers O (1986) Production of endolymph in the semicircular canal of the frog *Rana esculenta*. *Journal of Physiology* 371:17-28.

10 633

11 634

Bever MM, Jean YY, Fekete DM (2003) Three-dimensional morphology of inner ear development in *Xenopus laevis*. *Developmental Dynamics* 227:422-430.

12 635

13 636

Birkmann K (1940) Morphologisch-anatomische Untersuchungen zur Entwicklung des häutigen Labyrinthes der Amphibien. *Zeitschrift für Anatomie und Entwicklungsgeschichte* 110:443-488.

15 637

16 638

Blood DC, Studdert VP (1999) *Saunders Comprehensive Veterinary Dictionary, 2nd Edition*. Edinburgh: W.B. Saunders.

18 639

19 640

Burnham JA, Stirling CE (1984) Quantitative localization of Na-K pump site in frog inner ear dark cells. *Hearing Research* 13:261-268.

20 641

21 642

Deiters O (1862) Ueber das innere Gehörorgan der Amphibien. *Archiv für Anatomie, Physiologie und Wissenschaftliche Medicin* 1862:262-275, 277-310.

22 643

23 644

Dubois A (2007) Naming taxa from cladograms: a cautionary tale. *Molecular Phylogenetics and Evolution* 42:317-330.

24 645

25 646

Duellman WE, Trueb L (1986) *Biology of Amphibians*. Baltimore: The Johns Hopkins University Press.

27 647

28 648

Fay RR, Popper AN (1985) The octavolateralis system. In: *Functional Vertebrate Morphology* (Hildebrand M, Bramble DM, Liem KF, Wake DB, eds), pp 291-316. London: Belknap Press.

29 649

30 650

Frishkopf LS, Goldstein MH (1963) Responses to acoustic stimuli from single units in the eighth nerve of the bullfrog. *Journal of the Acoustical Society of America* 35:1219-1228.

31 651

32 652

Gaupp E (1904) A. Ecker's und R. Wiedersheim's Anatomie des Frosches, part 3, 2nd Edition. Braunschweig: Druck und Verlag von Friedrich Vieweg und Sohn.

33 653

34 654

Gridi-Papp M, Narins PM (2010) Seismic detection and communication in amphibians. In: *The Use of Vibrations in Communication: Properties, Mechanisms and Function across Taxa* (O'Connell-Rodwell CE, ed), pp 69-83. Kerala: Research Signpost.

36 655

37 656

Hagmann B, Giebel W (1978) Enzymhistochemische Untersuchungen am Innenohr des Frosches (*Rana temporaria*). *Archives of Oto-Rhino-Laryngology* 220:89-103.

39 657

40 658

Harrison HS (1902) On the perilymphatic spaces of the amphibian ear. *Internationale Monatsschrift für Anatomie und Physiologie* 19:221-261.

41 659

42 660

Hasse C (1868) *Das Gehörorgan der Frösche*, Reprinted from *Zeitschrift für wissenschaftliche Zoologie*, Bd. 18 Edition. Leipzig: Verlag von Wilhelm Engelmann.

44 661

45 662

Henson OW (1974) Comparative anatomy of the middle ear. In: *Handbook of Sensory Physiology*, volume V/1: Auditory System (Keidel WD, Neff WD, eds), pp 39-110. Berlin: Springer-Verlag.

46 663

47 664

Hillis DM (2007) Constraints in naming parts of the Tree of Life. *Molecular Phylogenetics and Evolution* 42:331-338.

48 665

49 666

Hoegg S, Vences M, Brinkmann H, Meyer A (2004) Phylogeny and comparative substitution rates of frogs inferred from sequences of three nuclear genes. *Molecular Biology and Evolution* 21:1188-1200.

50 667

51 668

Hossler FE, Olson KR, Musil G, McKamey MI (2002) Ultrastructure and blood supply of the tegmentum vasculosum in the cochlea of the duckling. *Hearing Research* 164:155-165.

52 669

53 670

Jørgensen MB, Kannevorff M (1998) Middle ear transmission in the grass frog, *Rana temporaria*. *Journal of Comparative Physiology A* 182:59-64.

54 671

55 672

56 673

57 674

58 675

59 676

60 677

61 678

62 679

63 680

64 681

65 682

674 Kuhn (1880) Ueber das häutige Labyrinth der Amphibien. Archiv für Mikroskopische Anatomie
1 675 17:479-550.

2 676 Lewis ER (1976) Surface morphology of the bullfrog amphibian papilla. Brain, Behavior and Evolution
3 677 13:196-215.

4 678 Lewis ER (1984) On the frog amphibian papilla. Scanning Electron Microscopy 1984 (IV):1899-1913.

5 679 Lewis ER, Narins PM (1999) The acoustic periphery of amphibians: anatomy and physiology. In:
6 680 Comparative Hearing: Fish and Amphibians (Fay RR, Popper AN, eds), pp 101-154. New York:
7 681 Springer.

8 682 Lewis ER, Leverenz EL, Bialek WS (1985) The Vertebrate Inner Ear. Boca Raton: CRC Press, Inc.

9 683 Lombard RE (1977) Comparative morphology of the inner ear in salamanders (*Caudata: Amphibia*).
10 684 Basel: S. Karger.

11 685 Mason MJ, Narins PM (2002) Vibrometric studies of the middle ear of the bullfrog *Rana catesbeiana*
12 686 I. The extrastapes. Journal of Experimental Biology 205:3153-3165.

13 687 Mason MJ, Wang M, Narins PM (2009) Structure and function of the middle ear apparatus of the
14 688 aquatic frog, *Xenopus laevis*. Proceedings of the Institute of Acoustics 31:13-21.

15 689 Paterson NF (1949) The development of the inner ear of *Xenopus laevis*. Proceedings of the
16 690 Zoological Society of London 119:269-291.

17 691 Paterson NF (1960) The inner ear of some members of the Pipidae (Amphibia). Proceedings of the
18 692 Zoological Society of London 134:509-546.

19 693 Pauly GB, Hillis DM, Cannatella DC (2009) Taxonomic freedom and the role of official lists of species
20 694 names. Herpetologica 65:115-128.

21 695 Purgue AP, Narins PM (2000a) A model for energy flow in the inner ear of the bullfrog (*Rana*
22 696 *catesbeiana*). Journal of Comparative Physiology A 186: 489-495.

23 697 Purgue AP, Narins PM (2000b) Mechanics of the inner ear of the bullfrog (*Rana catesbeiana*): the
24 698 contact membranes and the periotic canal. Journal of Comparative Physiology A 186: 481-
25 699 488.

26 700 Retzius G (1881) Das Gehörorgan der Wirbelthiere. Morphologisch-Histologische Studien. I. Das
27 701 Gehörorgan der Fische und Amphibien. Stockholm: Samson & Wallin.

28 702 Simmons DD, Meenderink SWF, Vassilakis PN (2007) Anatomy, physiology, and function of auditory
29 703 end-organs in the frog inner ear. In: Hearing and Sound Communication in Amphibians
30 704 (Narins PM, Feng AS, Fay RR, Popper AN, eds), pp 184-220. New York: Springer.

31 705 Smotherman M, Narins P (2004) Evolution of the amphibian ear. In: Evolution of the Vertebrate
32 706 Auditory System (Manley GA, Popper AN, Fay RR, eds), pp 164-199. New York: Springer.

33 707 Thévenaz P, Ruttimann UE, Unser M (1998) A pyramid approach to subpixel registration based on
34 708 intensity. IEEE Transactions on Image Processing 7:27-41.

35 709 van Dijk P, Mason MJ, Schoffelen RLM, Narins PM, Meenderink SWF (2011) Mechanics of the frog
36 710 ear. Hearing Research 273:46-58.

37 711 Wagner DS (1934) The structure of the inner ear in relation to the reduction of the middle ear in the
38 712 Liopelmidae (Noble). Anatomischer Anzeiger 79:20-36.

39 713 Werner YL (2003) Mechanical leverage in the middle ear of the American bullfrog, *Rana catesbeiana*.
40 714 Hearing Research 175:54-65.

41 715 Wever EG (1973) The ear and hearing in the frog, *Rana pipiens*. Journal of Morphology 141:461-477.

42 716 Wever EG (1978) Sound transmission in the salamander ear. Proceedings of the National Academy of
43 717 Sciences of the USA 75:529-530.

44 718 Wever EG (1985) The Amphibian Ear. Princeton: Princeton University Press.

54 719

55
56
57
58
59
60
61
62
63
64
65

Figure Captions

720

721

722 Fig. 1

723 A: Ernest Glen Wever's schematic diagram of the peripheral auditory apparatus of a ranid frog. The

724 original caption is included. From: Wever, E.G. (1973) The ear and hearing in the frog, *Rana pipiens*.

725 *Journal of Morphology* 141(4): 461-477. Copyright © 1973 Wiley-Liss, Inc. B: A representation of the

726 same diagram with the same colour-coding as used elsewhere in this paper, to facilitate comparison

727 between figures. Where Wever's nomenclature differs from that used in the present paper,

728 structures have been relabelled. Additionally, based on the interpretations of the present study, new

729 labels have been introduced for structures that were not explicitly identified in Wever's original

730 diagram, including the contact membranes which separate otic and periotic labyrinths.

731 Colour code: white = otic labyrinth (endolymph); green = periotic labyrinth (perilymph); red =

732 sensory epithelium; dark grey = limbic tissue; cream = bone; yellow = cartilage.

733

734 Fig. 2

735 WinSurf reconstructions of the left inner ear structures of (left) *Xenopus laevis*, male specimen,

736 (middle) *Rana pipiens*, (right) *Eleutherodactylus limbatus*. Lateral views are shown in the top row,

737 dorsal views in the bottom row. *Eleutherodactylus* reconstructions are 2.5× enlarged relative to the

738 others. In the *Eleutherodactylus* sections used for these reconstructions, the periotic cistern in the

739 region marked with an asterisk, which lies lateral to the very small saccular cavity, had collapsed. Its

740 approximate shape has been restored here by comparison with the contralateral ear and the extent

741 of the space available for it within the otic capsule. Colour code: white = otic labyrinth (endolymph);

742 green = periotic labyrinth (perilymph); red = sensory epithelium; semitranslucent grey = internal

743 walls of the otic capsule.

1
2
3
4
5
6
7
8
9
10
11
12
13
14
15
16
17
18
19
20
21
22
23
24
25
26
27
28
29
30
31
32
33
34
35
36
37
38
39
40
41
42
43
44
45
46
47
48
49
50
51
52
53
54
55
56
57
58
59
60
61
62
63
64
65

744 Key to this and subsequent figures: AR = amphibian recess (endolymph); AS = anterior semicircular
745 canal; B = brain; BR = basilar recess (endolymph); CA = contact membrane of amphibian recess; CB =
746 contact membrane of basilar recess; CC = *crus commune* (confluence of anterior and posterior
747 semicircular canals); CS = contact membrane of saccule; IS = inferior saccular chamber; LC = lateral
748 chamber; LP = lateral passage; LR = lagenar recess (endolymph); LS = lateral semicircular canal; LT =
749 limbic tissue; O = operculum; PC = periotic canal; POC = periotic cistern; POS = periotic sac; PS =
750 posterior semicircular canal; PT = periotic tissue; PU = posterior utricular cavity; RPB = *recessus partis*
751 *basilaris* (perilymph); RW = round window; S = saccule; SPI = stapes *pars interna*; SPM = stapes *pars*
752 *media*; SS = superior saccular chamber; TV = tegmentum vasculosum, or the saccular diverticulum
753 within which this epithelial lining is found; VIII = branch of eighth cranial nerve.

754

755 **Fig. 3**

756 WinSurf reconstructions of left inner ear structures of *Rana pipiens*, seen from an approximately
757 posterior view. The reconstruction on the left shows the otic labyrinth (white), sensory epithelia
758 (red) and contact membranes **separating endo- and perilymph** (purple). Part of the posterior
759 semicircular canal has been removed to reveal the diverticula of the superior saccule. The
760 reconstruction on the right shows the same, with the periotic labyrinth added in (semitranslucent
761 green). Scale bar 2.5 mm. See Fig. 2 caption for full list of abbreviations.

762

763 **Fig. 4**

764 **Composite photomicrographs of two approximately transverse sections through the posterior part**
765 **of the inner ear of *Rana pipiens*. Section B is in a plane 240 µm anterior to Section A. Relative to the**
766 **centre of each photomicrograph, dorsal is upwards and slightly away from the viewer, lateral is to**

1
2 767 the left. Scale bar applies to both A and B and represents 1 mm. See Fig. 2 caption for full list of
3 abbreviations.

4
5 769

6
7
8
9 **Fig. 5**

10
11 770 Photomicrographs of sections through the inner ear of *Rana pipiens*. A: Basilar recess (BR;
12 endolymph), *recessus partis basilaris* (RPB; perilymph) and contact membrane of basilar recess (CB)
13 separating the two. B: Amphibian recess (AR) and its contact membrane (CA), expanded from Fig.
14 4A. C: Periotic canal (PC) and contact membrane of the sacculle (CS), expanded from Fig. 4B. D:
15 Tegmentum vasculosum (TV), expanded from Fig. 4A. All scale bars 200 μ m. See Fig. 2 caption for full
16 list of abbreviations.
17
18
19
20
21
22
23
24
25

26 777

27
28
29
30 **Fig. 6**

31
32 778 WinSurf reconstructions of left inner ear structures of *Eleutherodactylus limbatus*, seen from an
33 approximately lateral view. Part of the lateral semicircular canal has been removed to reveal the
34 contact membrane of the amphibian recess (CA) and the contact membrane of the sacculle (CS). The
35 reconstruction on the left shows the otic labyrinth and associated structures only; the reconstruction
36 on the right includes the dorsal and posterior parts (only) of the periotic labyrinth. The asterisk
37 indicates the ventral diverticulum of the central part of the periotic canal, which is closely apposed
38 to the superior saccular chamber (SS). Scale bar 0.5 mm. Colour code: white = otic labyrinth
39 (endolymph); semitranslucent green = periotic labyrinth (perilymph); red = sensory epithelium;
40 purple = contact membrane separating endo- and perilymph. See Fig. 2 caption for full list of
41 abbreviations.
42
43
44
45
46
47
48
49
50
51
52
53
54
55
56
57
58
59
60
61
62
63
64
65

790 **Fig. 7**

791 Composite photomicrographs of two sections through the inner ear of *Eleutherodactylus limbatus*.
792 Section A is in an approximately transverse plane, through the posterior part of the inner ear.
793 Relative to the centre of the photomicrograph, dorsal is upwards and slightly away from the viewer,
794 lateral is to the left. Section B is in an oblique plane (between transverse and sagittal), taken from
795 the ear on the contralateral side to Section A and laterally inverted to aid comparison. Relative to
796 the centre of the photomicrograph, dorsal is upwards, lateral is to the left and away from the
797 viewer. Note in particular the membrane marked with an asterisk, located between the ventral
798 diverticulum of the central part of the periotic canal (PC) and the superior saccular chamber (SS). The
799 membranous labyrinth has pulled away from the otic capsule wall on the right hand side. Scale bar
800 applies to both A and B and represents 200 μm . See Fig. 2 caption for full list of abbreviations.

802 **Fig. 8**

803 Photomicrographs of sections through the inner ears of *Eleutherodactylus limbatus* and *Xenopus*
804 *laevis*. A: Tegmentum vasculosum (TV), amphibian recess (AR) and its contact membrane (CA) in *E.*
805 *limbatus*, scale bar 100 μm . B: Periotic canal (PC) and the contact membrane of the sacculle (CS) in *E.*
806 *limbatus*, scale bar 100 μm . C: Tegmentum vasculosum of *E. limbatus*, scale bar 50 μm . D: ~~Section~~
807 ~~through the~~ Basilar recess (BR) of *X. laevis* (female specimen), scale bar 200 μm . The asterisk
808 indicates the additional 'tympanal area' identified by Paterson (1949, 1960), located just
809 rostralateral to the basilar recess (see text). See Fig. 2 caption for full list of abbreviations.

811 **Fig. 9**

812 Photomicrograph of a transverse section through the head of *Eleutherodactylus limbatus*, at the
813 level of the posterior half of the otic capsule. The three fluid compartments collectively denoted '1'

1
2
3
4
5
6
7
8
9
10
11
12
13
14
15
16
17
18
19
20
21
22
23
24
25
26
27
28
29
30
31
32
33
34
35
36
37
38
39
40
41
42
43
44
45
46
47
48
49
50
51
52
53
54
55
56
57
58
59
60
61
62
63
64
65

814 appear to be separate in this section, but inspection of other sections in the same series suggests
815 that they are actually part of one continuous fluid system extending between the periotic labyrinths
816 of each ear and passing underneath the brain (B). The left-hand arrow marked '1' points to the left
817 periotic sac, which can be seen emerging from the left otic capsule. Within the capsule, it is
818 immediately adjacent to the amphibian recess (AR), from which it is separated by a thin contact
819 membrane. Between fluid space 1 and the base of the skull is a second fluid space (2), which is also
820 continuous across the head and extends between the two round windows (RW). Distortion resulting
821 from shrinkage may have changed the relative sizes of fluid spaces 1 and 2. Scale bar 0.5 mm. See
822 Fig. 2 caption for full list of abbreviations.

823
824 **Fig. 10**

825 WinSurf reconstructions of left inner ear structures of *Xenopus laevis* (female specimen), seen from
826 an approximately caudoventral view. Part of the posterior semicircular canal has been removed to
827 reveal the diverticula of the saccule. The reconstruction on the left shows the otic labyrinth and
828 associated structures only; the reconstruction on the right includes all but the most rostralateral
829 part of the periotic labyrinth too. The anterior semicircular canal had been obliterated in the slides
830 used to make this reconstruction and the saccular cavity was distorted owing to the presence of a
831 bubble. The presumed original shape of the saccule (S) has been restored here. The asterisk
832 indicates a short, blind branch of the periotic canal (see text). Scale bar 1.5 mm. Colour code: white =
833 otic labyrinth (endolymph); semitranslucent green = periotic labyrinth (perilymph); red = sensory
834 epithelium; purple = contact membrane separating endo- and perilymph. See Fig. 2 caption for full
835 list of abbreviations.

1
2
3
4
5
6
7
8
9
10
11
12
13
14
15
16
17
18
19
20
21
22
23
24
25
26
27
28
29
30
31
32
33
34
35
36
37
38
39
40
41
42
43
44
45
46
47
48
49
50
51
52
53
54
55
56
57
58
59
60
61
62
63
64
65

837 **Fig. 11**

838 Photomicrograph of an oblique section through the inner ear of *Xenopus laevis* (male specimen).

839 Note that the periotic cistern (POC), the contents of which have picked up only a small amount of

840 stain, is separated from the stapes footplate (SPI and SPM) by the lateral passage (LP), which is filled

841 with diffuse material staining pale blue. The contact membrane of the basilar recess is the thin

842 membrane between the basilar recess (BR) and the periotic sac (POS); the membrane marked with

843 an asterisk between the basilar recess and the periotic cistern (POC) is Paterson's (1949, 1960)

844 additional 'tympanal area' (see text). Relative to the centre of the picture, dorsal is upwards and

845 away from the viewer, lateral is to the left and towards the viewer. Scale bar 1 mm. See Fig. 2

846 caption for full list of abbreviations.

847
848 **Fig. 12**

849 Reconstructions created from a stack of serial section images of the ear of *Rana pipiens*, **digitally**

850 resectioned in a plane as close as possible to Wever's 1973 illustration (Fig. 1). See text for details.

851 The extrastapes, tympanic membrane, periotic sac and round window were not within the original

852 sections and are consequently not shown in these reconstructions. A: 'Virtual section'; the faint,

853 diagonal striations indicate the planes of the original section photomicrographs from which this was

854 reconstructed. B: Expanded, diagrammatic illustration of the same. Out of the plane of this particular

855 section, the periotic canal is in communication with the periotic fluid which abuts the contact

856 membranes of the amphibian and basilar recesses; these regions are all components of the periotic

857 labyrinth and are hence shaded in green. The asterisk indicates a process of the stapes *pars media*

858 which articulates with the otic capsule. C: WinSurf reconstructions of the right inner ear of *R. pipiens*

859 from (left) lateral, (middle) posterior and (right) dorsal views, showing the position of the 'virtual

860 section' as a grey plane. The stapes and operculum are included in these reconstructions but the

861 internal walls of the otic capsule are not. Both scale bars 2 mm. Colour code: white = otic labyrinth

862 (endolymph); green = periotic labyrinth (perilymph); dark grey = limbic tissue; lighter grey = looser

- 1
- 2
- 3
- 4
- 5
- 6
- 7
- 8
- 9
- 10
- 11
- 12
- 13
- 14
- 15
- 16
- 17
- 18
- 19
- 20
- 21
- 22
- 23
- 24
- 25
- 26
- 27
- 28
- 29
- 30
- 31
- 32
- 33
- 34
- 35
- 36
- 37
- 38
- 39
- 40
- 41
- 42
- 43
- 44
- 45
- 46
- 47
- 48
- 49
- 50
- 51
- 52
- 53
- 54
- 55
- 56
- 57
- 58
- 59
- 60
- 61
- 62
- 63
- 64
- 65

863 periotic tissue; cream = bone; yellow = cartilage.

864

Figure 1
[Click here to download high resolution image](#)

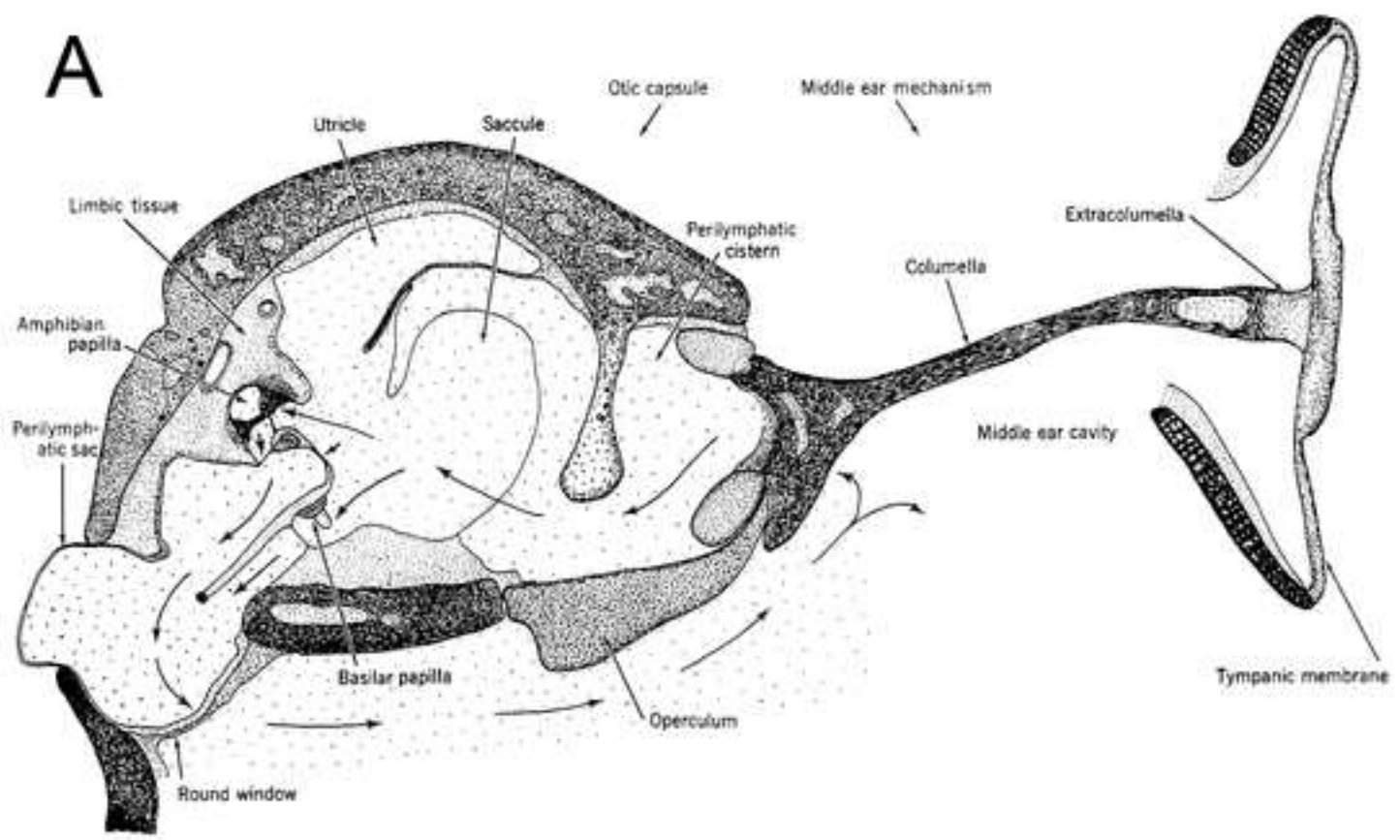


Fig. 1 A schematic representation of the ear and labyrinth of *Rana pipiens*, in frontal section. The large arrows indicate the paths of fluid flow for an inward thrust of the columella. Scale $\times 20$.

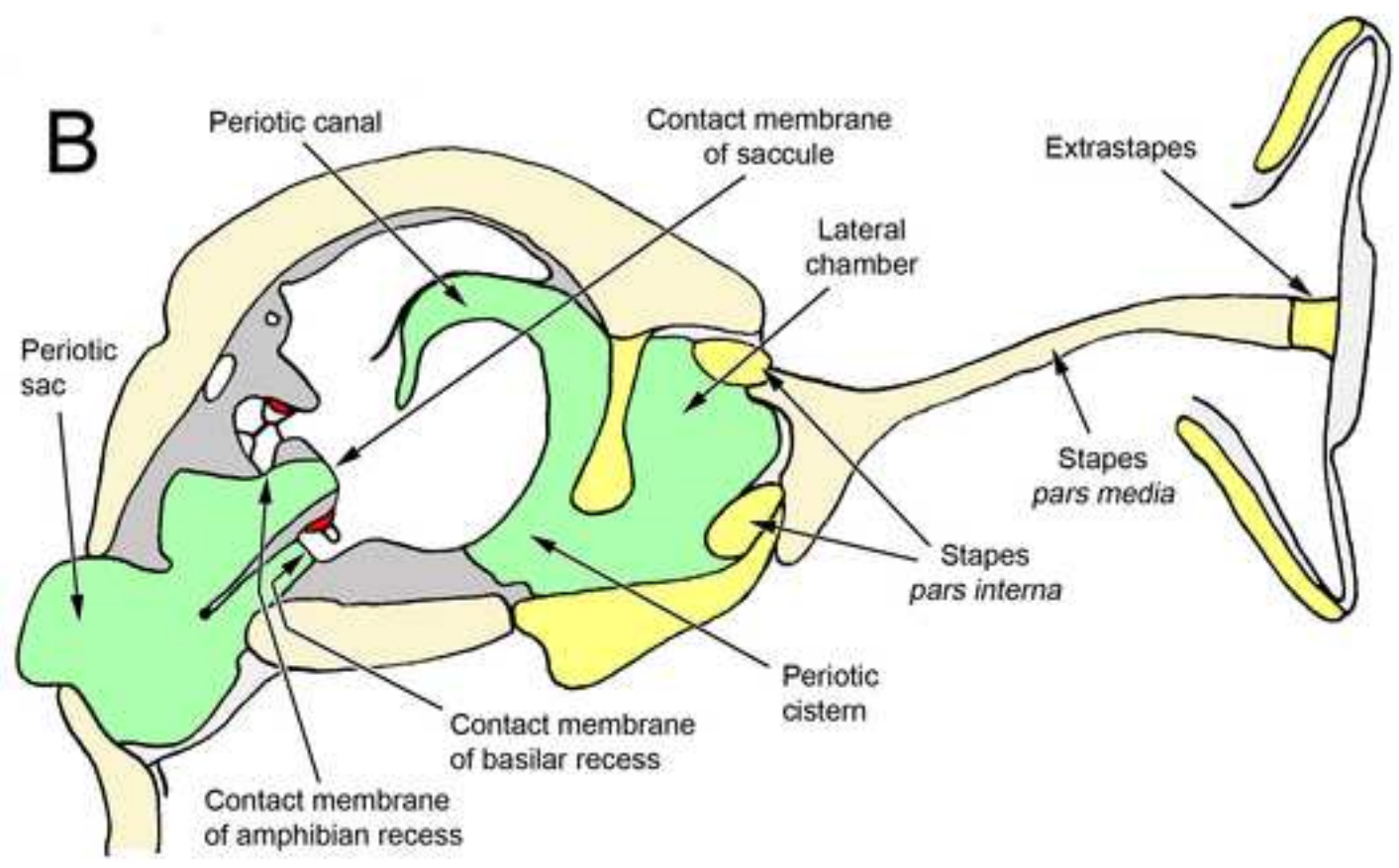


Figure 2
[Click here to download high resolution image](#)

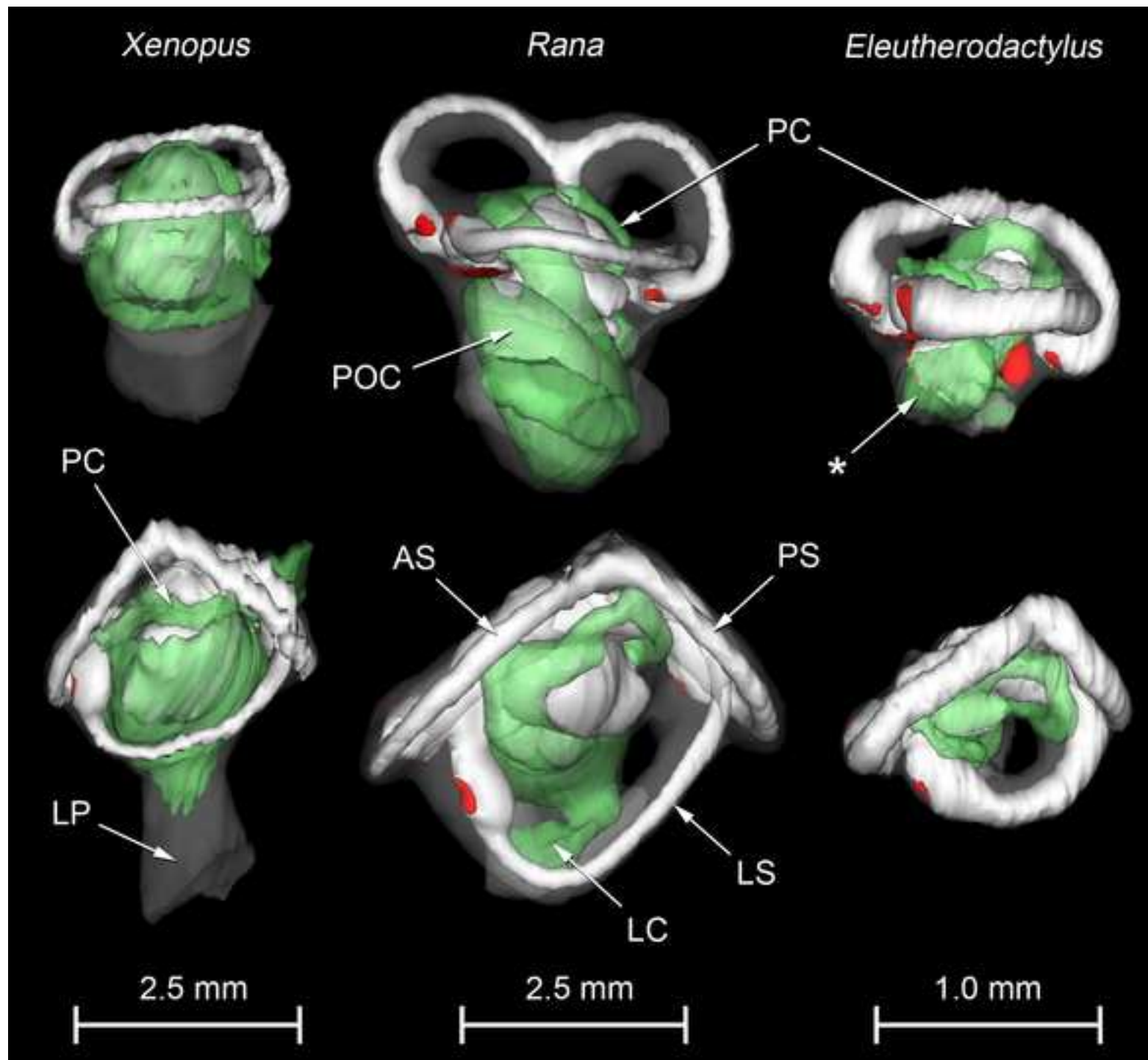


Figure 3
[Click here to download high resolution image](#)

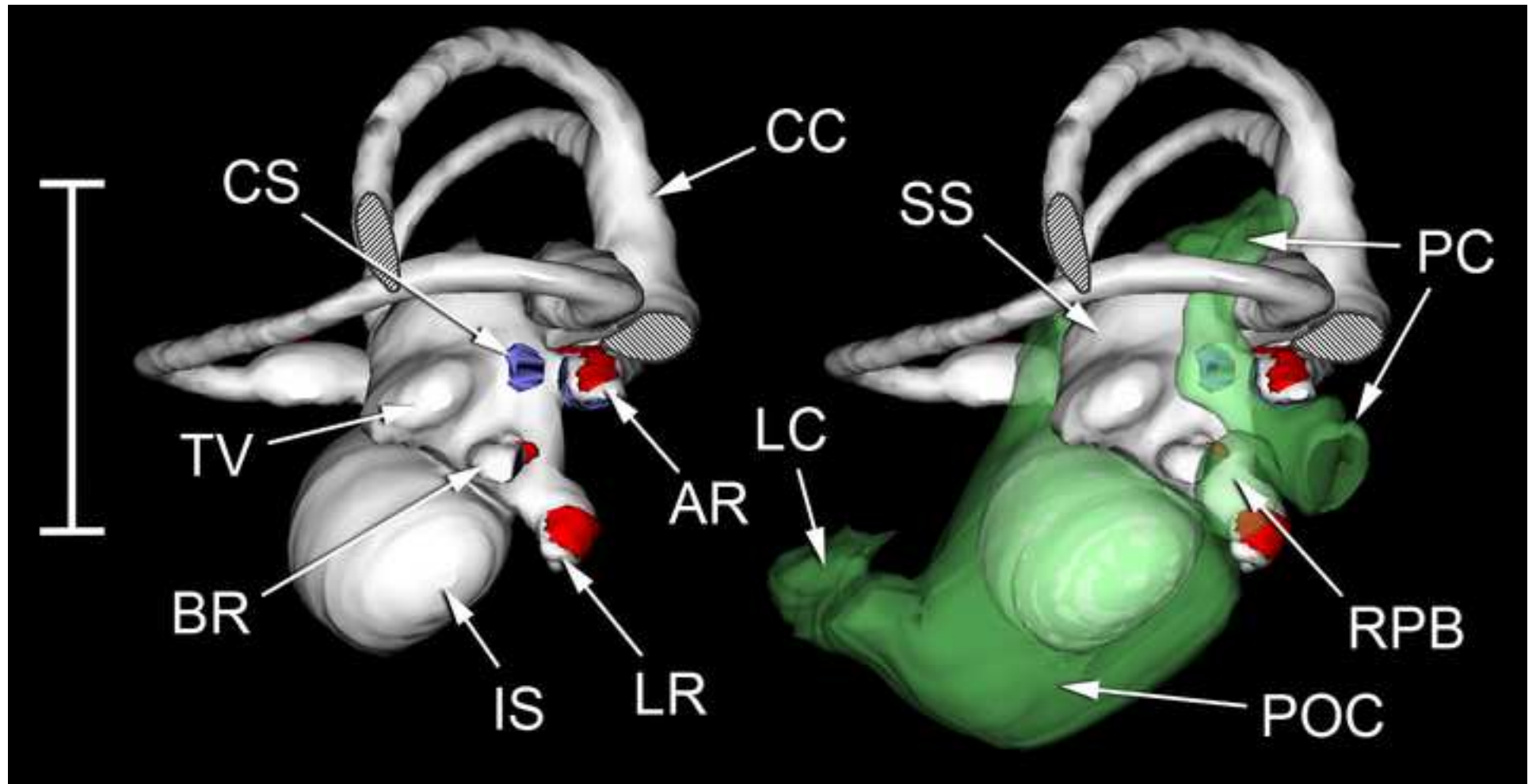


Figure 4
[Click here to download high resolution image](#)

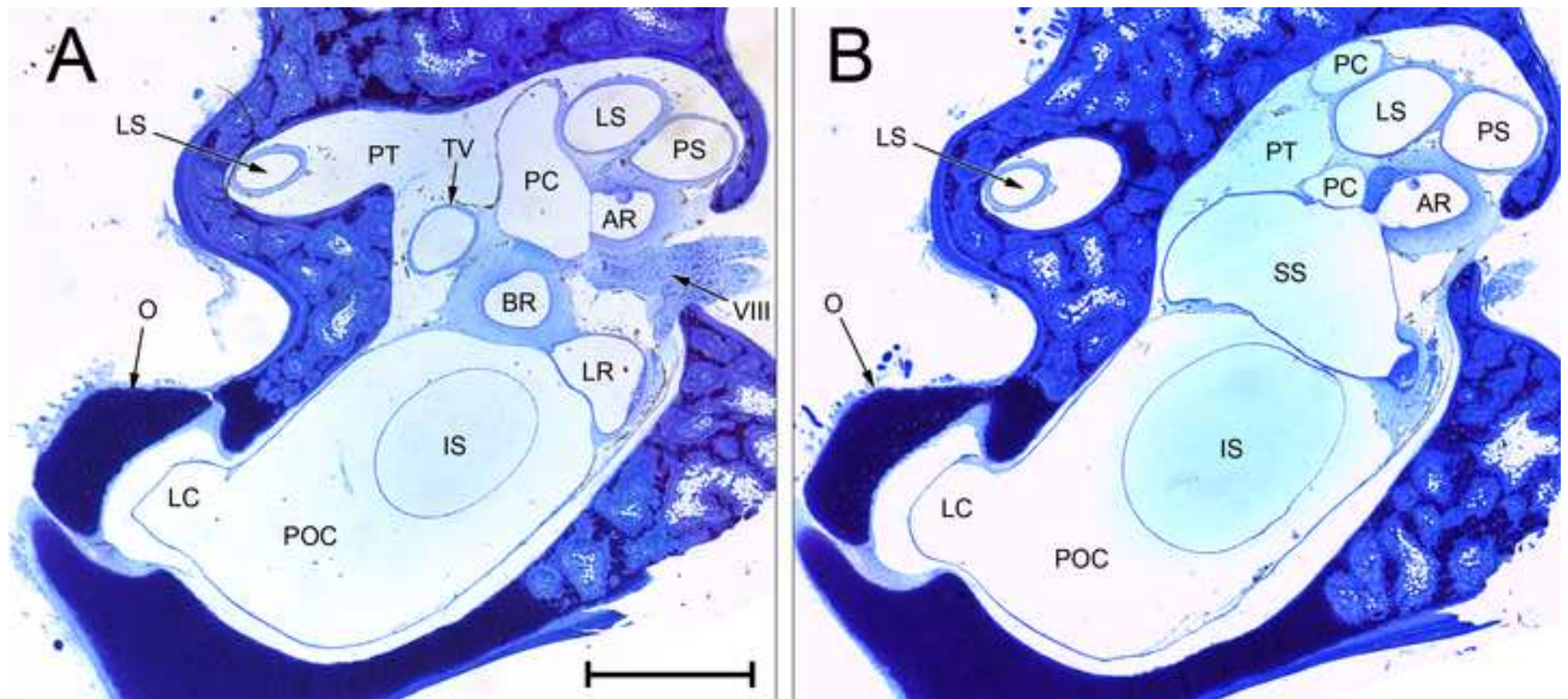


Figure 5
[Click here to download high resolution image](#)

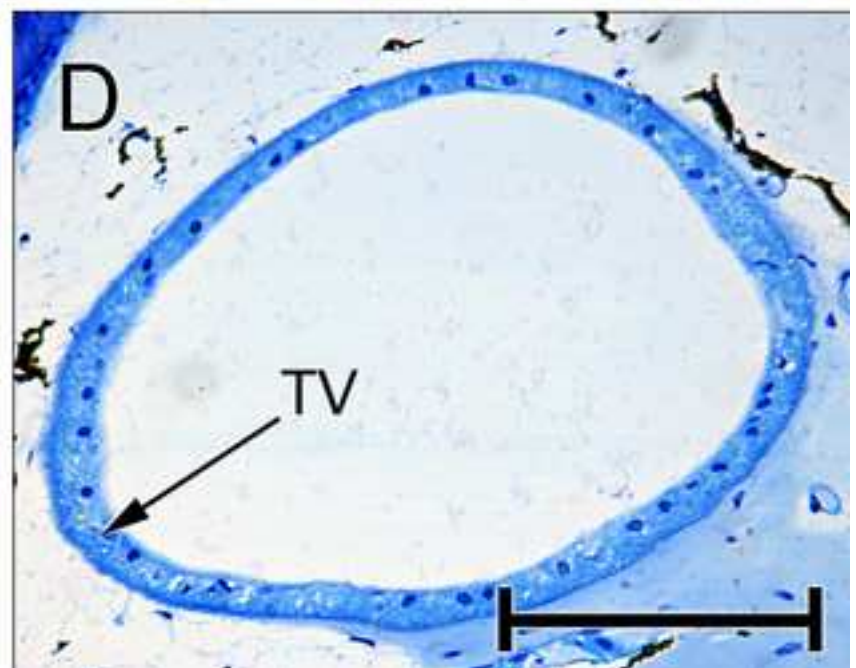
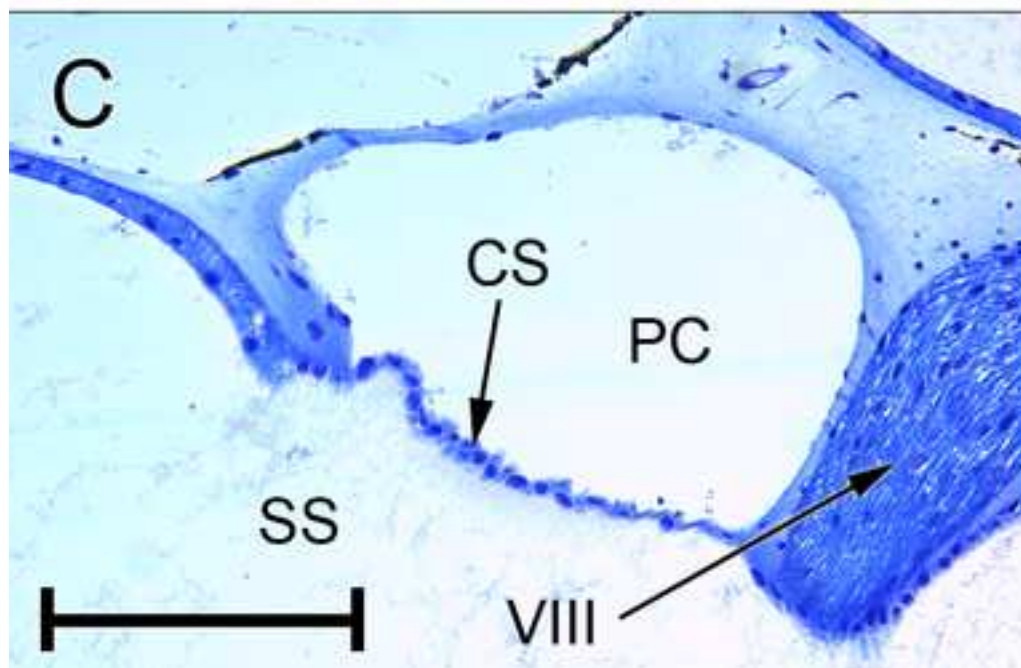
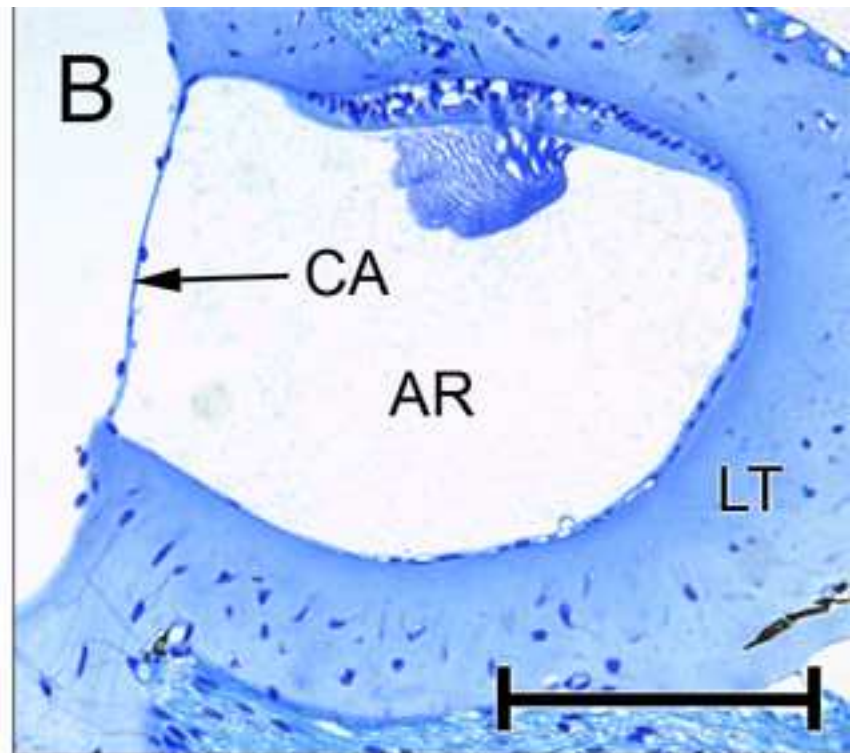
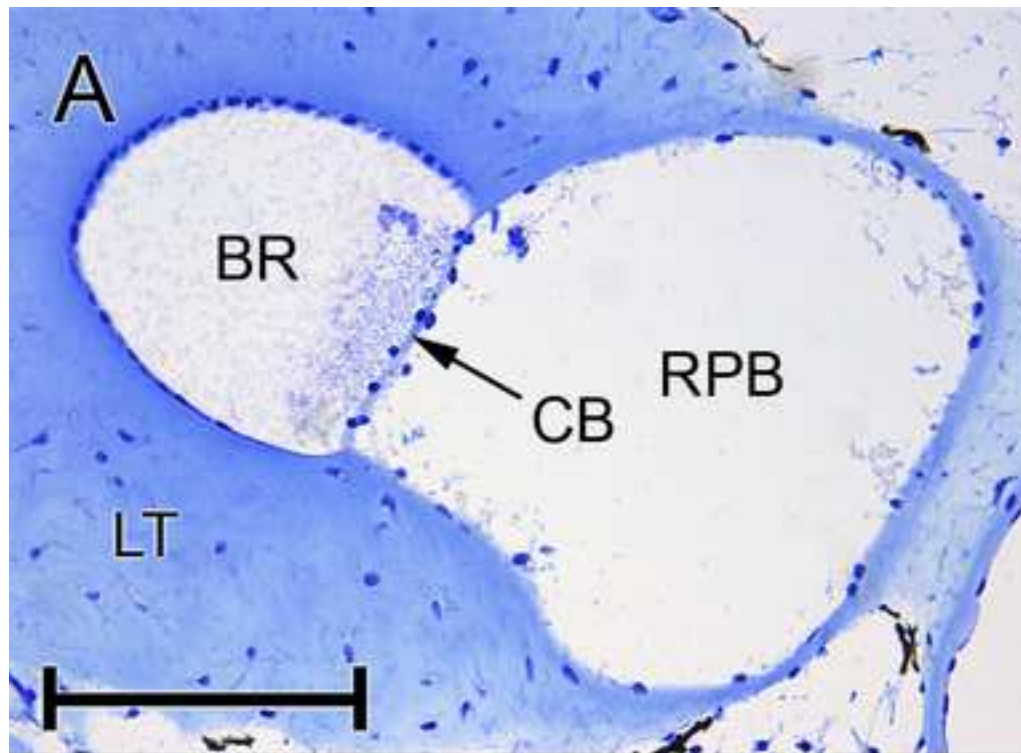


Figure 6
[Click here to download high resolution image](#)

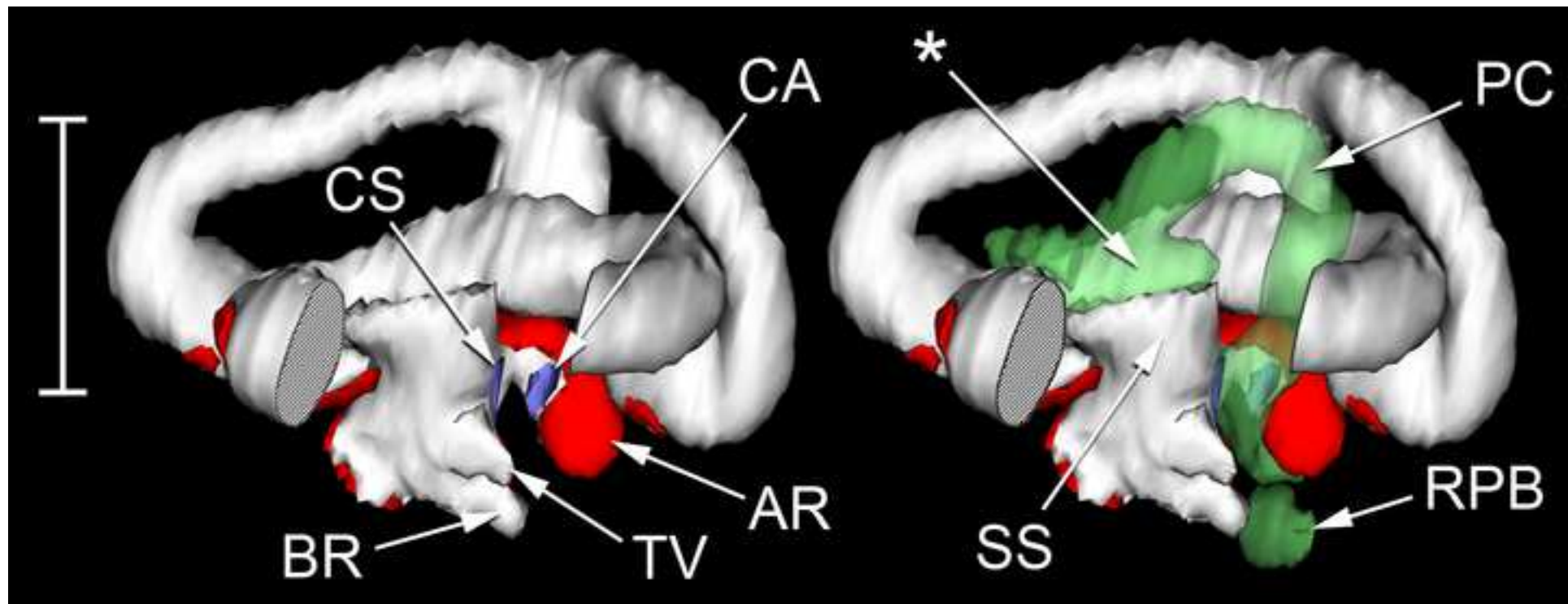


Figure 7
[Click here to download high resolution image](#)

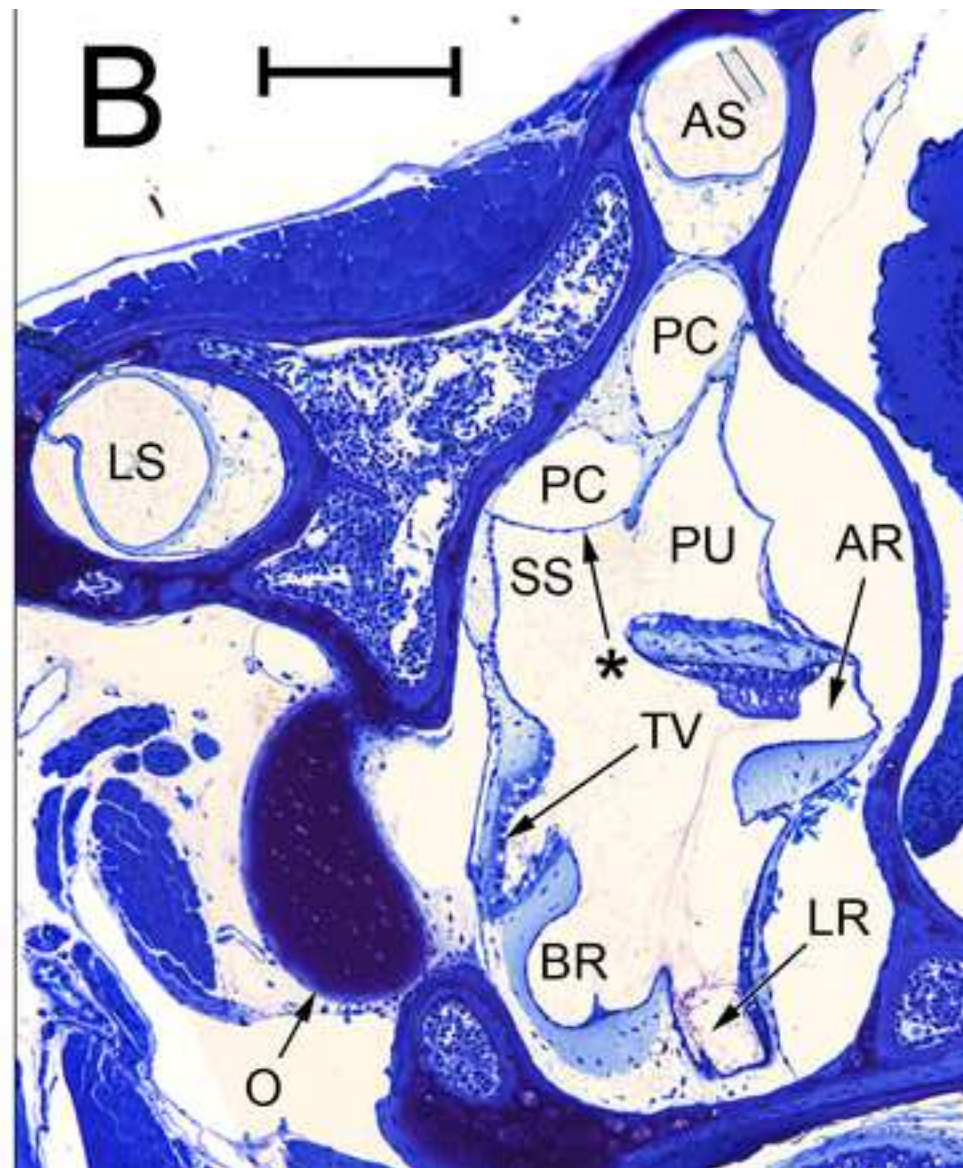
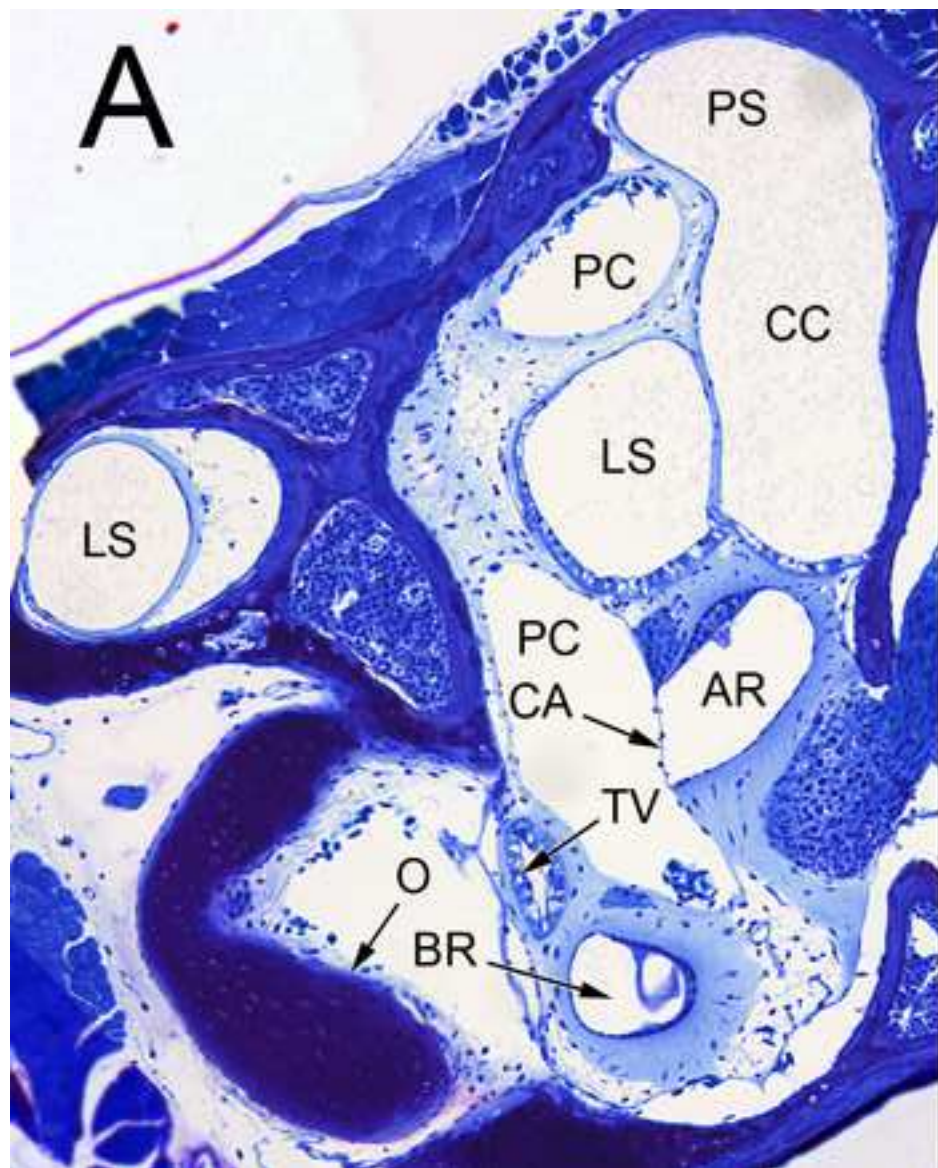


Figure 8
[Click here to download high resolution image](#)

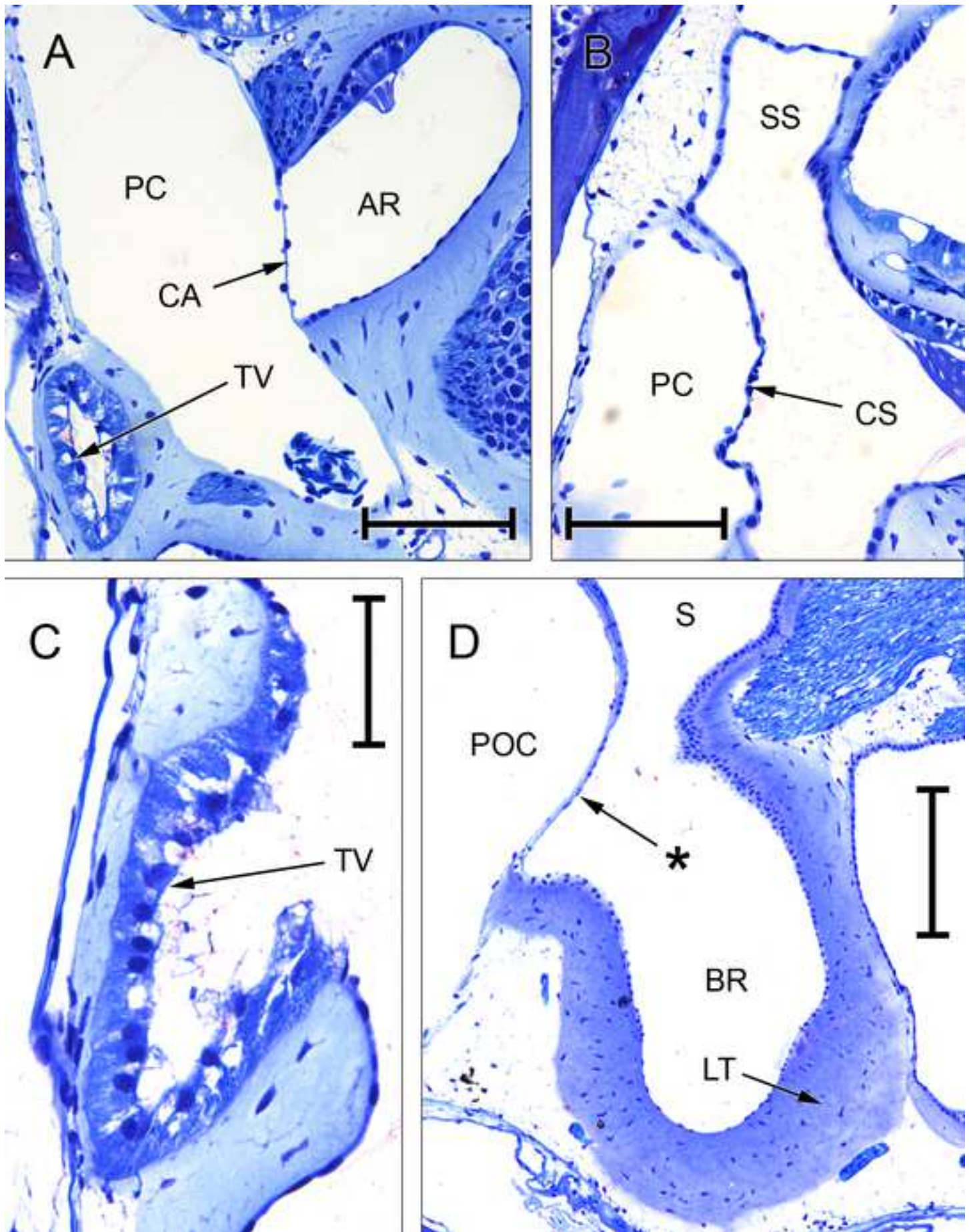


Figure 9
[Click here to download high resolution image](#)

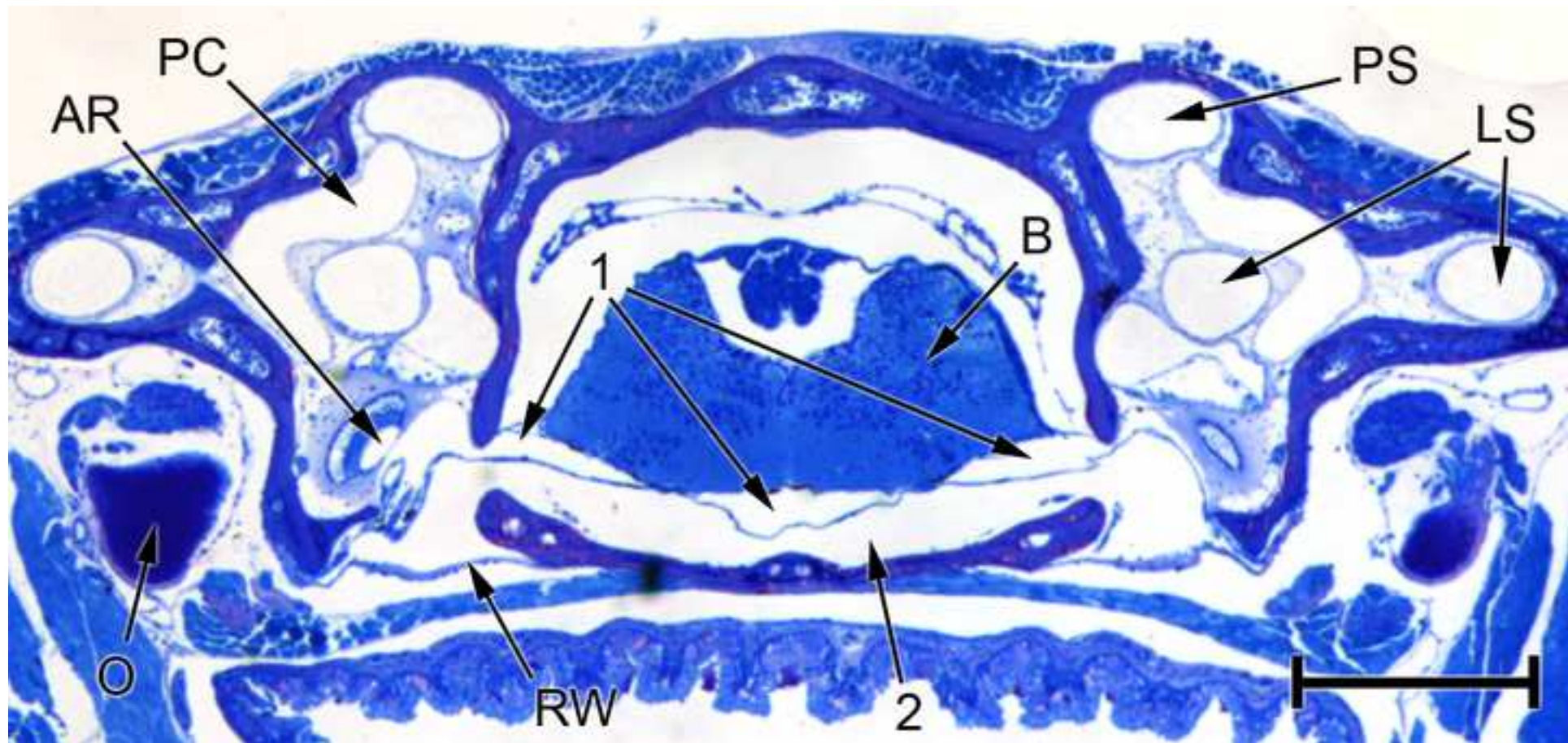


Figure 10
[Click here to download high resolution image](#)

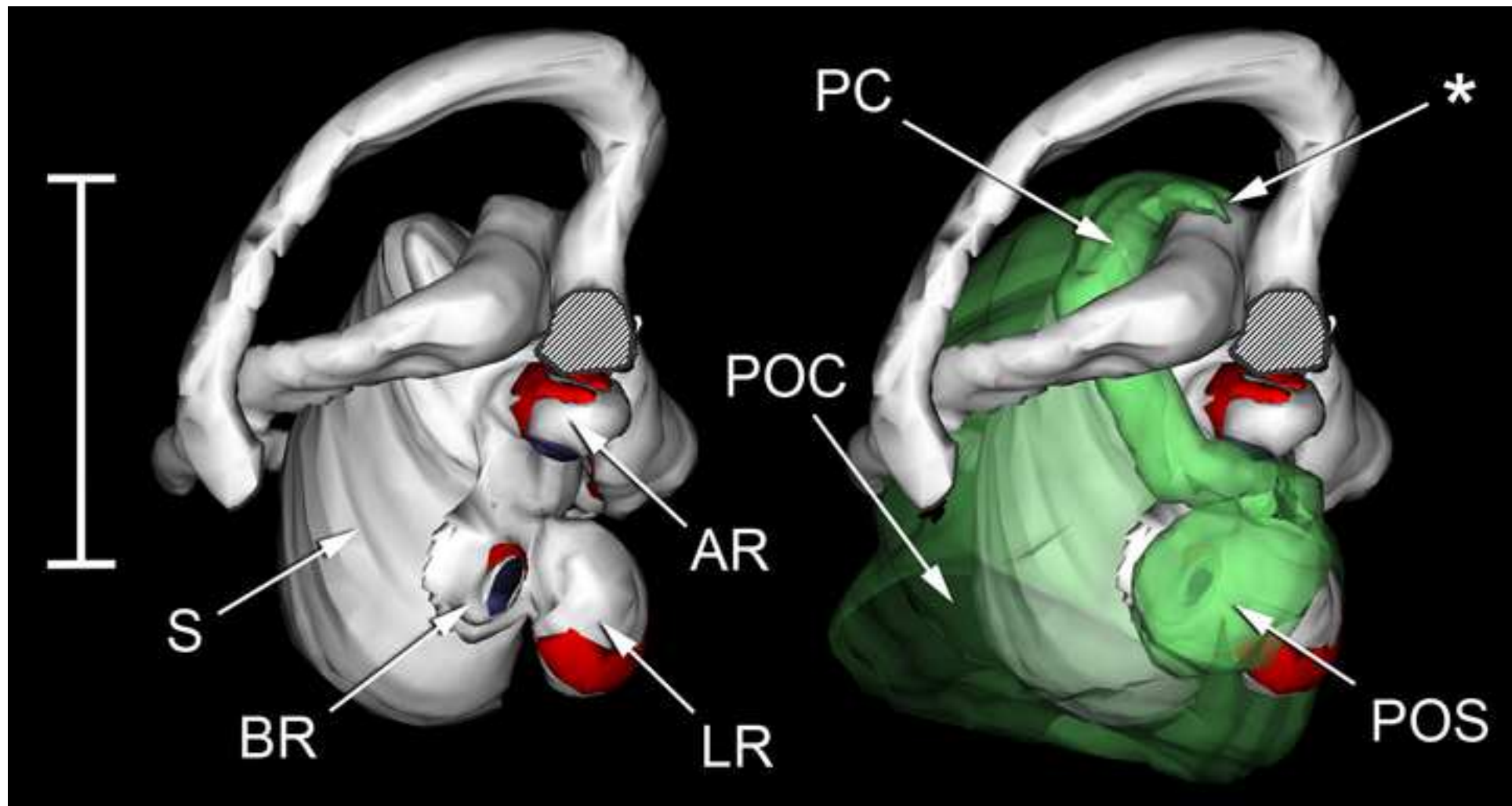


Figure 11
[Click here to download high resolution image](#)

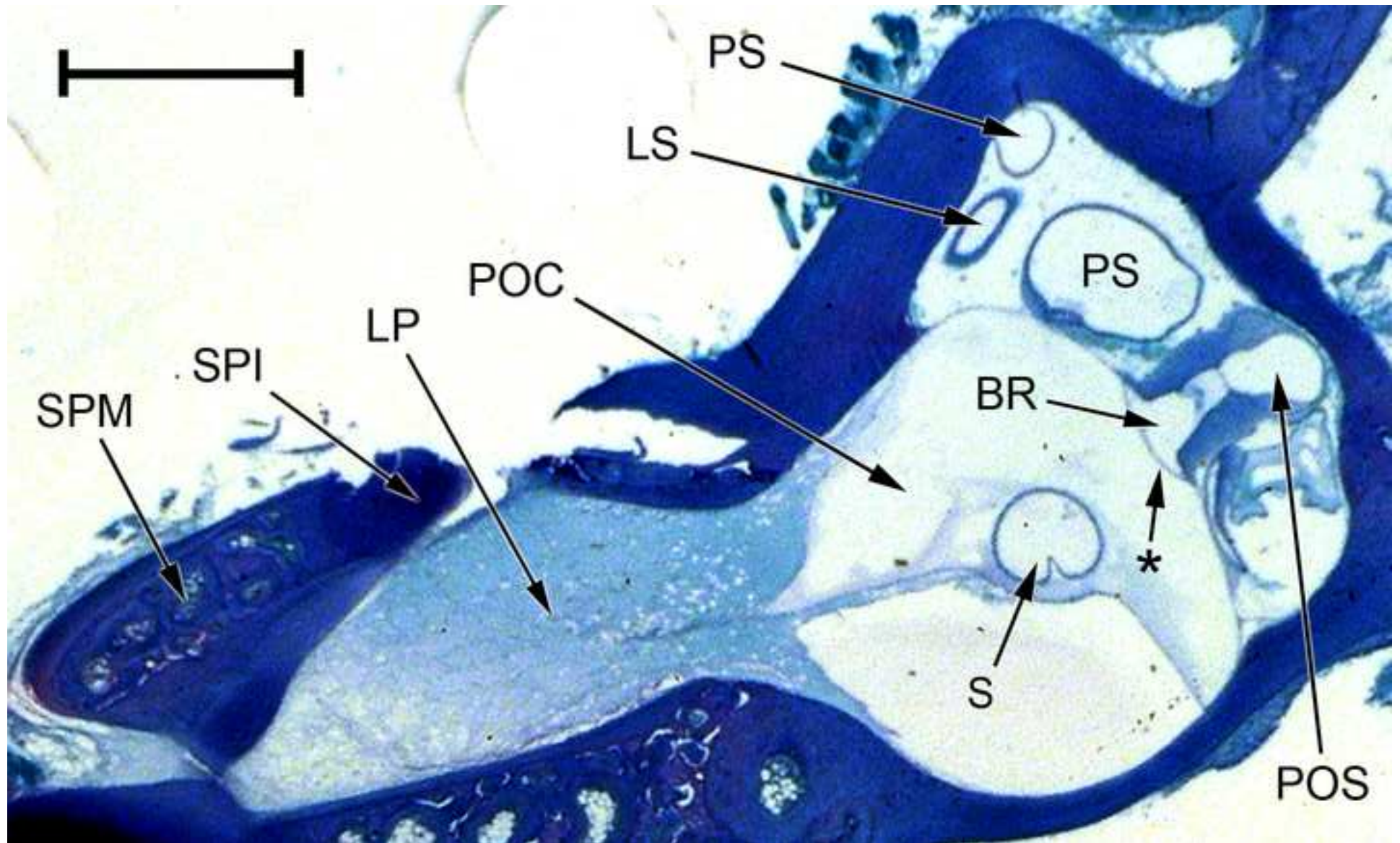
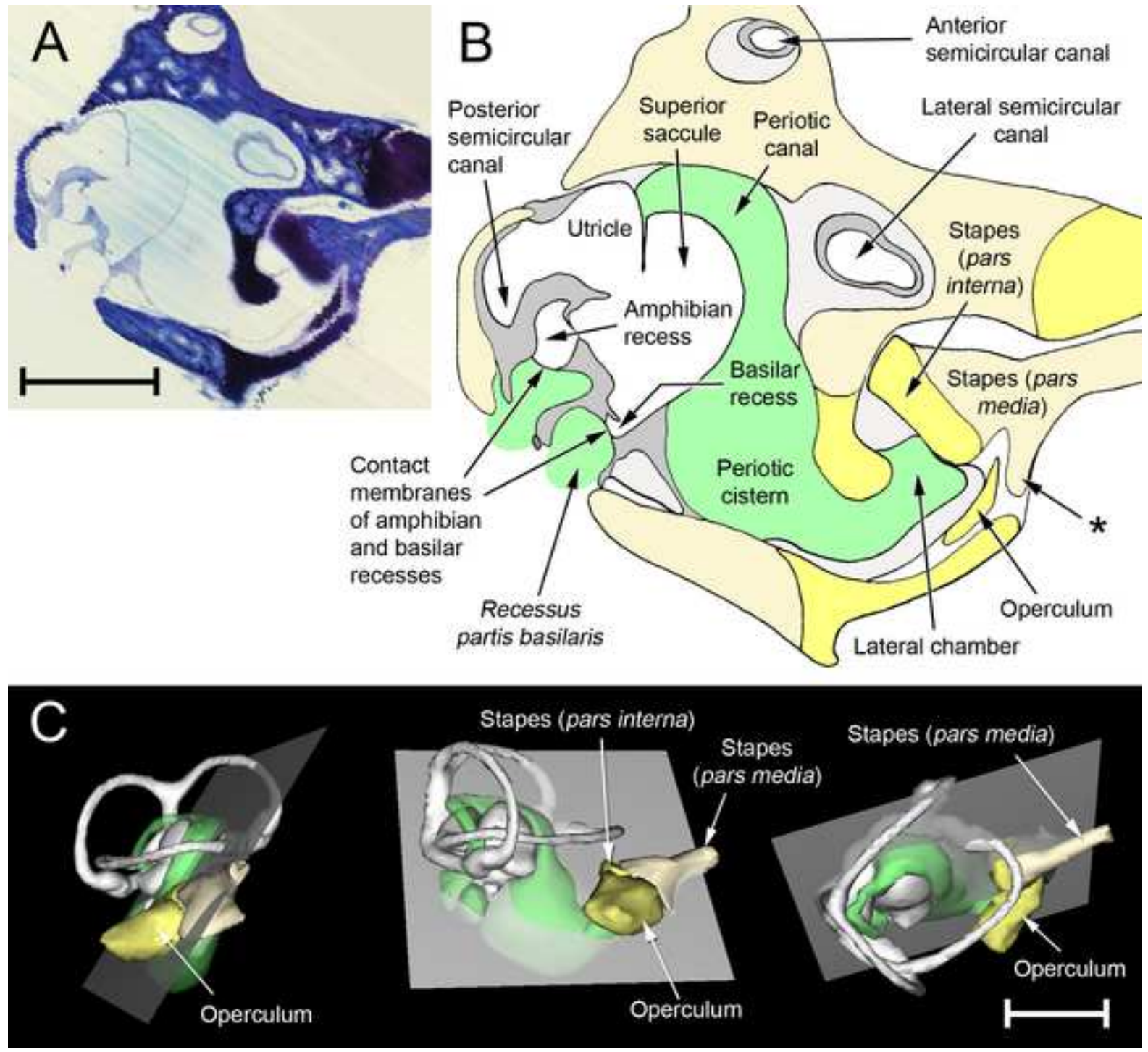


Figure 12
[Click here to download high resolution image](#)



Conflicts of interest disclosure statement

The authors declare that they have no conflicts of interest.